Summer 8-13-2021

Molecular Pathogenesis of a Novel Subgroup of Peripheral T-cell Lymphomas

Jiayu Yu
University of Nebraska Medical Center

Molecular Pathogenesis of a Novel Subgroup of Peripheral T-cell Lymphomas

by

Jiayu Yu

A DISSERTATION

Presented to the Faculty of the University of

the University of Nebraska Graduate College

in Partial Fulfillment of the Requirements

for the Degree of Doctor of Philosophy

Pathology &Microbiology

Graduate program

Under the Supervision of Professor Javeed Iqbal

University of Nebraska Medical Center,

Omaha, Nebraska

October 2019

Supervisory Committee

Kate Hyde, Ph.D. Shannon M. Buckley, Ph.D. Timothy C. Greiner, M.D.

Acknowledgments

First and foremost, I would like to express my sincere gratitude to my advisor Prof. Javeed Iqbal for the continuous support of my graduate study and research, for his patience, motivation, and knowledge. It has been an honor to be his first Ph.D. student. His hard-working, enthusiasm and intelligence have always motivated me. He always stimulates me to think independently, organized and schedule my work efficiently. Due to his trust, I can continue working on the most well-known tumor suppressor genes on T-cell lymphoma, which was of great interest to me.

Second, I would like to thank my committee members, Prof. Kate Hyde, Prof. Shannon M. Buckley and Prof. Timothy C. Greiner for their valuable time and suggestions regarding my research. I am especially grateful to Dr. Kate Hyde, thank you to teach me the technique of retro-orbital injection, give me advice for flow cytometric data analysis, suggestions for writing the research project grant (R01) for my comprehensive exam and the kind help for my future career. I want to thank heartily to Dr. Shannon M. Buckley, thank you so much to help me for the tail vein injection, the kind advice to take advantage of CD45.2 and CD45.1 antibodies to distinguish donor and host cells, the tip advice for the maxillary bleeding and the suggestions to define mouse lymphoma and leukemia. I would like to sincerely thank Dr. Timothy C. Greiner, thank you for your kind advice for making slides of my previous committee member presentations, the dedicated teaching on mouse tumor morphology, and provided me video conference just to fit my schedule even during your time of vacation.

The labmates of the Iqbal group have contributed immensely to my professional and personal life at UNMC. The group has been a source of good advice and friendships. Thanks to Dr. Alyssa C. Bouska and Dr. Waseem G. Lone, as senior postdocs, thank you for the stimulating discussions and insightful comments and deep thoughts on my projects. Thanks to my fellow graduate students, Tayla B. Heavican and Tyler A. Herek for your companion, suggestions on experiments and encouraging and supportive during the most difficult periods in graduate school. I am grateful to all of you for your companion just as family members during my 5 years of graduate study life, as well as the faithful support during the final stages of my Ph.D. I would like to give special thanks to Prof. Wing C. Chan, Prof. Timothy W. McKeithan and Dr. Yuping Li from City of Hope National Medical Center, who constitutively provide suggestions and supports on this project. I also want to thank the previous lab member Sneha Ganesh graduated as an M.S. and the visiting scholar Dr. Saumyaranhjan Mallick, and the current new lab members Sunandini Sharma and Sahil Sethi for your companion.

My sincere thanks also go to Dr. Chengfeng Bi (Andy) and Dr. Xuan Zhang in Prof. Kai Fu's lab who gave me lots of suggestions in vitro experiments and taught me to perform good Western blots. I am especially thankful for Jacob Robinson and Jun Li who performed all the mouse IHC staining and greatly thankful for Prof. Catalina Amador for her kind help with the diagnoses of all the mice H&E and IHC slides. I would like to thank Dr. Satyayanarayana Rachagani in Prof. Surinder K. Batra's lab who provide me *p53*^{R172H} mice breeders for my research and gave me advice for

primary mouse cell culture. I would also like to thank Dr. Kamiya Mehla in Prof. Michael A. (Tony) Hollingsworth's lab, who discussed with me many times about the intracellular staining on mouse cells and cell proliferation assay. I also own special thanks to Prof J. Graham Sharp who kindly taught me how to perform thymectomy on real mice, as well as the assistance from Prof. Geoffrey Thiele.

I have sincerely appreciated the help from Dr. Manju George in IACUC, who help me to go through every detail to establish the project protocol for mice study, especially when I had no experience in mice study at the beginning. I also sincerely thank the faculties in Comparative Medicine, Kristin Leland Wavrin who taught the basic techniques in the mouse study, including ear tag and maxillary bleeding and help me established the whole system for mouse thymectomy (Even though it didn't work eventually). I am especially thankful for Kris Puhl and Hua Yang, who helped to monitor tumor-bearing mice and treat me so kind as their daughter.

I would like to reserve a special thanks for Prof. Rakesh K. Singh, the program director, and Tuire Cechin, the program coordinator in PAMM. I cannot thank you sufficiently for your continuously tremendous support and always being there in my whole Ph.D. life.

My time at UNMC was made enjoyable in large part due to many friends. I am grateful to have my wonderful friends who provide me with so many memorable moments in my life, especially for the friends we started graduate school at about the same time. Thank you Tayla B. Heavican, Bushra Bakhsh, Saswati Karmakar, Chunyi

Zhou and Shashank Shrishrimal, for studying together for the exams at nights and weekends, providing me advice for experiments as much as you can, hanging out together for dinners, parties and trips, as well as being extremely supportive during my bad days in graduate school.

In regards to my personal life, I thank UNMC gave me the opportunities to works as the Friendship House manager for more than three years. Thus I got the chance to know the wonderful people, my “boss” Matthew Mitchell, and Connor Willingham, who gave me so much support whenever I asked for. I am grateful to meet, talk and live with people from different parts of China, India, Egypt, Sweden, and Pakistan.

I would also like to acknowledge the funding from the Chinese Scholarship Council for the financial support for the first four years and the financial support from Prof. Javeed Iqbal for the last year of my graduate study.

Last but not least, I would like to thank my family: my grandparents, parents, uncles and aunts, and cousins, for the support of my decisions. I own you so much for all the unconditional love you have given to me.

Molecular Pathogenesis of a Novel Subgroup of Peripheral T-cell Lymphomas

Jiayu Yu, Ph.D.

University of Nebraska Medical Center, 2019

Advisor: Javeed Iqbal, Ph.D.

Peripheral T-cell Lymphoma (PTCL) consists of numerous distinct disease entities. With the current diagnostic criteria over a third of the cases cannot be further classified and are called "not otherwise specified" (PTCL-NOS). Using gene expression profiling (GEP) of tumors, we identified two novels PTCL-NOS molecular subgroups either characterized by high expression of *GATA3* (33%), which is associated with Th2 cell differentiation, or high expression of *TBX21* (49%) which regulates Th1 cell maturation. Therefore, stratifying patients for diagnosis and identifying the underlying genetic basis to improve clinical therapy becomes critical to prognosis.

First, we performed DNA copy number analysis by using the OncoScan® platform, which revealed recurrent chromosomal imbalances are highly discordant between PTCL-GATA3 and PTCL-TBX21. Triple-deletion of *TP53;PTEN;CDKN2A* has

been detected in 23% verse 0% in PTCL-GATA3 and PTCL-TBX21, contributing inferior overall survival (OS) in this group. Most interestingly, a distinct molecular subtype characterized by heterozygous loss of *TP53* and *PTEN* accounts for 35% in PTCL-GATA3, with hot-spot *TP53*^{R175H} mutation identified to contributes to the dysfunction of *TP53* signaling.

Second, to evaluate the role of *TP53* and *PTEN* in T-cell lymphomagenesis, we disrupted *p53* and/or *Pten* with the Cre-loxP system, which induced *p53*^{R172H} mutation and *Pten* deletion specifically in CD4^{+} T cells. Impaired T-cell development was observed due to *p53*;*Pten* deficiency. Acute loss of *p53*;*Pten* results in SP CD4^{+} T cell and DN T cell lymphoma between 8-24.6 weeks after birth. In contrast, long-term *p53*; *Pten* deficiency characterized by markedly pleomorphic morphology at a latency of 27.7-89.1 weeks after birth. Strikingly, the predominant subset of heterozygous loss of *p53*;*Pten* tumor-bearing mice committed to a CD8^{+} immunophenotype.

To characterize the T-cell biology of *p53;Pten* deficiency, functional characterization of 4-week old age CD4^{+} splenocytes were isolated from 6 genotypes of mice for all the *in vitro* studies. As expected, *p53*^{R172H} switches CD4^{+} T cells from arrest into proliferation in the context of *Pten*-deficiency in an antigen-dependent and independent manner. Strikingly, we found the dose of *Pten* dictates cell growth by regulation of apoptotic cell death. We also demonstrated that IL-2 is not required for initial expansion, but is required for the long-term survival of primed T cells *in vitro*. Besides, heterozygous loss of *p53* and *Pten* has more capacity to skew naïve CD4^{+} T

cells into Th2 phenotypes. Lastly, we also observed that cell-intrinsic programming by genetic alterations imparts affects the differential engraftment fitness after adoptive transfer.

Table of Contents

List of Figures

List of Tables

List of abbreviations

HSC	hematopoietic stem cell
ETP	Early thymic precursor
TCR	T-cell receptor
DN1	Double negative $D44^{+}CD25^{-}$
DN2	Double negative $CD44^{+}CD25^{+}$
DN3	Double negative $CD44^{-}CD25^{+}$
DN4	Double negative $CD44^{-}CD25^{-}$
ISP	Immature single-positive (ISP) $CD8^{+}$
DP	Double positive $CD4^{+}CD8^{+}$
SP	Signal positive
RS	Recombination signals
DSBs	Double-strand breaks
TdT	Terminal deoxynucleotidyl transferase
MHC	Major histocompatibility complex
APCs	Antigen-presenting cells

SLOs	Secondary lymphoid organs
TFs	Transcription factors
MAPK	Mitogen-activated protein kinase
NF-κb	Nuclear factor-κB
HL	Hodgkin lymphoma
NHL	Non-Hodgkin lymphoma
HDC	Dendritic cell neoplasms
PTCL	Peripheral T-cell lymphoma
NKTCL	Natural killer/T-cell lymphoma
PTCL-NOS	Peripheral T-cell lymphoma, not otherwise specified
AITL	Angioimmunoblastic T-cell -cell lymphoma
ALCL	Anaplastic large cell lymphoma
ATCL	T-cell leukemia/lymphoma
T-PLL	T-cell prolymphocytic leukemia
ALL	Acute lymphoblastic leukemias
EATL	Enteropathy-associated T-cell lymphoma
HSTCL	Hepatosplenic T-Cell lymphoma
SPTCL	Subcutaneous panniculitis-like T-cell lymphoma

EBV	Epstein-Barr virus
CHOP	Cyclophosphamide, Doxorubicin, Vincristine, Prednisone
OS	Overall survival
ASCT	Autologous stem-cell transplantation
DLBCL	Diffuse large B-cell lymphoma
COO	Cell-of-origin
GCB	Germinal center B-cell-like
ABC	Activated B-cell-like
T_{FH}	Follicular T helper
GEP	Gene expression profiling
GATA3	GATA Binding Protein 3
TBX21	T-Box 21
Th1	T helper type 1
Th2	T helper type 2
LOH	Loss of heterozygosity
TP53	Tumor protein 53
DBD	DNA binding domain
PTEN	Phosphatase and tensin homolog deleted on chromosome 10

PBD	Phosphatidylinositol-4-5-bisphosphate-binding domain
C2-domain	C-terminal domain
PDZ BD	PDZ-binding motif
PI3K	Phosphatidylinositol 3-kinase
PIP3	Phosphatidylinositol (3,4,5)-trisphosphate
PIP2	Phosphatidylinositol (4,5)-bisphosphate
mTOR	Mammalian target of rapamycin
IFNγ	Interferon γ
IL	Interleukin
NGS	Next-generation sequencing
WES	Whole-exome sequencing
CNVs	Copy number variations
FF	Fresh frozen
FFPE	Formalin fixed, paraffin embedded
CCRCC	Clear cell renal cell carcinoma
AML	Adult acute myeloid leukemia
JAK/STAT	Janus kinase/signal transducers and activators of transcription
CDS	Coding sequence

HGG	High-grade gliomas
LGG	Low-grade gliomas
ES	Embryonic stem
TNBC	Triple-negative-like breast cancer
MEFs	Mouse embryonic fibroblasts
GOF	Gain-of-function
MT	Mutant
WT	Wild-type
ACT	Adoptive cell transfer
IPA	Ingenuity Pathway Analysis

Chapter 1: Introduction

Mature T-cell development and differentiation

T cells are a major component of the adaptive immune response, and play a central role in cell-mediated immunity in pathogen elimination[1,2] and tumor surveillance[3]. T cells are identified by a surface molecule CD3 and are comprised of two major groups: the $CD4^+$ T helper (T_H) cells and cytotoxic $CD8^+$ T cells[4]. The CD4 T cells display helper activities on other immune cells, and in turn are subdivided into Th1, Th2, Th9, Th17, Th22, Tfh and T regulatory (Treg) groups[5-9], each with a characteristic profile of production cytokines. The CD8 T cytotoxic population is the second major group of T lymphocytes that function in killing target cells; they are comprised of Tc1 and Tc2 subpopulations with similar cytokine profiles as Th1 and Th2 cells[10]. To ensure adaptive immune responses against foreign antigens and avoid attacking itself, the naïve T cell compartment in the thymus contains quite a number of cells with unique T cell receptors to construct a diverse T cell repertoire, which is a consequence of different V, D, J recombinations[11].

The generation of a functional T cell starts from hematopoietic stem cells (HSC) in the bone marrow, which gives rise to lymphoid progenitors that home to the thymus and, undergo a series of well-documented development steps in the thymus, and eventually differentiate into effector T cells in the periphery (Figure 1). This tightly regulated phase is a result of the TCR-mediated signal. The T cell development starts when TCRδ, TCRγ, and TCRβ gene rearrangement initiated in DN2 ($CD44^+CD25^+$)

stage. With the successful rearrangement of TCRβ chain via productive V(D)J recombination and surface expression of TCRβ co-assemble with pre-Tα[12], this process gives rise to a DN3 ($CD44^{-}CD25^{+}$) cells come with a functional pre-TCR complex. The pre-TCR signals are essential for rapid expansion, and maturation to the double-positive (DP, $CD4^{+}CD8^{+}$) stage and rearrangement of the TCR-α chain leading to the mature TCR-αβ receptor expression upon successful rearrangement[13]. TCR β selection is achieved at the late DN4 ($CD44^{-}CD25^{-}$) stage, which leads to the generation of double-positive (DP, $CD4^{+}CD8^{+}$) cells and initiates TCRα locus rearrangement. Next, αβ-T undergo positive and negative selection and eventually commit to the CD4 or CD8 single-positive (SP) lineages. DP thymocytes that recognize self-MHC receive a positive selection signal leading to either CD4 or CD8 single-positive (SP) cells depending on their interaction with either class II or class I MHC molecules, referred to as repertoire selection phase. After binding to MHC I molecules, cells retain CD8 expression, whereas binding to MHC II retains CD4 expression. Cells will be deleted by negative selection in the medulla if it exceeds a certain threshold avidity binding to MHC molecules. The rest will migrate out of the thymus into the peripheral blood and secondary lymphoid organs.

For mature T cells, an important part of the molecular development involves somatic alteration of the germline configuration of the T-cell receptor (TCR) genes to a unique configuration, in order to permit the development of a clone of T cells with an extracellular receptor specific to a given antigen[14,15]. T cells comprise two distinct

subsets by expressing either αβ- and γδ-TCRs formed by germline genetic rearrangement of the variable (V), diversity (D), and joining (J) gene segments. The TCR repertoire is established through a series of DNA recombination events that generate 10^{16} to 10^{18} different possible sequences from the VDJ gene segment random somatic recombination events shaped by the selection of self-antigens, which is regulated by Rag enzyme at the TCR loci. The TCR genes encoding the TCRβ chain are located at chromosomal positions 7q32–35[16]. The V, D, and J gene segments are flanked by recombination signals (RS) of 12- or 23-mer spacer length that direct recombination according to the 12/23 rule. At the *trb* locus, the 3′ end of TRBV or TRBD in TCRβ chains is a heptamer (CACAGTG)-23 base-pair (bp)-nonamer (ACAAAAACC) rearrangement of signal sequences (3′ TRBV 23 RSS and 3′ TRBD 23 RSS), whereas the 5′ end of TRBD or TRBJ is a nonamer-12bp-heptamer rearrangement of signal sequences (5′ TRBD 12 RSS and 5′ TRBJ 12 RSS)[17]. TCR chains are assembled by V(D)J recombination and can be divided into two phases: cleavage and repair. V(D)J is activated by activating gene RAG-1 and RAG-2[18] which introduce a pair of double-strand breaks (DSBs) between the V, D, and J coding segments and the RSSs[19]. The cleavage generates four new structures: a blunt signal end, a hairpin coding end, signal joints (SJ) and coding joints (CJ)[18]. The generation of junctional diversity is initiated by opening of hairpin coding ends, which are the substrates for nontemplate-dependent nucleotide additions by terminal deoxynucleotidyl transferase (TdT)[20]. The nonhomologous end-joining (NHEJ) pathway machinery recognizes and repairs the

RAG-generated breaks results in the rejoining of the DNA ends generated during V(D)J recombination[21]. This process occurs only between segments with the 23 RSS terminal and segments with the 12 RSS terminal, which act as recognition sites for the VDJ recombinase[22]. This results in the diversity and specificity of T cells that enables them to recognize a vast spectrum of antigens presented by major histocompatibility complex (MHC) molecules to provide sufficient immune coverage.

Substantial progress in elucidating the molecular genetic basis for the commitment from immature to mature T cells has been achieved, with several transcriptional factors (TFs) identified that are critical for T cell differentiation and maturation. The life of T cells begins after the B selection checking point, where DN3 thymocytes express the functional pre-TCR. PU.1 is a key differentiation regulator compared to its transcriptional partners since it can bind approximately 30000-75000 sites in early hematopoietic progenitors[23,24]. It modulates T cell development at the pre-thymic stage through regulating the expression of CD11b, CD16, CD18, and CD64 as well as gene targets expressed during myelopoiesis and hematopoietic stem cells homing[25,26]. The expression of *GATA3* is upregulated between DN3-DN4 stages[27]. Deletion of *GATA3* results in the accumulation of DN3 cells and a decreasing of DN4, DP and SP cells, which is mainly due to the impairment of β selection by dysregulation of Notch signaling upon absence of *GATA3*[28]. *Runx3* KO mice display abnormalities in CD4 expression during lineage decisions and impairment of $CD8^+$ T cell maturation in the thymus. In a double mutant Null *Runx3* and heterozygous *Runx1* (*Runx3*$^{-/-}$;

Runx1$^{+/-}$) mouse model, SP CD8^{+} T cells have been barely detected in periphery[29].

T cell activation, function, and plasticity

T cell receptor (TCR) signal transduction is initiated by the immunological synapses[30] formed by the engagement of the TCR to peptide-MHC (pMHC) expressed on antigen-presenting cells (APCs). TCR consists of the CD3εγ and CD3εδ heterodimers and the CD3ζζ homodimer, which form the TCR-CD3 complex[31] (Figure 2). There are three critical nodes in TCR signaling[32], including LCK, ZAP-70 and LAT, activation of which results in a cascade of phosphorylation events. The phosphorylation events start with the SRC family protein tyrosine kinase LCK binding to the cytoplasmic domains of CD4 or CD8 co-receptors. Then phosphorylation of CD3ζ and other ITAMs by LCK serves as a docking site to recruit the syk kinase family member ZAP-70 PTK. Activated ZAP-70 further phosphorylates LAT, the scaffolding transmembrane adaptor linker for T cell activation, to form the docking sites to recruit adaptor molecules such as GADS, GRB2, and PLCγ1, which results in the generation of a multi-molecular LAT signalosome[32]. The LAT effector molecules induce signal propagation through the Ca^{2+}-calcineurin, mitogen-activated protein kinase (MAPK) and nuclear factor-kB (NF-KB) signaling pathway. This process converts the TCR with no intrinsic enzymatic function to an active PTK to phosphorylate a spectrum of substrates leading to the cascade of downstream signal integration, which results in T cell proliferation, migration, cytokine production, and effector functions.

During T cell activation, signaling through TCR alone results in a non-

responsive state (anergy) and impaired T cell response upon re-stimulation[33]. Ligation of the CD28 receptor on T cells provides a critical second signal along with TCR signaling in T cell activation. CD28 is expressed on roughly 80% of human $CD4^+$ T cells and 50% $CD8^+$ T cells[34]. It has been demonstrated that CD28 promotes T cell proliferation through activation of downstream Akt signaling[33]. Phosphorylation of the CD28 cytoplasmic tail is followed by the engagement of its ligands CD80 (B7-1) and CD86 (B7-2) on APCs[35]. This recruits GRB2, which complexes with VAV1[36] and p85[37], the regulatory subunit of PI3K. The p85 regulatory subunit then allows the recruitment of p110, the catalytic subunit of PI3K[37], and further targets downstream Akt signaling.

The third signaling during T cell activation comes with the engagement of cytokine receptors to the cytokine environment[38]. Along with Ag and co-stimulation, this process leads to the activation of specific transcription factors (TFs) and initiates T cell differentiation. Naive $CD4^+$ T cells remain “poised” to adopt alternative subset transcriptional programs until they reach to the signals provided by antigen-presenting cells (APCs). In secondary lymphoid organs (SLOs) such as spleen and lymph nodes, naive $CD4^+$ T cells differentiate into functionally distinct effectors, including Th1, Th2, Th9, Th17, Th22, Tfh and T regulatory (Treg), which are regulated by the corresponding lineage defined transcription factors Tbx21, GATA3, TGFβ, Rorγt, AhR, Bcl6, and Foxp3, respectively. It has been well established that naïve $CD4^+$ T cell priming can be remarkably flexible in the response to cytokine stimuli. Although Th1 and Th2 cells display more stable phenotypes, *in vitro* experiments demonstrated that

Th1 populations arising after 1 wk of stimulation in Th1-polarizing condition could convert to Th2 cells when re-stimulated in IL-4, and vice versa[39]. However, long-term culturing could not reverse Th1/Th2 cell differentiation[39]. Th17 cells can readily switch to other T helper cell programs under certain cytokine conditions. *In vivo*, IFN-γ and IL-12 synergize to generated Th17 into Th1/Th17 cells through the upregulation of IL-12Rβ2 chain by IFN-γ and IL-12 for Th1 polarization[40]. Subsequently producing IFN-γ Th17 cells promote efficient immune support in intestinal inflammation in mouse models of IBD[41]. In contrast, Th17 cells can adopt a T_H1-like phenotype via IL-4 expression, which has been observed during helminth infection *in vivo*[42]. Besides, iTregs can become IL-17-producing cells upon stimulation with IL-6 and IL-21. In the presence of IL-6 or IL-21 along with TGF-β, naïve $CD4^+$ T cells differentiate into Th17 cells; however, in the absence of proinflammatory cytokines, TGF-β drives differentiation into Treg cells[43,44]. The differentiation decision is governed predominantly by the cytokines in the microenvironment and, to some extent, by the strength of the interaction of the T cell antigen receptor with antigen.

Lymphomas in the context of WHO classification

Lymphomas are a heterogeneous group of cancer that arises from lymphocytes in the immune system, including Hodgkin lymphoma (HL) (10%) and non-Hodgkin lymphoma (NHL) (90%)[45,46]. Several entities of non-Hodgkin lymphomas (NHLs) have been identified, including precursor lymphoid neoplasm (B- and T-cell), mature B-cell neoplasms, mature T and NK neoplasms, mature histiocytic and dendritic cell

neoplasms (HDC) based on the 2016 revision of the World Health Organization (WHO) classification system[47] (Figure 3).

Peripheral T-cell lymphoma (PTCL) and natural killer/T-cell lymphoma (NKTCL) are rare and heterogeneous forms of non-Hodgkin's lymphoma (NHL) that encompass a biologically and clinically heterogeneous group representing approximately 12-15% of the lymphoid neoplasms and are distinct from the more common cutaneous T-cell lymphomas[48]. The geographic variation in the relative frequency of PTCL and NKTCL has been well-documented previously[49], mainly due to genetic variations. Most of the aggressive T-cell lymphomas are included within the nodal, extranodal, and leukemic groups[48]. T-cell malignancies derived from early thymic precursor (ETP) or immature T cells results in leukemia-lymphoblastic T-cell lymphoma. Otherwise, the NHLs that originate from mature T lymphocytes or NK cells are recognized as peripheral T-cell lymphomas (PTCL)[50]. Nodal T-cell lymphomas represent rare neoplasias arising from post-thymic and activated T lymphocytes[50], and mainly include the following subtypes: peripheral T-cell lymphoma, not otherwise specified (NOS), which accounts for 25.9% of the lymphoma entities[51]; angioimmunoblastic T-cell lymphoma (AITL), which is the second-largest category, accounting for 18.5% of the cases[52]; anaplastic large cell lymphoma (ALCL), including the ALK+ (6.6%) and ALK− (5.5%) entities[53]; enteropathy-associated T-cell lymphoma (EATL) (5%)[54], hepatosplenic T-Cell Lymphoma (HSTCL) (1.4%)[55] as well as subcutaneous panniculitis-like T-cell lymphoma (SPTCL) (0.9%)[56] are relative rare compared to others. A PCR-based amplification of T-cell clonality

using genomic DNA from patients for diagnosis has been routinely applied in clinic. Rearranged T-cell receptor genes can be found in all T-cell lymphomas representing all stages of T-cell development[15]. Patients with PTCLs have significantly worse clinical outcomes compared to patients with aggressive B-cell lymphomas due to the misclassification by lacking reliable protein markers for diagnosis and less responsiveness to conventional B-cell lymphoma regimes because of its heterogeneity[48,57].

Peripheral T-cell lymphoma, not otherwise specified (PTCL-NOS), accounts for approximately 30-50% of mature T-cell lymphomas[51,57] and remains the most commonly diagnosed subtype of T-cell lymphoma, which cannot be further classified based on morphology, phenotype, and conventional molecular studies, and is often described as a “wastebasket” category. According to the International T-cell Lymphoma Project, the disease is equally common in Europe and North America but shows a slightly lower prevalence in Asia (34.3%, 34.4%, and 22.4% of PTCL, respectively)[57]. It mostly affects male patients, with a median age at presentation of 60 years[51]. Despite TCR gene rearrangements as the clinical markers, the diagnosis of PTCL-NOS is made by a standard panel of immunostains including CD20, CD2, CD3, CD4, CD5, CD8, CD30, CD56, TCR-β, TIA-1, Ki67, and in situ stains for EBV-encoded RNAs[57,58]. $CD4^+$ phenotype predominates in nodal cases[59]. Besides, $CD4^+CD8^+$ double-positivity or $CD4^-CD8^-$ double-negativity is at times seen[59,60], because of CD8, CD56, and cytotoxic granule expression. It usually characterized by the aberrant T-cell

immunophenotype, with a frequent loss of CD5, CD7, and CD52. High Ki67, Epstein-Barr virus (EBV)-positivity and CD56 expression at lesions are associated with a worse prognosis[61]. Patients are often seen with B-cell symptoms and accompany them with hemophagocytic syndrome at the time of diagnosis. PTCL-NOS involves nodal sites deriving from the clonal expansion of mature T-lymphocytes bearing clonally rearranged TCR genes. However, it probably encompasses more than one disease as suggested by the morphological, phenotypical and genetic heterogeneity. Anthracycline-containing regimens, including CHOP (cyclophosphamide, doxorubicin, vincristine, prednisone) and CHOP-like regimens were most wildly used, though it has not been proved to be the optimized therapy. Compared to other T-cell lymphoma entities, the long-term survival is quite low, with a remission rate of 50-65% and 5-year overall survival (OS) less than 37%[48,62], which is largely unsatisfactory both in first-line and in the refractory/relapsed settings. The addition of etoposide improves event-free survival in younger patients, but without a clear impact on OS[63]. Consolidative autologous stem-cell transplantation (ASCT) in the first remission may improve outcomes by random studies, but it still remains controversial[48]. This is why several new drugs are going on in clinical trials, and identifying genetic lesions, as well as oncogenic pathways in PTCL-NOS, are urgent needs.

Cellular origin of PTCL-NOS

Understanding the developmental mechanisms at which stage lymphoma derived from is relevant to the pathogenesis, which can also provide information of the

selection for new therapeutic agents. As defined and characterized by the Lymphoma/Leukemia Molecular Profiling Project (LLMPP)[64], diffuse large B-cell lymphoma (DLBCL) can be well categorized by its cell-of-origin (COO) which either derived from a germinal center B-cell (GCB) or activated B-cell (ABC) based on the patterns of gene expression[65]. However, the developmental biology of PTCLs is less well understood, as the T cell system is more complex and comprising numerous subsets with different biological changes. Nevertheless, AITL bears a close relation to the follicular T helper (T_{FH}) cell of the germinal center which was demonstrated by the molecular signatures in a GEP study[66], which also shares the same genetic changes with PTCL-NOS bearing T follicular helper (T_{FH}) phenotype[47].

Despite the heterogeneous nature of PTCL-NOS, molecular subgroups with distinct features have been identified by GEP (Gene expression profiling) studies[67]. Unsupervised hierarchical clustering of gene expression data identified two novel subgroups of PTCL-NOS[67], which provide the molecular basis of the heterogeneity of PTCL-NOS. PTCL-GATA3 associated with high expression of *GATA3* and its target genes such as *CCR4, IL18RA, CXCR7,* and *IK* which promote a Th2 phenotype during naïve T cell differentiation. Whereas the PTCL-TBX21 subtype is characterized by high expression of *TBX21* and *EOMES,* and its target genes including *CXCR3, IL2RB, CCL3,* and *IFNGG,* which has a prominent Th1 cytokine secretion pattern (Figure 4). Besides, PTCL-GATA3 and the enrichment of gene signatures highly associated proliferation and PI3K-mTOR-AKT signaling, while PTCL-TBX21 gene signatures are

enriched in the NF-κB pathway. Importantly, *GATA3* expression confers a poor prognosis, with a 5-year overall survival (OS) of 19%, whereas cases with a *TBX21* signature display more favorable outcomes (5-year OS, 38%)[67]. PTCL-GATA3 correlated with Th2-associated transcripts and cytokine production and indicated a high-risk subset of PTCL-NOS has been demonstrated in an independent study[68]. However, the genetic basis of the disease phenotype, as well as the pathogenesis and oncogenic pathway of PTCL-GATA3 and PTCL-TBX21 is still unclear.

Interestingly, it has been reported that patients with PTCL-NOS expressing one of Th1 or Th2 antigens tended to show a favorable prognosis as compared with cases not expressing Th1 or Th2 antigens[69]. This allows the identification of subgroups of PTCL-NOS patients based on cell-of-origin, which is designated as Th1 or Th2 phenotype, further points out the potential role of a genetic basis in naïve $CD4^+$ T cell differentiation and provide new insights into the stratification of patients from the heterogeneous PTCL-NOS group for novel therapies.

Genetic and epigenetic alterations and oncogenic pathways in PTCL-NOS

Compared to other T-cell lymphoma entities, the genetic alterations and pathogenic mechanisms underlying PTCL-NOS are largely unknown. Nevertheless, various recurrent mutations in PTCL-NOS have been identified. For instance, gene fusions and focal indel mutations of *VAV1* (11%)[70,71], encoding one of the components of the TCR signaling, has been reported by different groups in a relevant proportion of PTCL-NOS. Mouse *Vav1* knockout T cells fail to elicit TCR-induced intracellular $Ca2^+$

flux and to activate the MAPK/ERK pathway and NF-κB signaling[72], suggesting that increased *VAV1* signaling leads to activating genetic alterations in PTCL-NOS. *RHOA G17V* (26%) and *IDH2*^{R172} (8%) mutations are highly specific for T_{FH}-derived PTCL-NOS and were identified in a cohort of 142 patients study, with immunohistochemical validation of T_{FH} markers such as PD-1 and BCL6 in these cases[73], further demonstrating that specific mutations could drive genetic alteration in subtypes of PTCL-NOS. Epigenetic alterations such as DNA methylation genes *TET2* (11-49%)[74-76] and *DNMT3A* (3-36%)[75-77], histone acetylation genes *CREBBP* (4-7%)[74,76], and Histone methylation genes *SETD2* (4.8%)[76] have also been reported in PTCL-NOS. However, the frequency of these mutations varies among institutions, which could be due to the heterogeneity in classification and limits of sample size. Together, these suggest a potential role of lymphoma associated mutations in driving genetic and epigenetic alterations in the molecular pathogenesis of PTCL-NOS.

TP53, the guardian of the genome, which translates a sequence-specific DNA binding protein that regulates downstream transcription[78] in cell-cycle arrest, DNA repair, apoptosis, autophagy, and cellular senescence[79]. Mutation of *TP53* tumor suppressor gene is a frequent event in tumorigenesis, which gives rise to a stable mutant protein whose accumulation is regarded as a hallmark of cancer[80]. Mutations of *TP53* in PTCL-NOS are relatively low compared to other human cancer, with a frequency of 7-16%[74,81]. In physical condition, the level of p53 is low due to the continuous inhibition by MDM2 mediated ubiquitination and proteasomal degradation[82].

However, upon DNA damage, p53 is release from MDM2 inhibition and activated to promote the repair of damaged cells. More than 90% of *TP53* mutations are point mutations that occur most often in the DNA binding domain (DBD), most frequently affects codons 175, 248, and 273[80]. Recently, a distinct molecular subtype characterized by *TP53* alterations in non-T_{FH} PTCL-NOS has been identified[73]. *TP53* mutation has been found in 28% non-T_{FH} PTCL-NOS cases, with 51% of them accompanied with a biallelic lesion. The deletion of *CDKN2A* was co-occurring with *TP53* alteration. This finding demonstrates the biological relevance of tumor suppressor inactivation of genomic instability during T cell subtype tumorigenesis.

In addition to nucleotide mutations and epigenetic alterations, structural changes by chromosomal instability have an important role in tumorigenesis. Gene amplification promotes the oncogenic activity of a subset of proto-oncogenes such as *MYC,* which is well documented in B-cell lymphomas[83]. Conversely, the deletion of tumor suppressor genes results in the disruption of their function. Furthermore, loss of heterozygosity (LOH) is also frequently observed in the tumor cells, which is characterized by the deletion of one allele of a gene either without or with duplication of the remaining allele. Chromosomal abnormalities were observed in 71% PTCL-NOS[84]. Gains of the region 7q21 containing *CDK6*[85], 8q24 encompassing *EIF3H* and *MYC*[86], and losses of 9p21 covering *CDKN2A/2B*[87], 10q23 encompassing *PTEN*[88], 17p13 encompassing *TP53*[73,88] were frequently observed in previous cytogenetic studies of PTCL-NOS. Amplification of 4q, 8q and17q, and deletion of 9p, 10q were

more frequently involved in PTCL-NOS compared to AITL. Furthermore, deletions of 13q14 encompassing *RB1* affected by deletions of 17p13 covering *TP53* suggest an import role of cell cycle genes in PTCL-NOS [86].

Loss of *PTEN* was associated with germinal center B-cell-like (GCB) DLBCL, but not in activated B-cell-like (ABC) DLBCL[89], and has been identified as a PI3K/AKT-dependent GCB-DLBCL subtype[90] which could be targeted by a PI3K inhibitor as a promising therapeutic approach. Even though then deletion of 10q has rarely been reported in cytogenetic studies in T-cell lymphoma[91,92], recurrent losses of 10q encompassing *PTEN* have been detected in 28% PTCL-NOS (10/36), with 50% patients were at relapsed stage[88], suggesting the inferior prognosis of heterozygous loss of *PTEN*. This was supported by other studies, of which observed heterozygous loss of *PTEN* occurs frequently in many advanced-stage of solid tumors, such as glioblastomas (70%) and in advanced prostate cancers (60%)[93]. The phosphatase and tensin homolog deleted on chromosome 10 (*PTEN*) tumor suppressor, is a phosphatase that can act on both polypeptide and phosphoinositide substrates. Structural and mutational studies revealed that PTEN consists of five functional domains, including a phosphatidylinositol-4-5-bisphosphate-binding domain (PBD), a phosphatase domain, a C-terminal domain (C2-domain), a C-terminal tail and a PDZ-binding motif (PDZ BD)[94]. Compared to other types of cancer in which the mutational hotspot is located in exon 5 encoding the phosphatase domain, however, *PTEN* point mutations were enriched almost exclusively in exon 7, which encodes part of the C2-

domain and results in protein truncation and rapid degradation in T-ALL[95,96]. In contrast to tumors affected by point mutations, the phosphatase domain-coding exons 2-6 are targeted by genomic deletions. The unique PtdIns (3,4,5)P3 lipid phosphatase activity of PTEN that antagonizes phosphatidylinositol 3-kinase (PI3K) signaling makes it one of the most important tumor suppressors, regarded as the second guardian of the genome[97]. Following *PTEN* loss, the accumulation of PIP3 at the plasma membrane recruits and activates AKT family members which further stimulate mTORC1, resulting in phosphorylation of S6K and 4EBP1. As a consequence of *PTEN* inactivation, the elevated transcription and translation events in the gene network of the PI3K-AKT-mTOR pathway promote cell growth, proliferation, survival and metabolism, and further breaks down the balance of cell homeostasis[94].

As the molecular and genetic understanding of PTCL-NOS deepens (Figure 5), an increasing number of subtypes of PTCL-NOS will be further identified along with well-characterized morphological, biological and clinical features. Therefore, deciphering the genetic and biologic basis of PTCL-NOS is urgent to link the mechanisms of tumorigenesis and stratification patients to efficient targeted therapy.

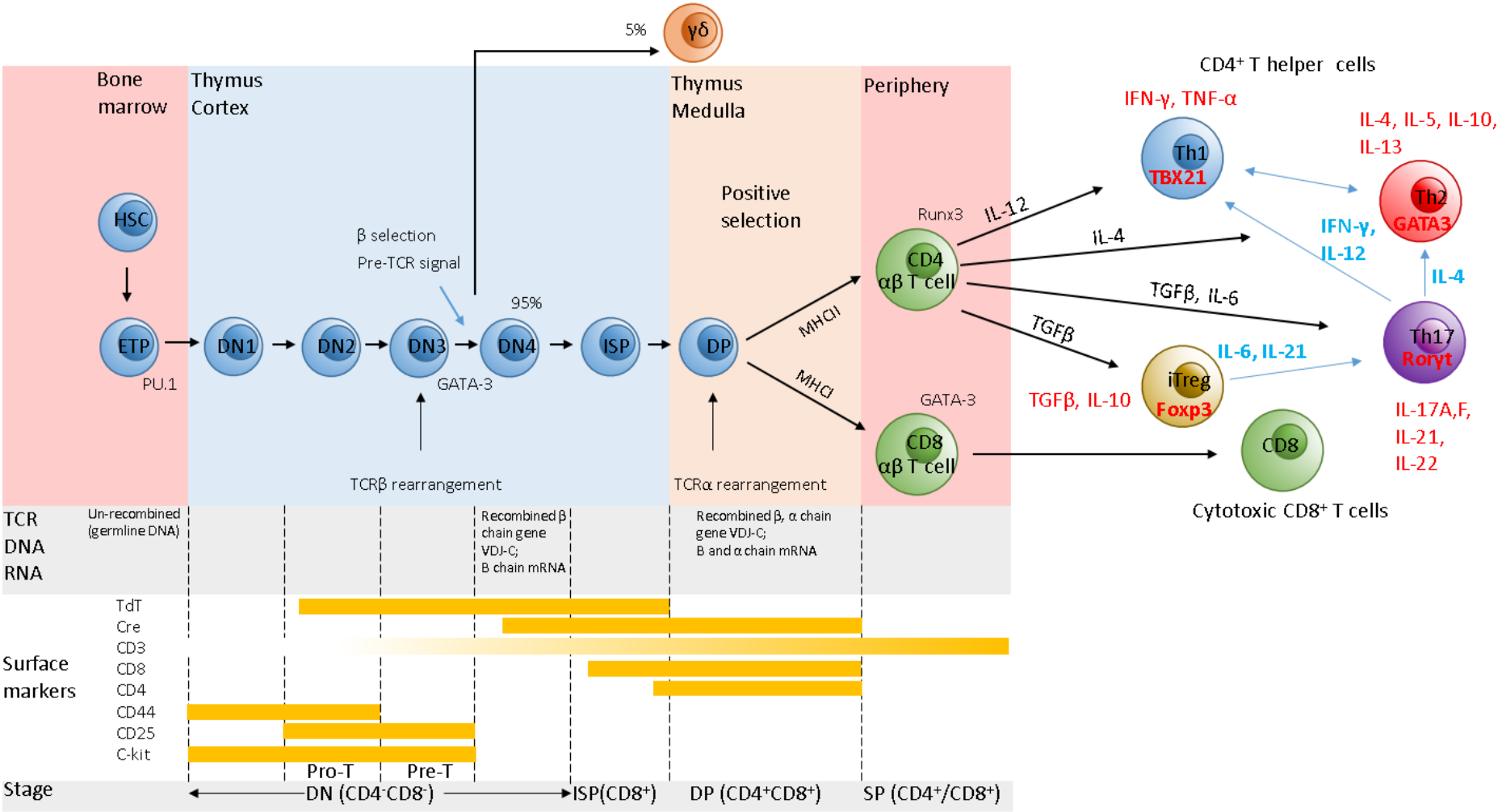
5%
γδ
Bone marrow
Thymus Cortex
Thymus Medulla
Periphery
Positive selection
HSC
β selection
Pre-TCR signal
95%
ETP
DN1
DN2
DN3
DN4
ISP
DP
PU.1
GATA-3
TCRβ rearrangement
TCRα rearrangement
MHCII
MHCI
Runx3
CD4 αβ T cell
GATA-3
CD8 αβ T cell
IL-12
IL-4
TGFβ, IL-6
TGFβ
TGFβ, IL-10
CD4+ T helper cells
IFN-γ, TNF-α
Th1
TBX21
IL-4, IL-5, IL-10, IL-13
Th2
GATA3
IFN-γ, IL-12
IL-4
iTreg
Foxp3
IL-6, IL-21
Th17
Rorγt
IL-17A,F, IL-21, IL-22
CD8
Cytotoxic CD8+ T cells
TCR DNA RNA
Un-recombined (germline DNA)
Recombined β chain gene VDJ-C; B chain mRNA
Recombined β, α chain gene VDJ-C; B and α chain mRNA
Surface markers
TdT
Cre
CD3
CD8
CD4
CD44
CD25
C-kit
Stage
Pro-T
Pre-T
DN (CD4-CD8-)
ISP(CD8+)
DP (CD4+CD8+)
SP (CD4+/CD8+)

Figure 1: T cell development and differentiation

T cell development begins in the thymus as early precursor thymocytes (EPTs) after travel out from bone marrow. The precursor thymocytes have still kept the capability to differentiate into B-, Myeloid-, NK- and dendritic lineage until they reach to DN3 stage when it committed to T cell lineage, which allows ETPs bypass of either the β selection checkpoint or differentiation into γδ T cells. Followed by α gene rearrangement at DN4 stage, as well as positive and negative selection upon TCR binding to MHC molecules, surviving single positive (SP) T cells travel to peripheral, differentiate into either $CD4^+$ T helper (Th) cells or cytotoxic $CD8^+$ T cells. Transcription factors (TFs) regulate T cell development at multipotent progenitor state as indicated above, such as PU.1, GATA3, and Runx3. Upon T-cell receptor (TCR) signaling activation, along with costimulatory signal and cytokine stimulation, naïve $CD4^+$ T cells differentiated into distinct effector subtypes that have critical roles in mediating immune response through the secretion of specific cytokines.

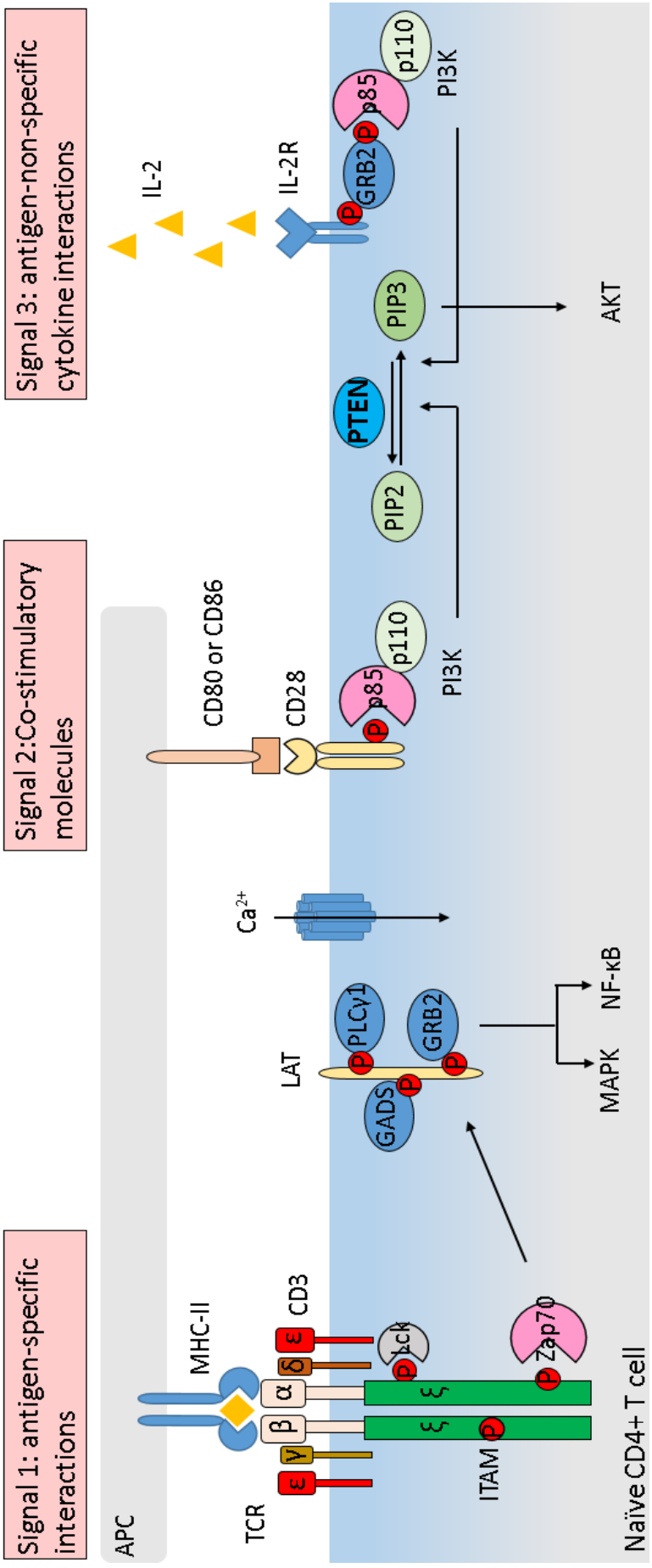
Signal 1: antigen-specific interactions
Signal 2:Co-stimulatory molecules
Signal 3: antigen-non-specific cytokine interactions
APC
MHC-II
TCR
CD3
ε
δ
α
β
γ
ε
ζ
ζ
ITAM
P
Lck
P
Zap70
P
Ca2+
LAT
PLCγ1
GRB2
GADS
MAPK
NF-κB
CD80 or CD86
CD28
p85
p110
PI3K
PIP2
PTEN
PIP3
AKT
IL-2
IL-2R
GRB2
p85
p110
PI3K
Naïve CD4+ T cell

Figure 2: Overview of the T-cell activation signaling pathways

T cell receptor (TCR) signal transduction is initiated by recognizing self or foreign antigens presented by major histocompatibility complex (MHC) molecules, which is the first signal required in T cell activation. Engagement of the TCR triggers a cascade of phosphorylation events through the formation of multi-molecular signalosomes. Major molecules involving in this process include LCK, ZAP-70, LAT, PCLγ1, GADS, and GRB2, which leads to the subsequent activation of multiple distal signaling pathways, such as $Ca2^{+}$-calcineurin-NFAT, mitogen-activated protein kinase (MAPK) and nuclear factor-κB (NF-κB) signaling pathway. Co-ligation of CD28 to CD80 (B7-1) or CD86 (B7-2) present on APCs augment TCR signals, thus promoting cell proliferation through one key downstream effector PI3K mediated activation of PI3K-Akt-mTOR signaling pathway. The third signal is delivered by combinations of cytokines which initiating the downstream signaling cascade to enhance cell expansion and differentiation. Upon IL-2/IL-2R ligation, the recruitment of Grb2 complex with PI3K which further leads to the phosphorylation of mTOR and Akt.

Figure 3: Lymphoma classification

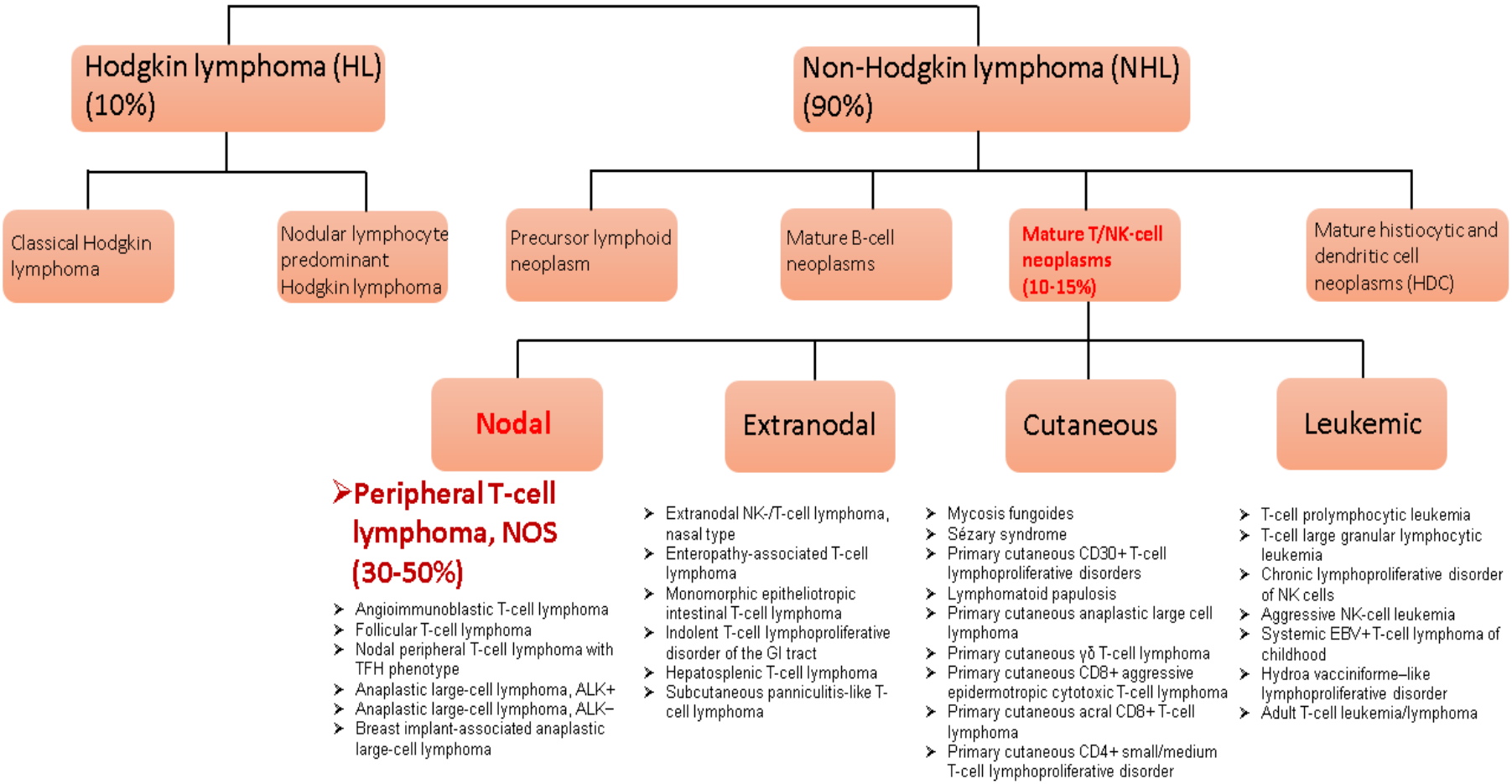
Hodgkin lymphoma (HL) (10%)
Non-Hodgkin lymphoma (NHL) (90%)
Classical Hodgkin lymphoma
Nodular lymphocyte predominant Hodgkin lymphoma
Precursor lymphoid neoplasm
Mature B-cell neoplasms
Mature T/NK-cell neoplasms (10-15%)
Mature histiocytic and dendritic cell neoplasms (HDC)
Nodal
Extranodal
Cutaneous
Leukemic
Peripheral T-cell lymphoma, NOS (30-50%)
Angioimmunoblastic T-cell lymphoma
Follicular T-cell lymphoma
Nodal peripheral T-cell lymphoma with TFH phenotype
Anaplastic large-cell lymphoma, ALK+
Anaplastic large-cell lymphoma, ALK–
Breast implant-associated anaplastic large-cell lymphoma
Extranodal NK-/T-cell lymphoma, nasal type
Enteropathy-associated T-cell lymphoma
Monomorphic epitheliotropic intestinal T-cell lymphoma
Indolent T-cell lymphoproliferative disorder of the GI tract
Hepatosplenic T-cell lymphoma
Subcutaneous panniculitis-like T-cell lymphoma
Mycosis fungoides
Sézary syndrome
Primary cutaneous CD30+ T-cell lymphoproliferative disorders
Lymphomatoid papulosis
Primary cutaneous anaplastic large cell lymphoma
Primary cutaneous γδ T-cell lymphoma
Primary cutaneous CD8+ aggressive epidermotropic cytotoxic T-cell lymphoma
Primary cutaneous acral CD8+ T-cell lymphoma
Primary cutaneous CD4+ small/medium T-cell lymphoproliferative disorder
T-cell prolymphocytic leukemia
T-cell large granular lymphocytic leukemia
Chronic lymphoproliferative disorder of NK cells
Aggressive NK-cell leukemia
Systemic EBV+ T-cell lymphoma of childhood
Hydroa vacciniforme–like lymphoproliferative disorder
Adult T-cell leukemia/lymphoma

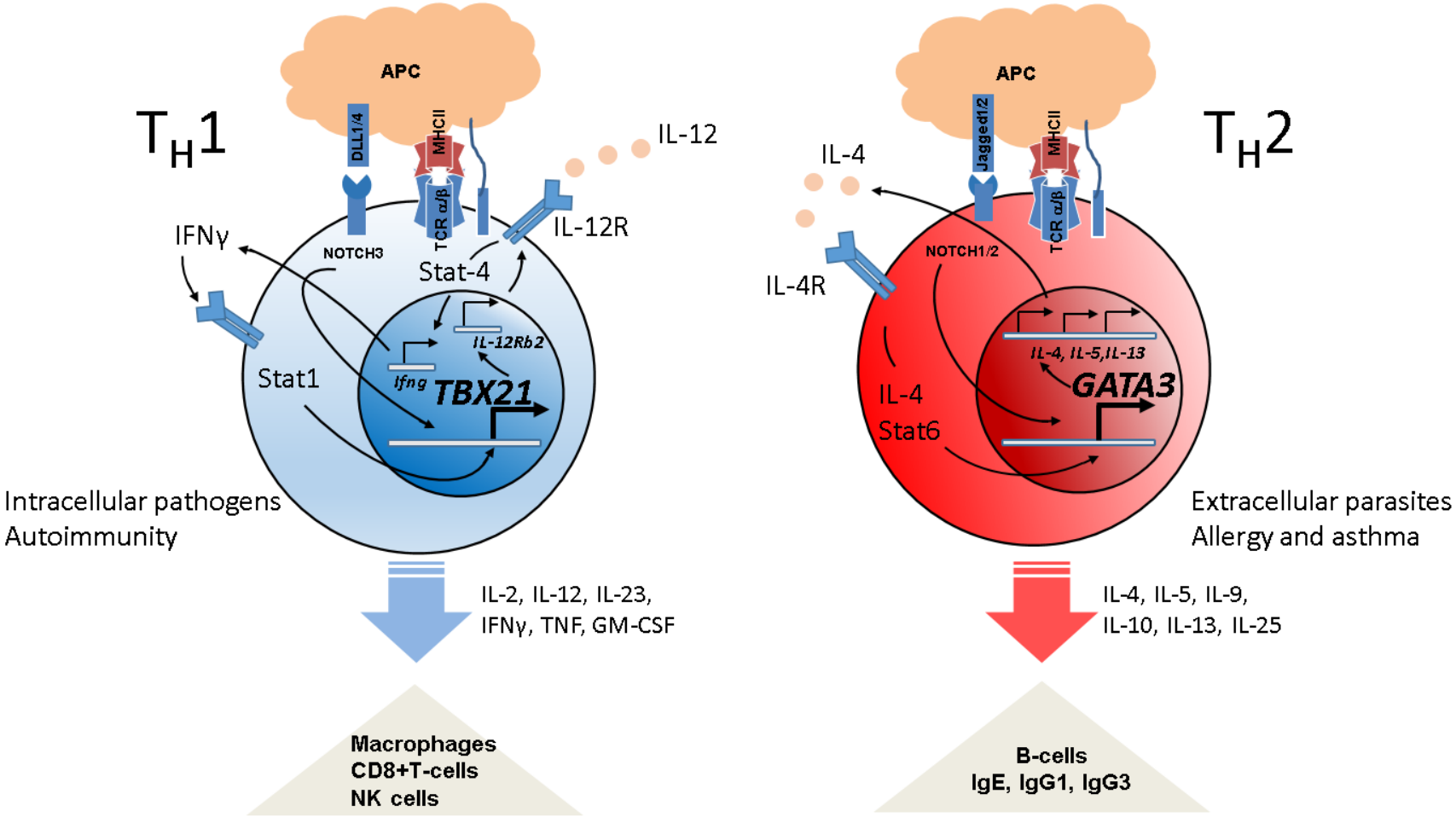
T_H1
APC
DLL1/4
MHCII
TCR α/β
IL-12
IL-12R
IFNγ
NOTCH3
Stat-4
IL-12Rb2
Stat1
Ifng
TBX21
Intracellular pathogens
Autoimmunity
IL-2, IL-12, IL-23,
IFNγ, TNF, GM-CSF
Macrophages
CD8+T-cells
NK cells
T_H2
APC
Jagged1/2
MHCII
TCR α/β
IL-4
IL-4R
NOTCH1/2
IL-4, IL-5,IL-13
GATA3
IL-4
Stat6
Extracellular parasites
Allergy and asthma
IL-4, IL-5, IL-9,
IL-10, IL-13, IL-25
B-cells
IgE, IgG1, IgG3

Figure 4: The lineage differentiation of T helper cells

Differentiated $CD4^+$ T cells can adopt alternate expression profiles and produce cytokines that are associated with alternate T cell lineages, such as Th1, and Th2 cells. TBX21 and GATA3 are the master transcriptional factors (TFs) that regulate the polarization response. Interleukin 12 (IL12) and interferon γ (IFNγ) induces the downstream signaling cascade to develop Th1 cell. Upon binding to IL-12 receptor, IL-12 signaling results in Stat4 mediated increase of Ifng expression. Binding of the IFNγ to its receptor further initiates Stat1 mediated promotion of transcription of TBX21, which initiates the Th1 differentiation program. On the contrast, IL-4 receptor signaling strongly promotes Stat6 mediated GATA3 transcription. GATA3 reorganizes chromatin structure in the Th2 locus, encompassing the IL-4, IL-5, and IL-13 genes, which increase their transcription competence. The increased production of IL-4 further enhances Th2 program by a positive feedback loop. The combination cytokines secret by Th1 cells are necessary for protection from intracellular bacterial infections and autoimmunity. Cytokines produced by Th2 cells are essential for the clearance of extracellular pathogens and the pathological allergic responses.

Figure 5: Evolution of molecular analysis techniques

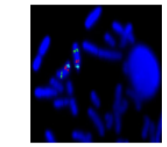

Fluorescent *in situ* hybridization(FISH):

- ✓ Detect specific DNA sequences.
- ✓ Metaphase chromosomes or interphase nuclei ;
- ✓ Fluorescent probes;
- ✓ Binds to parts of the chromosome with sequence complementarity;

1982

1992

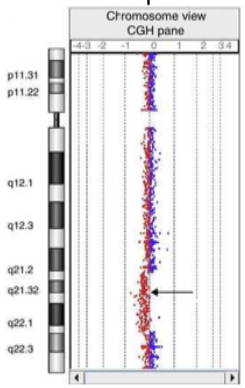

Array-based comparative genomic hybridization(aCGH)

- ✓ Whole genome chromosomal rearrangements;
- ✓ 10-15 times higher resolution than FISH;
- ✓ DNA; No needs for metaphase chromosomes;
- ✓ Low resolution.

2000

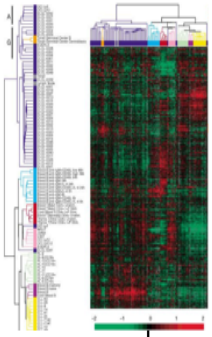

Gene expression profiling (GEP)

- ✓ Transcription level;
- ✓ Measure thousands of genes at a time;
- ✓ How cells function under specific circumstances

2003

Next generation sequencing (NGS)

- ✓ Single nucleotide changes;
- ✓ Massively parallel sequencing;
- ✓ Ultra-high throughput and speed;

2006

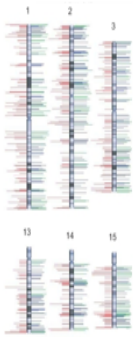

Copy number variation (CNV)

- ✓ DNA segment of one kb;
- ✓ Duplications, deletions, translocations, and inversions of one or more genes;
- ✓ High resolution.

Chapter 2 Genetic drivers and oncogenic pathways in PTCLs

Introduction

Peripheral T-cell Lymphoma (PTCL) consists of numerous distinct disease entities and is currently diagnosed using a complex and often fragmented diagnostic system with a combination of clinical, morphologic and immune-phenotypic features together with selected molecular assays[48,58]. The diagnosis of many cases is challenging even among expert hematopathologists, due to the wide spectrum of morphologic features and the lack of robust immunohistochemical markers, and more than a third of the cases cannot be further classified and are designed as peripheral T-cell lymphoma not otherwise specified (PTCL-NOS)[50,57]. Thus, this entity includes a mixed group of nodal and extra-nodal mature T-cell lymphomas that do not correspond to any of the defined T-cell entities in the WHO classification[57,98]. The clinical outcome of PTCL-NOS is highly variable, but overall aggressive, with a 5-year overall survival (OS) of 20-30%[99]. The introduction of new regimens, such as Pralatrexate[51], Romidepsin[100], Brentuximab vedotin[101] and Alemtuzumab[102] has not shown any major benefit and novel therapeutic targets need to be deciphered to improve the clinical outcomes of these patients.

Based on the gene expression profile (GEP), unsupervised hierarchical clustering of PTCL-NOS identified two novel molecular subgroups with biological meaning by Iqbal[67,103]. One subgroup, representing 33% of PTCL-NOS, is characterized by a high expression of *GATA3* and its target genes. *GATA3* is the master transcriptional regulator involved in Th2 cell differentiation, during which it controls

interleukin-4 (IL-4), IL-5, and IL-13 expression[104]. This subset of patients showed a significant association with poor OS[67]. The other subgroup, representing 49% of PTCL-NOS, had a high expression of *TBX21* and its target genes. *TBX21* is a master regulator of Th1 cell differentiation and cont rols the expression of the IFNγ[105] as well as the function of $CD8^+$ cytotoxic cells. Peripheral T-cell lymphomas (PTCL) are rare tumors derived from mature T-lymphocytes with different functional properties such as cytotoxic, helper, regulatory and follicular helper, and NK cells. However, it is not clear whether the two major subtypes of PTCL-NOS represent tumors derived from Th1 and Th2 cells regarding specific genomic defects, respectively. Naïve $CD4^+$ T cell with mTOR deficiency fails to differentiate into Th1 or Th2 due to failure of activation of specific STAT transcription factors[106], as for STAT4 for Th1 and STAT6 for Th2 differentiation. This could also be explained by the fact that the translation of *GATA3* could be enhanced through PI3K/mTOR axis[107]. Further evidence showed that Pten-deficient T cells could have a Th2 bias and that appropriate regulation of PI3K signaling is important for balancing effector cell differentiation in the periphery[108].

Genomic heterozygosity of PTCL-NOS has been delineated by array-based comparative genomic hybridization (CGH), as it represents the most common peripheral T-cell lymphomas (PTCL). For instance, losses of 5q10q/12q characterized by frequent expression of CD5, but negative for cytotoxic markers Granzyme B and TIA1 ($P<0.05$) due to the amplification of chromosome 12p13 in been observed in 53.3% (16/30) PTCL-NOS cases. This distinct group displayed a better survival compared to

cases without these alterations, indicating that PTCL-NOS should not be regarded as a “wastebasket” category, but comprises several distinct subtypes of mature T-cell malignancies on the basis of unique genetic profiles. Frequent recurrent gains were found on chromosome 7q22 (31-33%) and 8q24 (20-22%), losses of 6q (26-31%), 9p21 (30-31%), 13q21 (30-36%). Other genomic imbalances were detected significantly more often in PTCL-NOS than other T-cell entities, including gains of 1q, 3p, 5p, 17q, 22q, and losses of 5q, 10p, 10q, 12q. However, no well-characteristic genetic alterations have been identified so far due to the heterogeneous of PTCL-NOS and the small number of cases of the reported studies.

In this study, we investigated the genetic basis of PTCL-NOS using a combination of copy number variations (CNVs) and targeted sequencing and identified the distinct chromosomal abnormalities pattern in PTCL-GATA3 and PTCL-TBX21 subtypes with co-deletion of *TP53* and *PTEN* were frequently affects PTCL-GATA3. In addition, we identified $TP53^{R172H}$ mutation as the hotspot mutation in PTCL-GATA3. Therefore, the activation of PI3K-Akt-mTOR signaling in the absence of *PTEN* and dysregulation of the *TP53* pathway through *TP53* mutation in PTCL-GATA3 could be partially inhibited by PI3K inhibitors, suggesting a potential therapeutic option for these patients.

Results

Genetic basis of PTCL-NOS

Here we performed DNA copy number analysis on 21 cases of PTCL-NOS through the OncoScan™ platform on genomic DNA isolated from fresh-frozen (FF) and formalin-fixed, paraffin-embedded (FFPE) tissue. Specimens from FF were obtained from two consortiums including the International PTCL Project (IP-PTCL) and the Lymphoma and Leukemia Molecular Profiling Project (LLMPP). Patients had been diagnosed with PTCL-NOS between the years 2006-2015. Specimens from FFPE were obtained from Milan/Bologna University School of Medicine, Bologna. The classification of PTCL-NOS into PTCL-GATA3 (n=11) and PTCL-TBX21 (n=10) subtypes were performed using a robust molecular gene expression signatures based on previous GEP study[67].

Next, we determined the copy number variations (CNVs) by employing Nexus Express for OncoScan 3 program, an algorithm designed to estimate copy number frequencies by calculation of B-allele frequency (BAF) from the whole-genome view using data derived from the OncoScan™ platform. We found CNVs deviating from the diploid state of normal tissues in each chromosome in our cases represented by the

OncoScan™ platform. Overall, 100% penetrate of genetic imbalances were observed in PTCL-NOS (Figure 6A). In the previous study, chromosome gain of 7q22 (31-33%)[84,88] and 8q24 (20-22%)[84,87] were frequently observed in PTCL-NOS, but not in AITL or ALCL. Consistently, we observed chromosome gains mainly involved 7q22 (29%) and 8q24 (29%) (Figure 6B). Chromosome 7 gain has been reported as one of the repeated genomic events in glioblastoma multiforme[109], astrocytoma[110], and colorectal cancer[111], strongly correlates with inferior survival. Gains of material on chromosome 7q were identified in 1/3 of the PTCL-NOS[84]. The amplification of chr 7 is a common lesion in malignant neoplasms, even though no specific locus has been correlated with tumorigenesis in lymphoma or other types of cancer, it is usually regarded as a common secondary genetic lesion caused by other genomic abnormalities and results in an increased risk of tumor recurrence and disease progression[110,112]. 8q gain has been demonstrated to be an independent predictor of poor survival and associated with metastases in solid tumors, such as prostate cancer (29.6%-59.9%)[113,114], gastric carcinoma (18.2%)[115], and clear cell renal cell carcinoma (CCRCC) (8.3%)[116], as well as in blood malignancies, including adult acute myeloid leukemia (AML) (10%)[117] and splenic marginal zone B-cell lymphomas (8.8%)[118]. *MYC* up-regulation and/or translocation in B-cell neoplasms associated with aggressive clinical behavior were well documented. Frequent genomic alterations in 8q encompassing *MYC* oncogene amplification at 8q24.21 (28.6%) (Figure 6B) suggest MYC as the potential driver alterations in the underlying molecular pathogenesis

contributes to the development of malignancy. Other genomic amplification regions involved in 11q13.3 (14%), 14q32.2 (14%), 17q (24%) have been observed in our cohort (Figure 6B). Interestingly, we observed chr17q (24%) encompassing *STAT3* locus at 17q21.2 is highly penetrated in our cohort (Figure 6B). *STAT3* constitutively activates NF-κB signaling in ABC-DLBCL has been demonstrated[119] and frequently mutated *STAT3* in 22% adult T-cell leukemia/lymphoma without chromosomal abnormality has been detected in a 414-patients cohort study[120]. Highly amplification of *MYC* and *STAT3* in PTCL-NOS but not in other types of lymphomas, indicating the unique characteristic of this lymphoma entity and may contribute to the development of malignancy.

With regard to chromosomal losses, chr9p (19.0%), chr10q (23.8%) and chr17q (33.3%) were among the most frequent abnormalities besides the loss of chr8p, which accounts for 43% of the cases. 8p losses were found in 79% (15/19) leukemic mantle cell lymphoma, harboring a common segment 8p21-p23 and indicating poor prognosis[121]. However, no specific frequent gene copy gain was detected in this specific region or other PTCL-NOS studies, suggesting the structural deletion served as secondary genetic events caused by other genomic alterations. Consistent with other studies[84,87,122], the well-known tumor suppressors *TP53* located on 17p13.1, *PTEN* located on 10q23.31 and *CDKN2A* located on 9p21.3 were frequently affected by gene copy loss in human cancer, respectively, suggesting these genetic lesions contributes the inferior prognosis in PTCL-NOS.

The recurrent deletion was detected on chromosome 17p, with a minimally overlapping region at chr17p12-13.1 in 33.3% PTCL-NOS (Figure 6B). *TP53*, the guardian of the genome, spans 19114bp includes 11 exons on chromosome 17p13.1[81]. The coding sequence (CDS) from exons 2 to 11, which is translated into the canonical product of p53 consisting of 393 amino acids with several functional domains and motifs[81]. The deletion of *TP53*, an extensively studied tumor suppressor gene that is considered to be the major driver of 17p loss[123], has been highly detected in solid tumors, but relatively low in lymphoid malignancies[81,124]. Nevertheless, consistent with one of the recent studies, in which *TP53* deletion has been observed with a high incidence in 28% PTCL-NOS accompany with 13% focal deletion of *CDKN2A*, another tumor suppressor located at 9p21.3. *CDKN2A* loss has been observed in 19.0% PTCL-NOS in our cohort (Figure 6B), and with a penetrance of 30%-31% in PTCL-NOS in previous studies[87,88]. In activated B-cell (ABC) DLBCL, *CDKN2A* deletions and multiple genomic alterations of genes involved in the antiapoptotic nuclear factor-κB (NF-κB) signaling pathway indicating the specific DLBCL subgroups and bear potential prognostic value[89]. However, the incidence of *CDKN2A* loss has been revealed no differences between PTCL-NOS and AITL, irrespective of other chromosomal abnormalities[87], suggesting the prognostic value of *CDKN2A* status, but probably not the driving force in pathogenesis of PTCL-NOS.

Furthermore, recurrent deletions on chromosome 10q, with a minimally overlapping region at 10q22.2-q26.3 (24%) has been also observed in our cohort

(Figure 6B). The tumor suppressor *PTEN* is located at chromosomal band 10q23.3, a locus that is highly susceptible to aberrant genetic alterations in primary human cancers has been demonstrated to have an important role through negatively regulation of PI3K-Akt-mTOR signaling pathway in T cell development, activation and homeostasis by modulating the expression of survival and mitogenic facters[108,125]. *PTEN* loss defines a PI3K/AKT pathway-dependent GCB-DLBCL, and selectively toxic to PI3K inhibitor compare to PTEN-positive cells lines[90], suggesting therapeutically potential in stratifying patients according to their *PTEN* status. Losses of 10q23-24 have been reported in 28% of PTCL-NOS[88] in one study, which has a lower penetrance compare to our cohort, with 23.8% recurrent deletion has been detected. The significant-high penetrance of *PTEN* deletion further highlights the role of PI3K-Akt-mTOR signaling pathway in the pathogenesis of PTCL-NOS as well as the prediction of prognosis.

Recurrent chromosomal imbalances are highly discordant between PTCL-GATA3 and PTCL-TBX21

Due to the poor understanding of the cellular origin and the genetic and molecular pathogenesis of PTCL-NOS subtypes, we specifically compared the genomic lesions between PTCL-GATA3 and PTCL-TBX21 subgroups. As we expected, PTCL-GATA3 had more pronounced genomic aberration compared to PTCL-TBX21 (Figure 7A B), suggesting the complex genomic imbalance in PTCL-GATA3 contributes to its pathogenesis, clinical aggressiveness and poor response to clinical therapy.

Genomic imbalances predicting poor prognosis were specifically detected significantly more often in PTCL-GATA3 than PTCL-TBX21 (Figure 7B), including gains of chr7q, chr8q, chr17q (54.5% versus 0%, P=0.0124; 45.5% versus 10%, P=0.1486; 45.5% verse 0% P=0.0351), and losses of chr9p, chr10q, chr13q, chr17p (36.4% versus 0%, *P*=0.0902; 45.5% versus 10%, *P*=0.1486; 36.4% verse 0% *P*=0.0902, 54.5% verse 10% *P*=0.0124). With recurring amplification of chr8q encompassing oncogene *MYC* and frequently losses of chr17p, chr10q and chr9p, containing tumor suppressor *TP53*, *PTEN* and *CDKN2A* particularly in PTCL-GATA3, we further demonstrated PTCL-GATA3 and PTCL-TBCX21 are distinct entities due to the remarkable different genetic imbalance in these two subtypes, which also explained the genetic basis of the inferior prognosis in the PTCL-GATA3 subtype.

In contrast, gains on 5 (5q34-q35), 11 (11q13.3), 14 (14q32.2), 18 (18q11.1-q21.2) and losses on 1(1p36.11), 6 (chr6q26) were mainly detected in 30% of PTCL-TBX21, but not in PTCL-GATA3 (*P*=0.0902). Consistent with previous reports, loss of chr6q has been detected in 26-31% PTCL-NOS cases[84,88]. Among these genetic alterations, deletions of the long arm of chromosome 6 (6q) are among the most frequent chromosome aberrations in malignant T-NHLs such as adult PTCL-NOS, AITL, ALCL, T-Cell Leukemia/Lymphoma (ATCL), T-cell prolymphocytic leukemia (T-PLL), and acute lymphoblastic leukemias (ALLs)[84,126,127]. Therefore, the loss of chr6q restricted in PTCL-TBX21 but not in PTCL-GATA3 in our series provides improved diagnostic information to help stratify patients for therapy. Besides, chr8p was

predominantly lost in PTCL-TBX21 compare to PTCL-GATA3 (70% verse 18.2% *P*=0.0300). Loss of 8p is one of the most recurrently deleted genomic regions in a variety of human epithelial cancers including breast, lung, and colon cancers and governs tumor progression and drug response[128], but has been scanty reported regarding PTCL-NOS even though it has a 19% penetrance in one study[88]. Indeed, many genes located on chromosome 8p have been reported to have tumor-suppressive properties. However, none of the candidate genes fulfills the Knudson criteria for tumor suppressors[129], since no gene in the region shows an SNV event that reaches the 8p deletion frequency of ~50%[128,130]. The significant high level of 8p loss in PTCL-TBX21 compare to PTCL-GATA3 in our series emphasized consideration of the prognostic potential of this lesion specifically in this subtype.

A distinct molecular subtype characterized by *TP53* and *PTEN* alterations in PTCL-GATA3

Based on the distinct genomic alteration patterns identified in PTCL-NOS subgroups, we next enlarged the sample size to reach the largest cohort of molecularly classified PTCL-NOS (n=61) based on our knowledge, comprising of PTCL-GATA3 (n=31) and PTCL-TBX21 (n=30) subgroups. Highly concordant with the above observation, the overall frequency of genetic imbalance was detected significantly more often in PTCL-GATA3 than PTCL-TBX21 (Figure 7C). For instance, the most frequent gains on 8q and 17q were highly enriched in PTCL-GATA3 compare to PTCL-TBX21, which encompasses *Myc* (52% verse 13%) and *STAT3* (35% verse 10%)

(Figure 7C). The most frequent losses in PTCL-GATA3 compare to PTCL-TBX21 were detected on 17p, 10q, 9q, containing three well-known tumor suppressor (TS) genes *TP53* (58% verse 7%), *PTEN* (35% verse 3%) and *CDKN2A* (45% verse 7%) (Figure 7C), respectively.

Strikingly, co-inactivation of *TP53* and *PTEN* were detected in 29% (9/31) PTCL-GATA3 (Figure 8A B C). Co-deletion of *TP53* and *PTEN* conferred the inferior prognosis to PTCL-GATA3 (*P*=0.0147) as well as total PTCL-NOS (*P*=0.0048) compare to patients without *TP53* and *PTEN* co-alterations (Figure 9A B). Even though the co-deletion of *TP53* and *PTEN* has been widely observed in solid tumors, such as triple-negative breast cancer[131], high-grade astrocytoma[132], high grade glioma[133,134], prostate cancer[135], it has been rarely reported in blood malignancies. To our knowledge, we were the first to report the co-occurrence of *TP53* and *PTEN* in PTCL-NOS, especially only in PTCL-GATA3. Further comparison of *TP53; PTEN* copy loss status among different T-cell lymphoma subtypes in our series confirmed the high incidence of these genomic alterations specifically in PTCL-GATA3 (Figure 8E). Deregulation of p53 and PI3K-Akt-mTOR pathways in PTCL-GATA3 most probably contributes to the genetic basis of pathogenesis of the disease, pinpointing the therapeutic value of PI3K inhibitor in *PTEN* deleted patients since *TP53* deletion is not targetable partially due to the fact that the use of WT-*TP53* activators is the acquisition of *TP53* mutations during treatment[136].

$p16^{INK4A}$ and $p14^{ARF}$ ($p19^{ARF}$ in mice) encoded by *CDKN2A*, have been linked to each of the two major tumor suppressor pathways in human carcinogenesis[137]. $p16^{INK4A}$ inhibits CDK4/6 in the RB1 pathway, whereas $p14^{ARF}$ interacts with the p53 pathway by targeting MDM2[138], leading to the arrest of the cell cycle in G1 phase and effectively blocking entry into S phase. *TP53* and *CDKN2A* are frequently co-inactivated in human cancers, including PTCL-NOS, which results in chromosomal instability and conferred an adverse prognostic impact[73]. Consistently with the previous reports[73,122], co-deletion of *TP53* and *CDKN2A* were found in 35% (11/31) PTCL-GATA3 in our cohort (Figure 8 A B C). Patients carrying co-deletion of *TP53* and *CDKN2A* had significant inferior survival compared with patients without co-deletion of *TP53* and *CDKN2A* in PTCL-NOS (*P*=0.0122), or within PTCL-GATA3 subgroup (*P*=0.0375) due to the activation of both RB and p53 pathways (Figure 9 C D).

Triple-deletion of *TP53; PTEN; CDKN2A* has been detected in 23% verse 0% in PTCL-GATA3 and PTCL-TBX21 (Figure 8A C). Patients carrying triple genetic alteration of *TP53; PTEN; CDKN2A* had a poor prognosis compared to cases without triple-deletion either within PTCL-GATA3 subtype (*P*=0.0007), or in the total PTCL-NOS (*P*=0.0001) (Figure 9E F). The genomic alterations of *TP53*, *PTEN,* and *CDKN2A* genes were further validated within the aberrant recurrent loci in PTCL-GATA3 by NanoString Cancer CNV analysis (Figure 8D).

$TP53^{R175H}$ mutation contributes to the dysfunction of *TP53* signaling in PTCL-GATA3

On the basis of the above results, we carried out targeted sequencing on 28 molecularly diagnosed PTCL-NOS (PTCL-GATA3, n=17; PTCL-TBX21 n=11) at the genomic aberrant loci with a custom panel covering 334 most frequent mutated lymphoma associated genes with a mean depth of 268-fold coverage for the coding regions.

In PTCL-NOS, both GATA3 and TBX21 subgroups harboring *TP53* mutation, with a frequency rate of 29.4% (5/17) and 9.1% (1/11), respectively. Deletion of 17p encompassing the *TP53* locus was seen in 100% of the *TP53* mutated cases in PTCL-GATA3, but the deletion of 17p was not associated with *TP53* mutation in PTCL-TBX21 (Figure 10A). Interestingly, either *PTEN* or *CDKN2A* mutation has not been detected in any of these cases. We found *TP53* mutations in 5 of 17 (29%) PTCL-GATA3, including missense mutation (60%, 3/5) and frameshift deletion/splicing (40%, 2/5) involved in DNA binding and tetramerization domains (Figure 10B), suggesting the structural abnormalities and deregulation of the *TP53* pathways may be driven by *TP53* mutation in *TP53* deleted cases. The p53 pathway is commonly dysregulated in more than 50% of all types of cancer caused by *TP53* mutation[139]. Interestingly, *TP53* mutation has been rarely reported in lymphoid malignancies, especially in T-cell lymphoma entities. As it has been well-established that the majority of p53 mutations in hematologic malignancies are point mutations[81] and 79.9% of which are missense mutations most frequently at codons 248, 273 and 175[80], similar distribution pattern has been observed in our series. Missense mutations were identified in the majority

(60%) PTCL-GATA3, affecting codons at R175H, V274D, V274L. Hotspot *TP53*^{R175H} mutation was identified in 67% (2/3) of the cases in this subgroup (Figure 10B). In contrast, 1 of 11 (9%) PTCL-TBX21 harboring *TP53* missense mutation at codon Y236H accompany with the splicing site, however, no correlation of copy loss was identified.

Co-alteration of heterozygous loss of *TP53* and *PTEN* was significantly high, which accounts for 26% (8/31) of total PTCL-GATA3 in our cohort, suggesting heterozygous loss of one *TP53* and *PTEN* allele is the major aberrant genomic events in this subtype, which also gives a strong rationale for considering the cooperatively and complementary role of *TP53* and *PTEN* in the pathogenesis of PTCL-GATA3. Of note, 18% (3/17) of our targeted sequenced PTCL-GATA3 harboring *TP53* mutations concomitant with *PTEN* heterozygous deletion, indicating that *TP53* is a key tumor suppressor in the PTCL-GATA3 subtype. This hypothesis is further supported by our results that the co-deletion of *TP53* and *PTEN* has not been observed in the PTCL-TBX21 subgroup (Figure 10B).

Discussion

Little is known about the genetic basis in the pathogenesis of PTCL-NOS. The distinct expression pattern identified in GEP, characterized with corresponding molecules and associated with different clinical behavior suggesting PTCL-GATA3 and PTCL-TBX21 are two distinct molecular subtypes of PTCL-NOS[67]. Therefore,

stratifying patients for diagnosis and identifying the underlying genetic basis to improve clinical therapy becomes critical to prognosis.

Unlike PTCL-TBX21, the aberrant DNA copy loss of chr17p and chr10q, as well as *TP53* mutation were significantly correlatively with PTCL-GATA3, emphasizing the importance of the co-occurrence of genetic alterations in lymphomagenesis in this unique subgroup. In our study, *TP53* abnormalities (mutation and/or heterozygous deletion) occurred in 18/31 (58%) PTCL-GATA3, but only in 2/30 (7%) PTCL-TBX21. *TP53* heterozygous deletion was more frequent than mutations and was detected in 18/31 (58%) and 5/17 (29%) cases of PTCL-GATA3 respectively, which is concordant with previous reported genetic profiles of glioma[134] and mantle cell lymphoma[140], that higher incidence of *TP53* deletion than gene mutation was observed in cancer. *TP53* mutation followed by a full penetrance of *TP53* heterozygous deletion in PTCL-GATA3 further supports the idea that *TP53* is considered to be the major driver of 17p loss and highlight its role as the driving force in the pathogenesis in PTCL-GATA3. More than 50% of human malignancies have been reported mutations and/or deletion of the *TP53* gene, and the alteration of *TP53*-dependent DNA damage response is important in the pathogenesis of most cancers. However, loss of both *TP53* alleles is not a prerequisite in tumorigenesis and progression since the majority of tumors in heterozygous animals preserved a wild-type *TP53* allele[141]. *TP53* point mutations in lymphoid malignancies occur most often in the *TP53* DNA-binding domain, most frequently at codons 248, 273, and 175, similar to the codon distribution pattern in other types of cancer[80].

Consistently, in our study, *TP53* mutation has been enriched in the DNA-binding domain (DBD), of which hotspot *TP53*^{R175H} mutation was identified in 67% (2/3) of PTCL-GATA3. *TP53*^{R175H} mutation[142] has been characterized with gain-of-function mutations, such mutation has additional functions not seen in wild-type p53 and is expected to abrogate the tumor suppressor function of the affected p53 allele[143]. *TP53* mutation is relatively rare in lymphoid malignancies (19.3%) compare to other types of cancer but still indicate an unfavorable prognosis, including in DLBCL, AML, ALL, CLL/SLL, FL, MCL and MM based on IARC database[81]. Surprisingly, we have observed a 29% penetrance of *TP53* mutation in PTCL-GATA3 in our cohort. This exclusivity is highly interesting since it raises the possibility that the consequence of dysfunction of the *TP53* signaling pathway by *TP53* mutation could be the primary genomic event involved in the pathogenesis of PTCL-GATA3.

One of the most interesting characteristics in PTCL-GATA3 is the high incidence of co-alteration of *TP53* and *PTEN*, which has been detected in 35% of the cases in this subtype. This result supports the “two-hit” concept of cancer development in which pinpoints that the gain-of-function (GOF) of *TP53* mutation is a fundamental event in the development of PTCL-GATA3, which followed by *PTEN* heterozygous deletion to activate PI3K-Akt-mTOR pathway in skewing towards PTCL-GATA3 tumorigenesis. Even though contradicting with other studies in glioma[144] which showed a high frequency of homozygous deletion of *PTEN* accompany with *TP53* alteration, the co-occurrence of heterozygous but not homozygous deletion of *TP53* and *PTEN* were

detected in 20% (8/40) glioma specimen in one study[134]. Consistently, we observed 10q chromosomal copy number abnormalities in 35% (11/31) PTCL-GATA3, of which 91% (10/11) cases were characterized with heterozygous loss of *PTEN*. Co-occurrence of genetic alterations in *TP53* and *PTEN* has been reported in several tumor types, however, no study of combined inactivation of *TP53* and *PTEN* has been reported in PTCLs based on our knowledge. Our data, therefore, is the first to identify the genetic basis of PTCL-GATA3, characterized by combined inactivation of *TP53* and *PTEN*.

However, the predominant prevalence of heterozygous deletion of *TP53* and *PTEN* in PTCL-GATA3 compared to the homozygous deletion of the two genes also leads to an alternative mechanism in which considering the heterozygous loss of *PTEN* as the primary genomic events. Complete loss of *PTEN* elicits the activation of a fail-safe response in the prostate, but one copy loss of *PTEN* might benefit from “hypomorphing' due to the bypass of fail-safe responsiveness initiated by *TP53* has been demonstrated in prostate cancer[145]. Since the heterozygous deletion of *PTEN* has never occurred simultaneously with mutations in *PTEN* genes in our series, the increased instability of genomic balance could possible inactivate the second *TP53* allele, supporting the “two-hit” concept of tumorigenesis. Therefore, the dosage is critical for *PTEN* function. With the second genomic alteration occur as a “double hit”, in our case, further loss of *TP53* function removed the fail-safe response and results in lymphomagenesis in PTCL-GATA3. In contrast, neither *PTEN* nor *TP53* copy loss

has been observed in PTCL-TBX21. Given the presence of co-deletion of *TP53* and *PTEN* in PTCL-GATA3, but not in PTCL-TBX21, it highly suggests that *TP53* and *PTEN* collaboratively play a unique role in the pathogenesis of PTCL-GATA3 subgroup.

Triple deletion of *TP53*, *PTEN*, and *CDKN2A* has an incidence of 23% in PTCL-GATA3 in our series. When tumor grade was taken into account in gliomas, a significant increase in the frequency of co-occurrence of genetic alterations in *TP53*, *PTEN* and *CDKN2A* have been detected in high-grade gliomas (HGG) than in low-grade gliomas (LGG)[134], indicating that combined alterations of tumor suppressors are involved in malignant tumor progression. Although there is a lack of information on grading for the tumors in our series, the high incidence of triple deletion of three well-known tumor suppressor genes in PTCL-GATA3 indicated a distinct molecular subtype compare to PTCL-TBX21 and association with a more advanced stage of tumor formation.

Genetic analysis demonstrated a significantly higher prevalence of *TP53, PTEN and CDKN2A* alteration in PTCL-GATA3, and heterozygous deletion was the most frequent event, suggesting an alteration of cellular homeostasis by CDKN2A/TP53 and PI3K-Akt-mTOR signaling pathways in this subtype. The initiation and progression of PTCL-GATA3 are probably a consequence of sequential genetic events, such as point mutations and copy number alterations which result in dysregulation of cellular homeostasis through different signaling pathways. Therefore, it is critical for investigation of the independent and combined alterations in *TP53* and *PTEN* tumor

suppressor genes to evaluate a possible association between our findings and clinical heterogeneous behaviors.

A

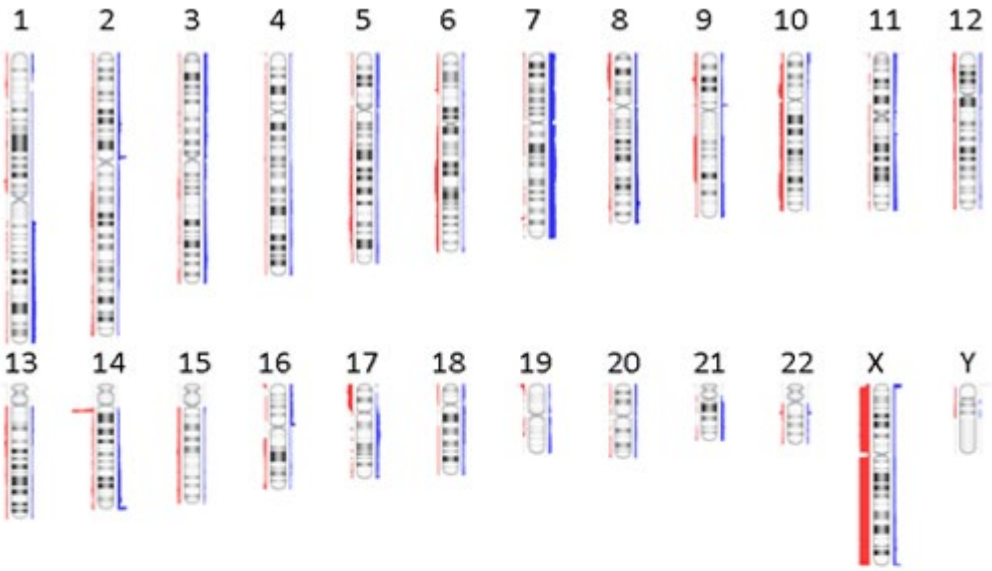
1
2
3
4
5
6
7
8
9
10
11
12
13
14
15
16
17
18
19
20
21
22
X
Y

B

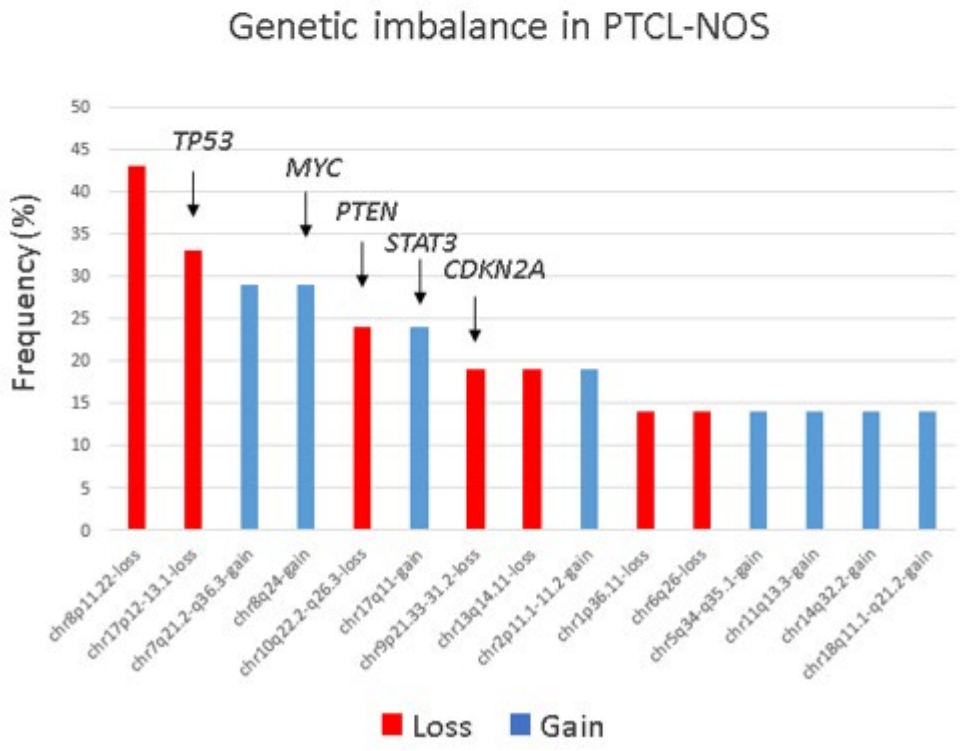
Genetic imbalance in PTCL-NOS
Frequency (%)
50
45
40
35
30
25
20
15
10
5
0
TP53
MYC
PTEN
STAT3
CDKN2A
chr6p11.22-loss
chr17p12-13.1-loss
chr7q21.2-q36.3-gain
chr8q24-gain
chr10q22.2-q26.3-loss
chr17q11-gain
chr9p21.33-31.2-loss
chr13q14.11-loss
chr2p11.1-11.2-gain
chr1p36.11-loss
chr6q26-loss
chr5q34-q35.1-gain
chr11q13.3-gain
chr14q32.2-gain
chr18q11.1-q21.2-gain
Loss
Gain

Figure 6: Summary profile of genetic gains and losses for total PTCL-NOS

(A) Ideogram of the distribution of gains and losses of genetic material detected by OncoScan™ platform and plotted by Nexus Express for OncoScan 3 program in 21 PTCL-NOS cases. Red bars to the left of the chromosomes represent areas of loss; Blue bars to the right of the chromosomes represent areas of gain. PTCL-GATA3, n=11; PTCL-TBX21, n=10. (B) Bar graph of the overall frequency of minimal overlapping region (MR) of genomic imbalances in PTCL-NOS. Red bar, loss of chromosomal material; Blue bar, gain of chromosomal material.

A

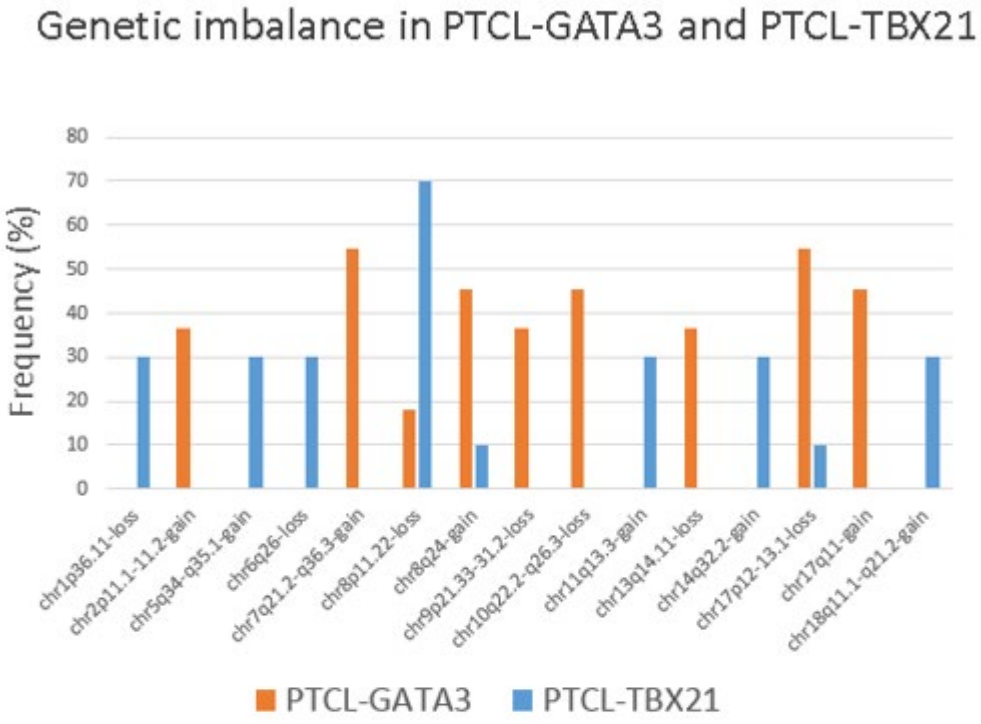
Genetic imbalance in PTCL-GATA3 and PTCL-TBX21
Frequency (%)
80
70
60
50
40
30
20
10
0
chr1p36.11-loss
chr2p11.1-11.2-gain
chr5q34-q35.1-gain
chr6q26-loss
chr7q21.2-q36.3-gain
chr8p11.22-loss
chr8q24-gain
chr9p21.33-31.2-loss
chr10q22.2-q26.3-loss
chr11q13.3-gain
chr13q14.11-loss
chr14q32.2-gain
chr17p12-13.1-loss
chr17q11-gain
chr18q11.1-q21.2-gain
PTCL-GATA3
PTCL-TBX21

B

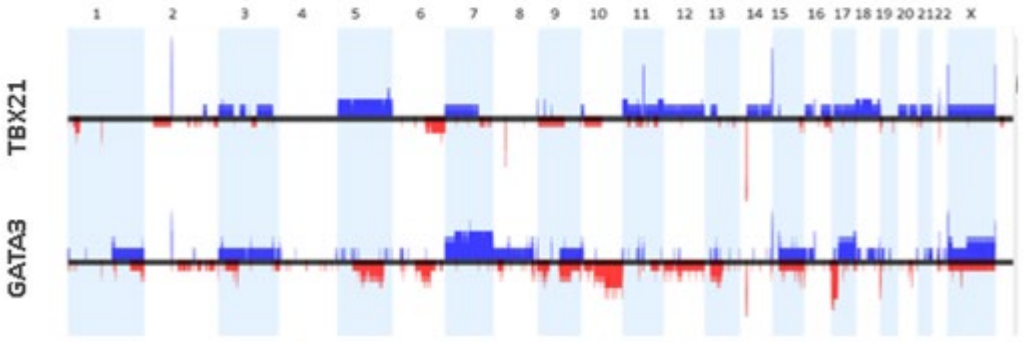
1 2 3 4 5 6 7 8 9 10 11 12 13 14 15 16 17 18 19 20 2122 X
TBX21
GATA3

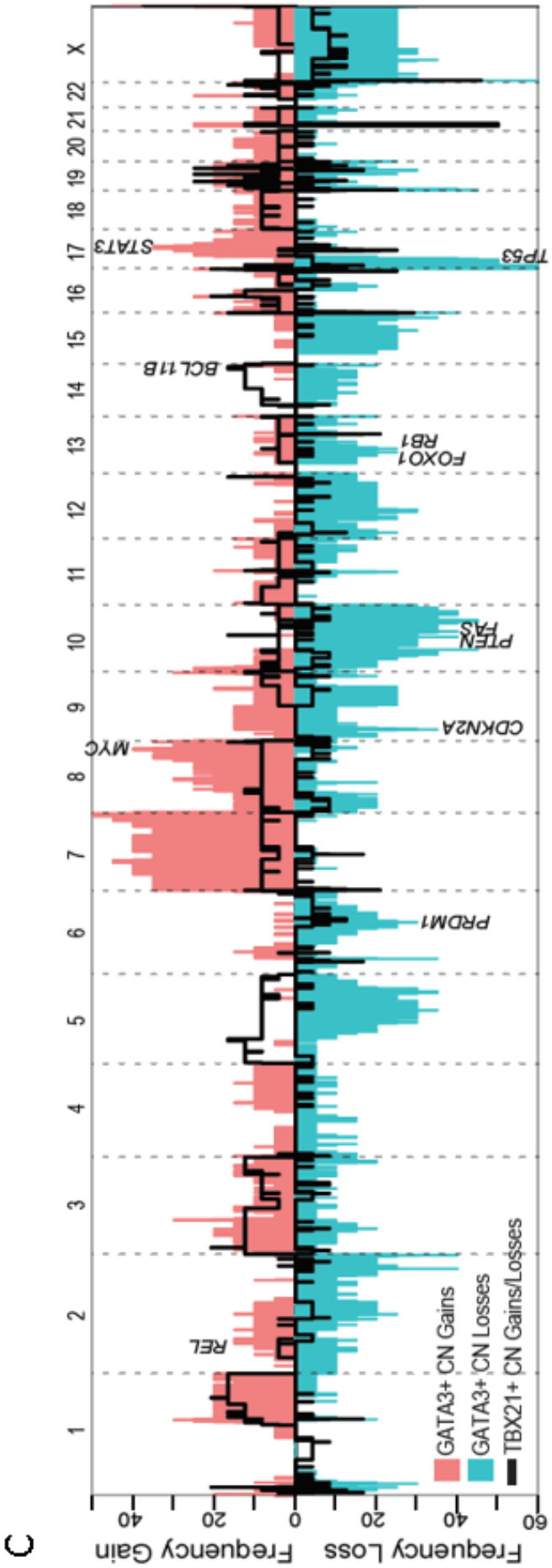
C
Frequency Loss
Frequency Gain
60
40
20
0
20
40
GATA3+ CN Gains
GATA3+ CN Losses
TBX21+ CN Gains/Losses
REL
MYC
PRDM1
CDKN2A
PTEN
FAS
FOXO1
RB1
BCL11B
STAT3
TP53
1
2
3
4
5
6
7
8
9
10
11
12
13
14
15
16
17
18
19
20
21
22
X

Figure 7: Whole-genome view of copy gains and losses in PTCL-GATA3 and PTCL-TBX21

(A) Bar graph of the overall frequency of minimal overlapping region (MR) of genomic imbalances in PTCL-GATA3 and PTCL-TBX21. Orange bar, PTCL-GATA3 n=11; Blue bar, PTCL-TBX21 n=10. (B) Distribution of copy gains and losses across all chromosomes in PTCL-GATA3 and PTCL-TBX21 respectively. Top view: aggregate copy number gains and losses in PTCL-TBX21, n=11; Bottom view: aggregate copy number gains and losses in PTCL-GATA3, n=10. Red area, loss of chromosomal material; Blue area, gain of chromosomal material. (C) Penetrance plots showing the frequency of gains and losses of genomic regions of PTCL-GATA3 (n=31) and PTCL-TBX21 (n=30). Each chromosome is represented on the x-axis, and the y-axis indicates the proportion of gain or loss of the corresponding genomic region. Representative tumor suppressor genes or oncogenes were indicated in focal regions. Gains are shown in red, and losses in blue in PTCL-GATA3. Gains and losses are shown in black lines above and below x-axis in PTCL-TBX21, respectively.

A

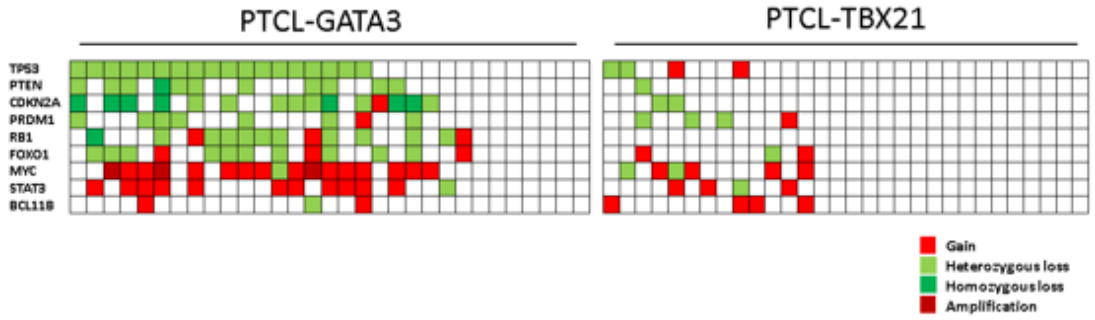
PTCL-GATA3
PTCL-TBX21
TP53
PTEN
CDKN2A
PRDM1
RB1
FOXO1
MYC
STAT3
BCL11B
Gain
Heterozygous loss
Homozygous loss
Amplification

B

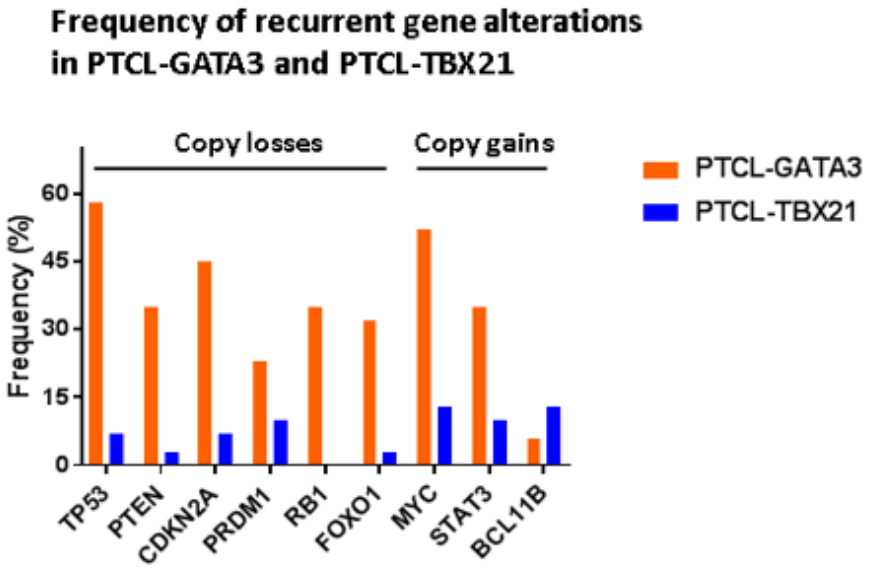
Frequency of recurrent gene alterations
in PTCL-GATA3 and PTCL-TBX21
Copy losses
Copy gains
PTCL-GATA3
PTCL-TBX21
Frequency (%)
60
45
30
15
0
TP53
PTEN
CDKN2A
PRDM1
RB1
FOXO1
MYC
STAT3
BCL11B

C

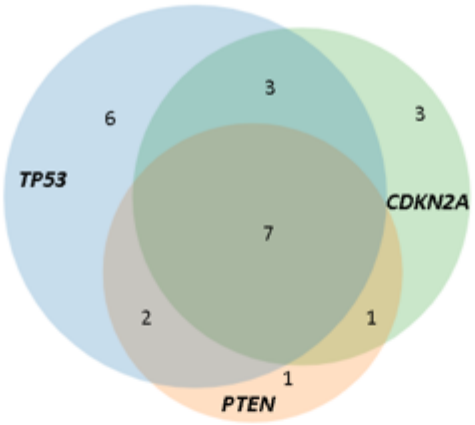
6
3
3
TP53
CDKN2A
7
2
1
1
PTEN

D

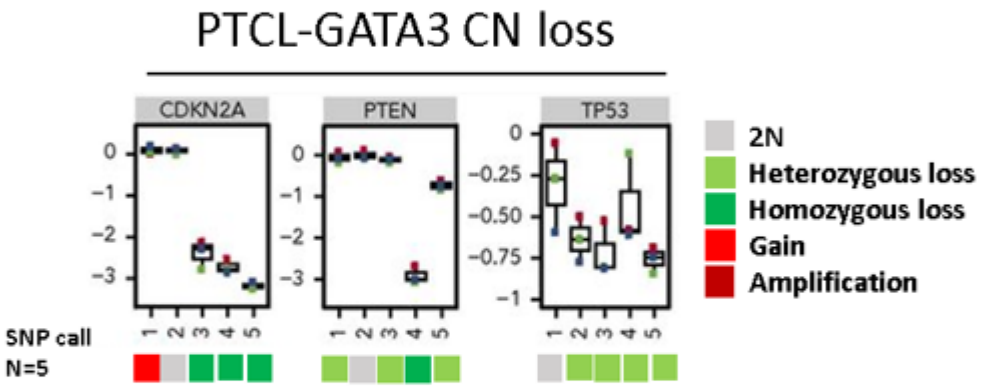
PTCL-GATA3 CN loss
CDKN2A
PTEN
TP53
SNP call
N=5
2N
Heterozygous loss
Homozygous loss
Gain
Amplification

E

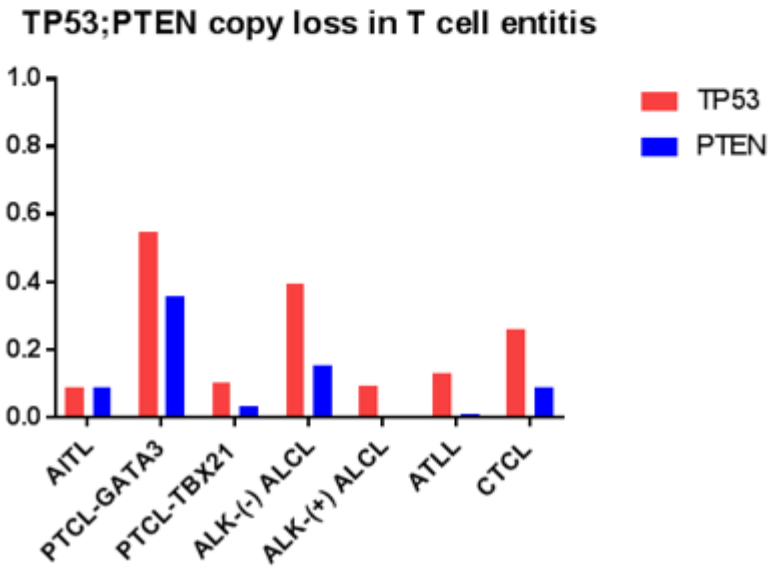
TP53;PTEN copy loss in T cell entitis
TP53
PTEN
AITL
PTCL-GATA3
PTCL-TBX21
ALK-(-) ALCL
ALK-(+) ALCL
ATLL
CTCL

Figure 8: Spectrum of recurrently altered genes in PTCL-GATA3 and PTCL-TBX21

(A) The status of copy number alterations of the recurrent genes in PTCL-GATA3 (n=31) comparing to PTCL-TBX21 (n=30). Each column represents one case, and each row indicates the representative genes. Red: copy gain; Light green: Heterozygous loss; Dark green: Homozygous loss; Dark red: Amplification/high gain; Blank: 2N/normal. (B) Bar graph of the frequency of the recurrently altered genes in PTCL-GATA3 and PTCL-TBX21. Orange bars represent PTCL-GATA3, n=31; Blue bars represent PTCL-TBX21, n=30. (C) Validation of *CDKN2A*, *PTEN* and *TP53* tumor suppressor genes within recurrent aberrant loci of PTCL-GATA3 by the NanoString Cancer CNV assay. Red: copy gain; Light green: Heterozygous loss; Dark green: Homozygous loss; Dark red: Amplification/high gain; Blank: 2N/normal. (D) Venn diagram depicts the overlap between *TP53*, *PTEN*, and *CDKN2A* copy loss in PTCL-GATA3. (E) Comparison of *TP53; PTEN* copy loss status among different T-cell lymphoma subtypes in our series. Red bar: *TP53* copy loss; Blue bar: *PTEN* copy loss.

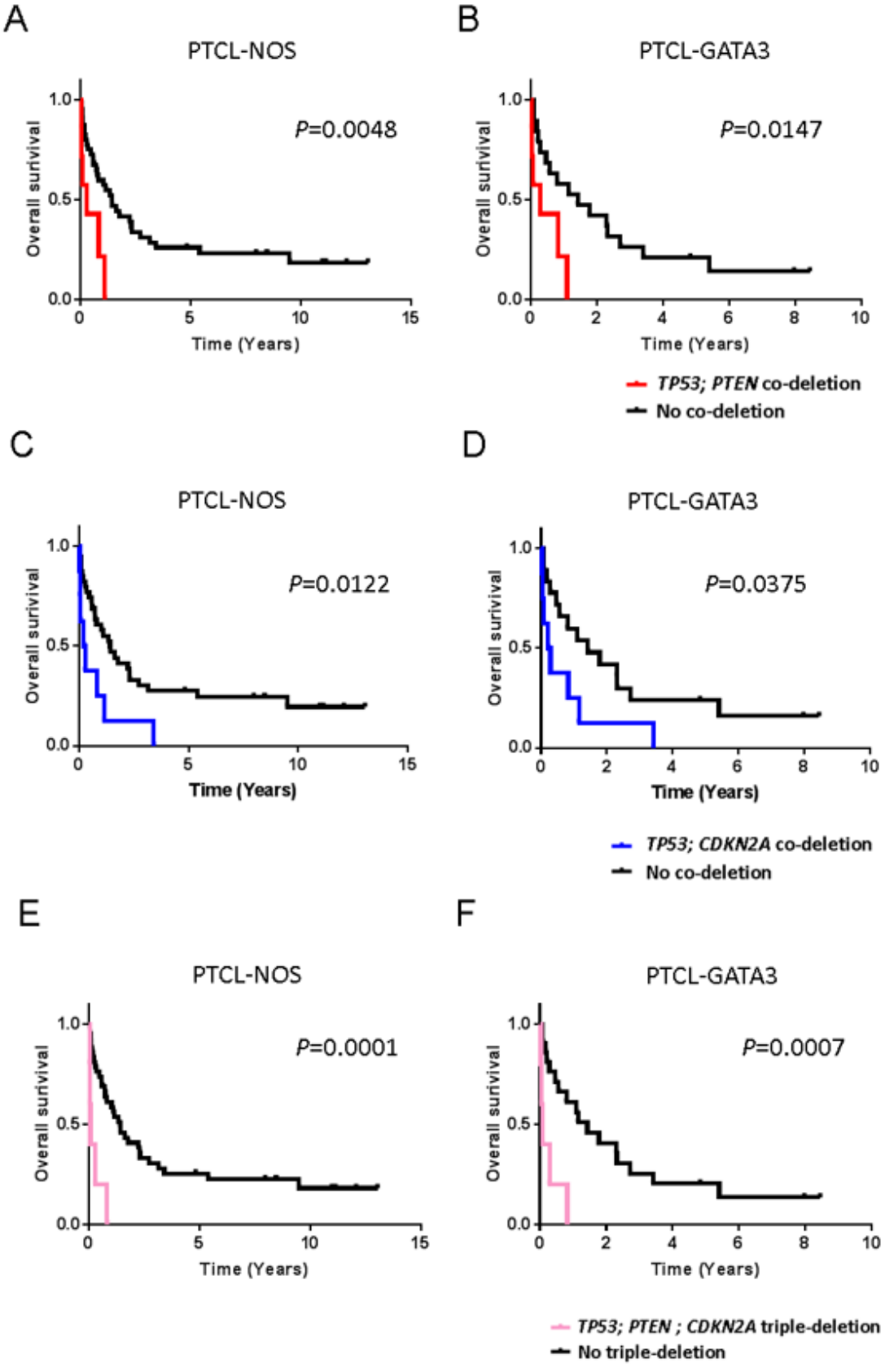
A
PTCL-NOS
P=0.0048
Overall survival
Time (Years)
B
PTCL-GATA3
P=0.0147
Overall survival
Time (Years)
TP53; PTEN co-deletion
No co-deletion
C
PTCL-NOS
P=0.0122
Overall survival
Time (Years)
D
PTCL-GATA3
P=0.0375
Overall survival
Time (Years)
TP53; CDKN2A co-deletion
No co-deletion
E
PTCL-NOS
P=0.0001
Overall survival
Time (Years)
F
PTCL-GATA3
P=0.0007
Overall survival
Time (Years)
TP53; PTEN ; CDKN2A triple-deletion
No triple-deletion

Figure 9: Association between co- or triple-deletion of tumor suppressor genes and survival in PTCL-NOS and PTCL-GATA3

(A) (C) (E) Kaplan-Meier survival curves of PTCL-NOS cases stratified by *TP53; PTEN, TP53; CDKN2A*, and *TP53; PTEN; CDKN2A* copy number status. Co-deletion of *TP53; PTEN*, n=7; no co-deletion of *TP53; PTEN*, n=40; Co-deletion of *TP53; CDKN2A*, n=8; no co-deletion of *TP53; CDKN2A*, n=39; Triple-deletion of *TP53; PTEN; CDKN2A*, n=5; no triple-deletion of *TP53; PTEN; CDKN2A*, n=42. (B) (D) (F) Kaplan-Meier survival curves of PTCL-GATA3 cases stratified by *TP53; PTEN, TP53; CDKN2A*, and *TP53; PTEN; CDKN2A* copy number status. Co-deletion of *TP53; PTEN*, n=7; no co-deletion of *TP53; PTEN*, n=19; Co-deletion of *TP53; CDKN2A*, n=8; no co-deletion of *TP53; CDKN2A*, n=18; Triple-deletion of *TP53; PTEN; CDKN2A*, n=5; no triple-deletion of *TP53; PTEN; CDKN2A*, n=21. All of the prognostic impacts on survival was evaluated by the log-rank test.

A

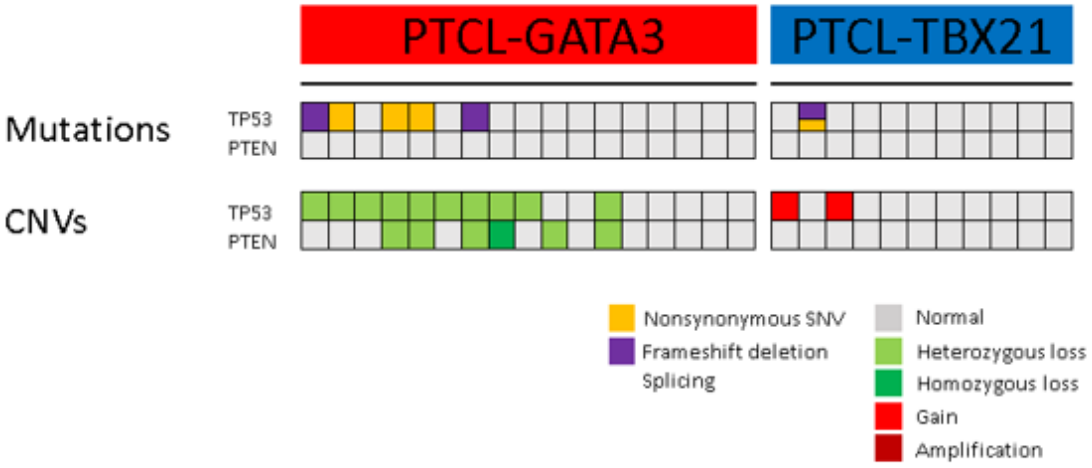
PTCL-GATA3
PTCL-TBX21
Mutations
TP53
PTEN
CNVs
TP53
PTEN
Nonsynonymous SNV
Frameshift deletion
Splicing
Normal
Heterozygous loss
Homozygous loss
Gain
Amplification

B

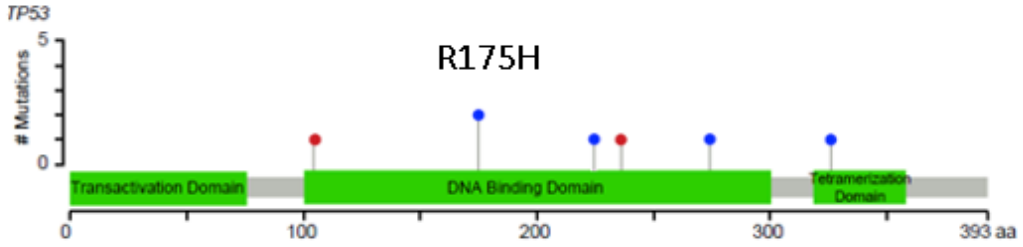
TP53
R175H
Mutations
5
0
Transactivation Domain
DNA Binding Domain
Tetramerization Domain
0
100
200
300
393 aa

Figure 10: *TP53; PTEN* mutation status in PTCL-GATA3 and PTCL-TBX21

(A) Co-mutation plot showing the spectrum of somatic alterations in *TP53* and *PTEN* genes and copy number status across PTCL-GATA3 (n=17), and PTCL-TBX21 (n=11). The color-coding is as follows: yellow, nonsynonymous SNV; purple, frameshift deletion/splicing; grey, normal; light green, heterozygous loss; green, homozygous loss; red, gain; dark red, amplification. (B) Schematic structure of *TP53 by* Mutation Mapper. Locations of coding mutations across PTCL-GATA3 tumor samples were indicated, including hotspot mutation R175H (n=2).

Chapter 3 *p53*$^{R172H/+}$*;Pten* mouse models generation and characterization

Introduction

A useful way to analyze the biology of human lymphoma and to examine the functional role of genes involved in the process is to establish a model system. Currently, no PTCL-NOS cell lines have been established over the years for this purpose, due to the rarity and the diagnosis of PTCL-NOS is currently performed on an “exclusion criteria” model since PTCL-NOS lack pathognomonic features[146]. The advent of gene expression profiling (GEP) and next-generation sequencing (NGS)

approaches revolutionized the understanding of the genetic landscape of PTCL-NOS. With the frequently altered genes identified in PTCL-NOS, two subgroups of PTCL-NOS have been identified, which are either characterized by high expression of GATA3 or TBX21 transcription factors and suggest either a Th2 or Th1 cellular origin[67].

More recently, the revised 2016 World Health Organization (WHO) classification refined the nodal PTCL-NOS with the T_{FH} phenotype as a provisional entity, with recurrent genetic abnormalities including *TET2*, *IDH2*, *DNMT3A*, *RHOA*, and *CD28* mutations, as well as gene fusions such as *ITK-SYK* or *CTLA4-CD28*[47]. However, the molecular pathogenesis of the cases in the PTCL-NOS category are still poorly understood.

Based on the observations of our copy number study to genetically characterize a large panel of molecularly classified PTCL-GATA3 and PTCL-TBX21, we identified frequent co-alteration of *TP53* and *PTEN* tumor suppressor genes in the PTCL-GATA3 in our cohort[147]. We, therefore, hypothesize co-occurring defects of *TP53* and *PTEN* could classify PTCL-NOS into the PTCL-GATA3 subtype, as they represent alterations in independent cellular pathways compared to PTCL-TBX21, and therefore could be the potential genetic drivers in the pathogenesis of this subtype. This also suggests that *TP53* and *PTEN* have specific functions critical to tumor development in independent cellular pathways since the alteration of two well-known tumor suppressor genes in the same pathway would be unnecessary and unlikely[133]. Therefore, *TP53* and *PTEN* co-alteration probably ultimately serve as the representative model system

for PTCL-GATA3 out of the genetically heterogeneous PTCL-NOS tumor type, and being the vehicles for the development of the new treating strategy for this disease.

Disrupted germline *p53* alleles in mouse embryonic stem (ES) cells have shown enhanced susceptibility to spontaneous tumors including malignant teratomas and lymphoma in both C57BL/6J (B6) and 129/Sv strains over the first 6 months, and more than ¾ of the lymphomas were of thymic origin and contained primarily immature $CD4^+CD8^+$ T cells, whereas the remainder originated in the spleen and peripheral lymph nodes and were of B-cell type[148]. Whole-exome sequencing (WES) of *p53* knockout thymic lymphoma showed high frequency of genomic instability and revealed that all of the independently derived oligoclonal mouse tumors had a deletion in the *Pten* gene prior to the formation of the TCRβ rearrangement[125], indicating the presence of a germline *p53* alteration sets an order to the selection of possible genes such as *Pten*, which contributes to lymphomagenesis[149]. Germline $p53^{R172H/+}$ mutant mice developed similar tumor spectrum compared to $p53^{+/-}$ mice, including lymphomas, carcinomas, and sarcomas, but tumors from $p53^{R172H/+}$ mice were highly metastatic, indicating a gain-of-function mutation inferred mutant *p53* additional properties which allow metastasis[142]. This has been supported by many studies suggesting that the presence of *p53* mutations in tumors was correlated with resistance to chemotherapy and worse prognosis compared to tumors lacking *p53* mutations[150,151]. Thus, the relevance of the tumor profile of the *p53* deficiency mouse models is highly related to the *p53* mutation status in human lymphoma.

Loss of heterozygosity (LOH) at 10q23 is a very common event in most primary tumors such as glioblastoma (60-74%)[152-154], gastric cancer (20-30%)[155], prostate cancer (32-63%)[156], and several series of ovarian cancers (27.3-56.5%)[157,158], which has been demonstrated associated with late-stage, more aggressive and metastatic tumors[159], suggesting *PTEN* is involved in transformation process in a dose-depended manner. The abrogation of *PTEN* in T cells during thymic development stage has shown to cause lymphomagenesis by different groups[160-162]. Monoallelic loss of *PTEN* mainly generated SP $CD4^+$ lymphomas, and some accompany with DP populations[163]. Biallelic loss of *PTEN* mediated by *Lck-Cre* gave rise to lymphomas with the majority classified as a mixture of DN/DP and SP $CD4^+/CD8^+$[162], with SP $CD4^+$, SP $CD8^+$, and DP also seen. The majority of mice with *PTEN* deficiency inactivated by *CD4-Cre* were DP lymphomas. However, these tumors were demonstrated to have thymic origins, and the majority gave rise to malignant peripheral T-cell populations, often displaying typical thymic phenotypical characteristics[162]. In contrast, conditional deletion of *Pten* from CD4 helper T cells by $OX40^{Cre}Pten^{f}$ mice did not show signs of lymphoma[164], indicating that the timing of *PTEN* deletion during T cell development and differentiation is critical to tumorigenesis.

Combined deletion of *TP53* and *PTEN* was detected in over 18.7% of triple-negative-like breast cancer (TNBC), characterized by the worst prognosis compared to other TNBCs with normal level of these tumor suppressors, and has been shown have the potential to estimate the pathobiological behavior and prognosis of TNBC that

exhibited hyper-activated AKT signaling and more mesenchymal claudin-low features relative to *Pten* or *p53* single-mutant tumors *in vivo*[131]. However, unlike *p53* deletion, induction of *p53*^{R270H} mutation plus *Pten* deletion skew tumors toward basal-like breast cancer[165], suggesting tumor subtype transformation is dictated by both the cell-of-origin (COO) and the oncogenic/tumor suppressor networks. Similarly, conditional inactivation of *p53* in the mouse prostate fails to produce a tumor phenotype, whereas complete *Pten* inactivation in the prostate triggers non-lethal invasive prostate cancer after long latency[145]. Strikingly, combined inactivation of *Pten* and *p53* elicits invasive prostate adenocarcinoma as early as 2 weeks after puberty and is invariably lethal by 7 months of age, while the transformation potential deceases in a *p53* or *Pten* copy-dependent manner which has been demonstrated *in vitro*[145].

The impact of combined inactivation of *TP53* and *PTEN* tumor suppressor genes, which frequently occurs in PTCL-GATA3, is poorly understood. In order to have any predictive value, the models must share central drivers of disease with the human disease they are representing. Intervention with recurrent known main mechanisms in tumorigenesis will give us more information about which pathways are central for the model so that the test compound can be acted on. Therefore, in the present study, we disrupted *p53* and *Pten* in $CD4^+$ T cells by mutation/deletion either alone or in combination and determined the effect on tumor formation, tumor-initiating and infiltrating cells, as well as prognosis.

Results

Generation of CD4$^+$ T lineage specific *p53* and/or *Pten* deficiency mouse model

To study whether the loss of *p53* and *Pten* causes tumorigenesis in PTCL-GATA3, we utilized the Cd4-Cre transgene to delete *p53* alone or in combination with *Pten*, and vice versa, in all CD4 lineages using conditional *p53* and *Pten* alleles. We crossed Cd4-Cre transgenic mice with *p53*$^{LSL\text{-}R172H+/-}$ and *Pten*$^{fl/fl}$ mice to obtain >300 mice of six genotypes, including *Cd4-Cre*$^{+/-}$;*Pten*$^{fl/+}$, *Cd4-Cre*$^{+/-}$;*Pten*$^{fl/fl}$, *Cd4-Cre*$^{+/-}$;*p53*$^{LSL\text{-}R172H+/-}$, *Cd4-Cre*$^{+/-}$;*p53*$^{R172H+/-}$*Pten*$^{fl/+}$, *Cd4-Cre*$^{+/-}$;*p53*$^{LSL\text{-}R172H+/-}$*Pten*$^{fl/fl}$ (hereafter referred to as *Pten*$^{fl/+}$, *Pten*$^{fl/fl}$, *p53*$^{LSL\text{-}R172H+/-}$, *p53*$^{LSL\text{-}R172H+/-}$*Pten*$^{fl/+}$, *p53*$^{LSL\text{-}R172H+/-}$*Pten*$^{fl/fl}$) as well as age-matched wild-type mice (Figure 11A B C D). All mice in this study are in the C57BL/6 genetic background. Germline point mutant *p53*$^{LSL\text{-}R172H+/-}$ mice present the LoxP-flanked transcriptional STOP cassette into intron 1 of the *p53* gene. Site-directed mutagenesis was used to introduce an arg to his mutation at codon 172 in the *p53* gene, which corresponds to the hot spot mutation at arg 175 in humans (Figure 11D). *Pten*$^{fl/fl}$ mice possess loxP sites flanking exon 5, which encodes the phosphatase domain of *PTEN* in which many tumor-associated mutations have been detected[96] (Figure 11E). Although the floxed allele was present across the tissue of the mouse, the mutant allele was specifically activated in CD4$^+$ T cells in the offspring upon Cre-mediated deletion of a loxP-flanked stop cassette and loxP sites. Of note, one allele of *p53* is truncated throughout the tissue due to the germline presence of the LoxP-flanked transcriptional STOP cassette. Successful generation of conditional and germline *p53* point mutation and *Pten* deletion were confirmed by several means. The

presence of the STOP cassette in *p53* and deletion of *Pten* was confirmed by standard PCR using genomic DNA extracted from ear notch biopsies (Figure 12A B C). Gene recombination was detected by standard PCR using genomic DNA extracted from $CD4^+$ T cells isolated from spleen. Primers spanning the mutant and deleted region were used to amplify the genomic DNA. The band indicating Cre-mediated recombination was only observed in $Pten^{fl/+}$, $Pten^{fl/fl}$, $p53^{LSL\text{-}R172H+/-}$, $p53^{LSL\text{-}R172H+/-}Pten^{fl/+}$, $p53^{LSL\text{-}R172H+/-}Pten^{fl/fl}$ cells, and a remaining floxed band indicated incomplete deletion (Figure 12D E F G).

The first clinical signs of spontaneous lymphomagenesis in $p53^{LSL\text{-}R172H+/-}Pten^{fl/fl}$ (n=12), $Pten^{fl/fl}$ (n=28), $p53^{LSL\text{-}R172H+/-}Pten^{fl/+}$ (n=18), and $p53^{LSL\text{-}R172H+/-}$ (n=11) mice were observed 8.1-, 8.3-, 27.7-, 49.7- weeks after birth, presenting with enlarged abdomen, weight loss and arched back. These findings were absent in age-matched wild-type mice. $Pten^{fl/fl}$, $p53^{LSL\text{-}R172H+/-}Pten^{fl/fl}$ and $p53^{LSL\text{-}R172H+/-}Pten^{fl/+}$ mice showed a 100% penetrance of lymphomagenesis. All average spleen, thymus, and body weights per group and genotype are listed in Table 1. $Pten^{fl/fl}$ and $p53^{LSL\text{-}R172H+/-}Pten^{fl/fl}$ mice developed lymphomas with significantly shorter latency of 8.1-24.6 weeks than $p53^{LSL\text{-}R172H+/-}$ and $p53^{LSL\text{-}R172H+/-}Pten^{fl/+}$ mice of 27.7-81.9 weeks (Table 1, Figure 13A). Biallelic loss of *Pten* causes a strong reduction of overall lifespan compared to monoallelic loss of *Pten,* which further support the previous finding of a gene dose-to effect relation of progression in *Pten*[166]. In the context of the *Pten*-null background, $p53^{LSL\text{-}R172H+/-}Pten^{fl/fl}$ and $Pten^{fl/fl}$ mice have a median time to a fatal illness of 10.5- and 13.2 weeks,

respectively (*P*=0.0042) (Figure 13A). *p53* inactivation leads to earlier tumor formation in *Pten* knock out mice, suggesting in combination with loss of the two genes synergize to accelerate the transformation of tumorigenesis. In contrast, *p53*$^{LSL\text{-}R172H+/-}$*Pten*$^{fl/+}$ and *p53*$^{LSL\text{-}R172H+/-}$ mice developed tumors after a long latency of median time to 44.5 and 64.7 weeks, respectively (*P*=0.0001), indicating heterozygous loss of *Pten* accelerates tumor formation in the context of *p53* deficiency (Table 1, Figure 13A). All wild-type mice remained healthy during the course of the study.

Acute loss of *p53;Pten* results in massive thymic and splenic enlargement in *Pten*$^{fl/fl}$ and *p53*$^{LSL\text{-}R172H+/-}$*Pten*$^{fl/fl}$ mice compared to age-matched wild-type control mice (Table 1, Figure 13B C). However, in the long-term *p53;Pten* deficiency, the thymic and splenic size was significantly increased in *p53*$^{LSL\text{-}R172H+/-}$*Pten*$^{fl/+}$ but not in *p53*$^{LSL\text{-}R172H+/-}$ mice compared to control mice (Table 1, Figure 13B). Drastically physically enlarged thymus was observed in *Pten*$^{fl/fl}$ and *p53*$^{LSL\text{-}R172H+/-}$*Pten*$^{fl/fl}$ mice at fatal illness, however, thymocytes count after red blood cell lysis didn't show a significant change compared to wild-type controls (Figure 13C E). This could be due to highly variable thymus cell counts among tumor-bearing subjects, thus the significance was not reached. Splenocytes count of *Pten*$^{fl/fl}$ and *p53*$^{LSL\text{-}R172H+/-}$*Pten*$^{fl/fl}$ tumor-bearing mice were significantly higher than wild-type mice (Figure 13F). However, no difference was observed in the long-term deficiency of *p53;Pten* tumor-bearing mice compared to the controls (Figure 13F). Interestingly, 5/10 *p53*$^{LSL\text{-}R172H+/-}$ tumor-bearing mice were observed to have enlarged axillary or inguinal lymph nodes (Figure 13D), accompanied

with neurological symptoms such as paralysis.

Histologically, *p53;Pten* alteration in lymphoid organs disrupt their architecture by recurrent histological features, with irregular nuclei containing prominent nucleoli and mitoses (Figure 13G, Table 2). Tumor cells have been completely or partial involved in spleen, thymus, liver, lymph node and kidney. The morphology of $p53^{LSL\text{-}R172H+/-}Pten^{fl/fl}$ and $Pten^{fl/fl}$ mice was similar, a pattern that shows a striking degree of highly proliferative large cells, intermediate chromatin, and $CD3^+$ on most of the tumor cells found in the spleen, lymph nodes, liver and kidney. Compared to $p53^{LSL\text{-}R172H+/-}Pten^{fl/fl}$ mice, which are mostly $CD4^-$ and $CD8^-$, the majority of $Pten^{fl/fl}$ mice are SP $CD4^+$ T-cell lymphomas.

In $p53^{LSL\text{-}R172H+/-}Pten^{fl/+}$ mice, however, the cases still show a range of histopathological features, consisting primarily of a proliferation of small-medium cytotoxic $CD8^+$ neoplastic T cells, which were classified as mature T-cell lymphoma when judged by the absence of surface TdT. Loss of expression of CD3 are less common. Marker expression analysis of the tumor subtypes on two individual mice revealed either a mixed expression of CD19 and Myeloid lineage or a plasma cell neoplasms with non-specific $CD19^+$ staining. DP T-cell lymphoma was also seen in one case, on the basis that they featured with $CD3^+Cd4^+CD8^+$, $CD19^-$ and TdT^+.

Impaired T cell development caused by *p53* and *Pten* deficiency

To evaluate the role of *p53* and *Pten* in T cell development, thymocytes of the various genotypes were isolated and analyzed for the expression of CD4 and CD8.

Flow cytometry analysis of the thymus of *Pten*$^{fl/fl}$, *p53*$^{LSL\text{-}R172H+/-}$*Pten*$^{fl/fl}$, *p53*$^{LSL\text{-}R172H+/-}$ and *p53*$^{LSL\text{-}R172H+/-}$*Pten*$^{fl/+}$ mice showed a remarkably reduced percentage of DP cells in all genotypes of tumor-bearing mice (Figure 14B, 15A), indicating defects in T cell differentiation by *p53* and *Pten* ablation. Upon acute loss of *p53* and *Pten*, the size and cell number for the thymus of *Pten*$^{fl/fl}$ and *p53*$^{LSL\text{-}R172H+/-}$*Pten*$^{fl/fl}$ mice were markedly increased compared with wild-type control mice (Figure 13E, Table 1). The significantly enlarged thymus observed in these tumor-bearing mice was partially due to an elevated proportion of CD4^{+} SP cells in *Pten*$^{fl/fl}$ thymocytes, an increased CD8^{+} SP subsets in *p53*$^{LSL\text{-}R172H+/-}$*Pten*$^{fl/fl}$ thymocytes, and a mildly increased percentage of DN cells in both genotypes (Figure 14B, 15A). In regards to the long-term *p53* and *Pten* deficiency, thymic and splenic cellularity was not been increased in the majority of the *p53*$^{LSL\text{-}R172H+/-}$*Pten*$^{fl/+}$ and *p53*$^{LSL\text{-}R172H+/-}$ mice. However, mice still displayed a severely altered CD4/CD8 expression profile accompanied by significantly increased proportion of DN cells in some individual mice, with *p53*$^{LSL\text{-}R172H+/-}$*Pten*$^{fl/+}$ thymocytes skewed more to a CD8^{+} SP phenotype (Figure 14B, 15A).

Interestingly, significant increased splenic cellularity has been observed in both *Pten*$^{fl/fl}$ and *p53*$^{LSL\text{-}R172H+/-}$Pten$^{fl/fl}$ mice, however, the size and cell number for the spleen in the majority of the *p53*$^{LSL\text{-}R172H+/-}$ and *p53*$^{LSL\text{-}R172H+/-}$Pten$^{fl/+}$ mice was similar to age-matched control mice resulting largely from a decrease of the DP population during T cell development (Figure 13F, 14B, 15A). An excessive amount of CD3^{+} T cells have been detected in the spleen and peripheral blood of both Pten$^{fl/fl}$ and p53$^{LSL\text{-}R172H+/-}$

Pten$^{fl/fl}$ mice, with a corresponding drop in the percentage of B-cells, suggesting the infiltration of expanded thymic populations into the periphery (Figure 14A B G). Compared to a previous report[162] in which deregulated distribution of DN, DP, SP CD4$^+$, and SP CD8$^+$ populations were present in the periphery in tumor-bearing *Pten*$^{flox/flox}$ × *Lck-Cre* and *Pten*$^{flox/flox}$ × *CD4-Cre* mice in a B6/D2 strain, complete loss of *Pten* in CD4$^+$ T cells predominantly gave rise to SP CD4$^+$ in the peripheral in our series which leads to increased splenic cellularity (Figure 14C D). Consistently, SP CD8$^+$ malignant cells were never observed in the periphery upon acute loss of *Pten* (Figure 14C D). The explanation for the variable proportion of expanded peripheral SP CD4$^+$ T cells could be attributable to the differences in genetic background and the number of mice analyzed. Even though T-cell-specific *p53;Pten*-deficient mice were phenotypically and histologically nearly indistinguishable from *Pten*-deficient mice, the significantly increased number of DN T cells in *p53*$^{LSL\text{-}R172H+/-}$*Pten*$^{fl/fl}$ but not in *Pten*$^{fl/fl}$ cells suggests that the transformation events was accelerated by genetic alteration of *p53* during T cell development (Figure 14 B 15A). Additionally, excessive expansion and infiltration of B220$^+$ B-lineage, CD335$^+$ NK-linage, and Mac-1$^+$/Gr-1$^+$ Myeloid-linage lymphocytes were never observed in either model (Figure 14A C E).

In contrast to acute loss of *p53* and *Pten*, reduced numbers of peripheral T cells were observed in some of the *p53*$^{LSL\text{-}R172H+/-}$ and *p53*$^{LSL\text{-}R172H+/-}$*Pten*$^{fl/+}$ mice, which is most likely a consequence of the diminished numbers of DP cells (Figure 14 C E F). Flow cytometric analysis of splenocytes revealed the distribution of differentially

expressing CD4/CD8 peripheral T cell populations among various genotypes of tumor-bearing mice, indicating the distinct but cooperative role of *p53* and *Pten* in T cell development (Figure 14D, 15C). Highly enriched SP $CD4^+$ T cells in the thymus and significantly increased DN cells were exclusively detected in $Pten^{fl/fl}$ and $p53^{LSL\text{-}R172H+/-}$ $Pten^{fl/fl}$ mice, respectively (Figure 14A, 15A). In contrast, the frequency of $CD4^+$ and $CD8^+$ T-cell thymocytes in the majority of $p53^{LSL\text{-}R172H+/-}$ mice was indistinguishable from those in age-matched *p53*-WT mice (Figure 14A). Strikingly, combined one copy loss of *Pten*, $p53^{LSL\text{-}R172H+/-}Pten^{fl/+}$ thymocytes skewed to an SP $CD8^+$ phenotype and infiltrated into the periphery, which has not been observed in other genotypes (Figure 14B D, 15A C).

Lack of peripheral T cells was observed in the lymph nodes of $p53^{LSL\text{-}R172H+/-}$ and $p53^{LSL\text{-}R172H+/-}Pten^{fl/+}$ mice, resulting largely from a decrease in the DP population during thymic development (Figure 14B E). Moreover, $p53^{LSL\text{-}R172H+/-}$ mice displayed a loss of T cells in the lymph nodes, while the number of $B220^+$ B cells was increased comparable to other genotypes (Figure 14E 15D).

Long-term deficiency of *p53* and *Pten* commits T cells to the CD8-lineage differentiation

Strikingly, a strong accumulation of $CD8^+$ T cells was detected in the periphery of $p53^{LSL\text{-}R172H+/-}Pten^{fl/+}$ mice, characterized by a mixture of $CD3^{low}CD8^+$ and $CD3^{high}$ $CD8^+$ subsets (Figure 14D F 15A C).

On one hand, the dramatic loss of DP cells in *p53*$^{LSL\text{-}R172H+/-}$*Pten*$^{fl/+}$ thymocytes could be explained by a stronger phenotype due to a partial block at immature CD8 single-positive (ISP) stage, which is indicated by a high level of CD8$^+$ thymocytes, suggesting differentiation of DP into CD8$^+$ SP is regulated by *Pten* expression in a dose-dependent manner (Figure 14 B, 15 A). The expanded ISP cells further acquired the capacity to infiltrate the periphery which accounts for the CD3^{low}CD8$^+$ population (Figure 14D F, 15 C). On the other hand, despite the reduced percentage of DP thymocytes, mature SP CD4$^+$ and SP CD8$^+$ were still present in periphery, characterized by a significant increase in SP CD8$^+$ and a corresponding reduction of SP CD4$^+$ T cells (Figure 14D F). This indicates positive selection is impaired in SP CD4$^+$ differentiation, but the pathway of SP CD8$^+$ differentiation appears favored in *p53*$^{LSL\text{-}R172H+/-}$*Pten*$^{fl/+}$ cells. In addition, the impairment of thymic T cells possibly leads to the alterations of genes in the regulation of B- and Myeloid- lineage commitment, since the abnormally increased percentage of B- and Myeloid-lineage population has been observed in the thymus of *p53*$^{LSL\text{-}R172H+/-}$*Pten*$^{fl/+}$ mice (Figure 14 A). The relative and absolute elevated amount of thymic B- and Myeloid-lineage could be due to the changes of thymic microenvironment which resulted from the disruption of thymic T cell development[167], or could have been derived from circulating B- and Myeloid-lineage that had entered the thymus. CD8$^+$ T cells comprised the majority population in periphery, accompanied with enrichment of the Myeloid-lineage, indicating a unique lymphoma entity identified upon the long-term deficiency of *p53* and *Pten* (Figure 15 E

F G).

Discussion

T cells undergo a series of well-documented differentiation steps in the thymus, which are typically defined based on the cell-surface expression of CD4 and CD8, with thymocytes starting as DN, DP, $CD4^+$ SP, and $CD8^+$ SP T cells[168]. To evaluate the role of *TP53* and *PTEN* in T-cell lymphomagenesis, we disrupted *p53* and/or *Pten* with the Cre-loxP system, which induced *p53* point mutation and *Pten* deletion specifically in $CD4^+$ T cells. By disruption of these two key tumor suppressor genes *in vivo*, we evaluated whether the genomic alterations cause pathogenesis and provide a selective advantage in T cell transformation, as well as the cooperative role of both genes in lymphomagenesis. In our study, the Cre-mediated *p53* mutation and *Pten* deletion were under the control of the CD4 promoter. The block of *p53* point mutation was removed and *Pten* expression was abolished as thymocytes upregulated CD4 expression during T cell differentiation toward the DP stage. As expected, $CD4^+$ T cell development and maturation were disrupted in $p53^{LSL\text{-}R172H+/-}$, $Pten^{fl/+}$, $Pten^{fl/fl}$, $p53^{LSL\text{-}R172H+/-}Pten^{fl/+}$, and $p53^{LSL\text{-}R172H+/-}Pten^{fl/fl}$ mice.

In our model system, the earlier onset of tumors arising from $p53^{LSL\text{-}R172H+/-}Pten^{fl/fl}$ and $Pten^{fl/fl}$ mice, were characterized by drastic enrichment of T cells in the peripheral lymphoid organs, which is consistent with previous findings that T-cell-specific *Pten*-deficiency mice inevitably developed T-cell lymphomas 5-23 weeks after birth[162]. We have shown that both $p53^{LSL\text{-}R172H+/-}Pten^{fl/fl}$ and $Pten^{fl/fl}$ mice were born alive

and appeared physical healthy up until 8 weeks of age. However, the transformation occurred as early as 6 weeks of age in some of the individual *p53*$^{LSL\text{-}R172H+/-}$*Pten*$^{fl/fl}$ and *Pten*$^{fl/fl}$ mice accompany with abnormal forward and side scatter characteristics in lymphoid cells, indicating the early onset of tumorigenesis developing immediately after the biallelic loss of *Pten*. Tumor-bearing mice from both *p53*$^{LSL\text{-}R172H+/-}$*Pten*$^{fl/fl}$ and *Pten*$^{fl/fl}$ genotypes inevitably developed increased thymic and splenic cellularity, partially due to massive thymic expansion and infiltrating T cells, which leads to premature death at 14.3 and 24.6 weeks, respectively. The main difference between the two genotypes was that the majority of the *Pten*-null mice show increased numbers of CD4^{+} SP T cells while combined loss of *p53* in the context of *Pten*-null background gave rise to more DN T cells in the periphery, suggesting a more severe block at the DN stage in *p53*$^{LSL\text{-}R172H+/-}$*Pten*$^{fl/fl}$ thymocytes compared to *Pten*$^{fl/fl}$ thymocytes. Alternatively, DN cells may survive better with *p53* mutation. Although tumor latency was shorter in *p53*$^{LSL\text{-}R172H+/-}$*Pten*$^{fl/fl}$ (median, 10.5 weeks) compared to *Pten*$^{fl/fl}$ (median, 13.2 weeks) mice, morphology and histology revealed that tumors driven by these two models were nearly indistinguishable, indicating the diagnosis of lymphoblastic lymphoma which originated from the thymus and partial or complete involvement of the spleen, liver, lymph nodes and metastasis to the kidneys.

In contrast to the short-term *p53;Pten* deficiency, *p53*$^{LSL\text{-}R172H+/-}$*Pten*$^{fl/+}$ mice displayed a severely altered CD4/CD8 expression profile. 50% (5/10) of the *p53*$^{LSL\text{-}R172H+/-}$*Pten*$^{fl/+}$ mice had a considerable increase in the percentage of CD8^{+} SP and DN

cells, and a corresponding decrease in DP population, which led to a remarkable reduction in thymic cellularity compared to *p53*$^{LSL\text{-}R172H+/-}$*Pten*$^{fl/fl}$ mice. This can be explained by the block in T cell development at the immature single-positive (ISP) stage in the absence of *p53* with an allele dosage of *Pten*, which results in an increased proportion of ISPs and a failure of normal developmental processes. Although future studies are needed to define the elevated $CD8^+$ SP populations in the thymus, such as whether or not they contain mature TCRβ (V to DJ) rearrangements and retain the expression level of CD34, the reduction in the peripheral T cell pool in *p53*$^{LSL\text{-}R172H+/-}$ *Pten*$^{fl/+}$ mice suggests the cooperative role of *p53* and *Pten* in T cell development. Normally, thymic B cells represent only a small subset (0.2%) of thymic cells characterized as immature $B220^+IgM^-$ and mature $B220^+IgM^+$ B-cells co-expressing CD19, but the commitment potential into B cells rather than T cells varies among genetic backgrounds *in vivo*[167,169,170]. However, a significantly increased number of B- and Myeloid-linage were observed in *p53*^{R172H} mice, indicating the severe impairment of the thymic microenvironment due to the genetic defects in T cell development. This was in agreement with the findings from several studies that thymic B-cell lymphopoiesis was remarkably enhanced in T cell-deficient mice, including CD3-ε knockout[170], TCR-β-deficient[167], and *iNotch1*$^{-/-}$ mice[171]. Similarly, early thymic progenitors (ETPs) such as IL-$7R\alpha^{+/-}Rag^{+/-}pT\alpha^+$ cells possess plasticity for myeloid lineage differentiation regulated by representative myeloid-related transcription factors such as PU.1 and C/EBPα/β, but inhibited by Notch signaling. Therefore, it is most

likely due to the alteration of gene networks through the changes of functional thymic microenvironment upon disruption of p53 signaling and PI3K-Akt-mTOR signaling pathway, which selectively skews the commitment of immature thymic progenitor toward the B- and Myeloid-lineage before their commitment to T cell lineage, or could also have delayed/impaired expression of Notch, especially in the C57BL/6 strain.

Compared to *p53*$^{LSL\text{-}R172H+/-}$*Pten*$^{fl/+}$ mice, 30% of the *p53*$^{LSL\text{-}R172H+/-}$ mice showed delayed tumor onset with incomplete penetrance, indicating *Pten* haploinsufficiency accelerates lymphomagenesis by activating PI3K-Akt-mTOR pathway in the context of *p53* deficiency. Low penetrance of tumor formation observed in *p53*$^{LSL\text{-}R172H+/-}$ mice is supported by other studies. One of which, for example, showed 20% of *p53*-cKO in CD4^{+} T cells developed lymphoma-like diseases with marked splenomegaly compared to the high penetrance of autoimmune disease in the majority of *p53* deficient mice[172]. Moreover, 50% (3/6) *p53*$^{LSL\text{-}R172H+/-}$ mice showed increased B cells in the periphery such as in lymph nodes, which is consistent with the findings in a previous study that reported complete deletion of *p53* in CD4^{+} T cells caused an increased B cell population in splenocytes, suggesting the effects on B cell development probably conferred by disruption of T cell signaling which is mediated by *p53* deficiency. Defective T cell apoptosis could either lead to autoimmunity or the development of lymphomas. Several studies[172,173] showed the ablation of *p53* in CD4^{+} T cells leads to the development of spontaneous autoimmunity by dysregulation of FoxP3 and STAT-5. In our study, 70% of the *p53*$^{LSL\text{-}R172H+/-}$ mice don't show signs of lymphomagenesis

but succumb to a fatal illness, suggesting that, in this scenario, “hotspot” *p53* mutation most likely results in spontaneous immunopathogenesis rather than tumorigenesis.

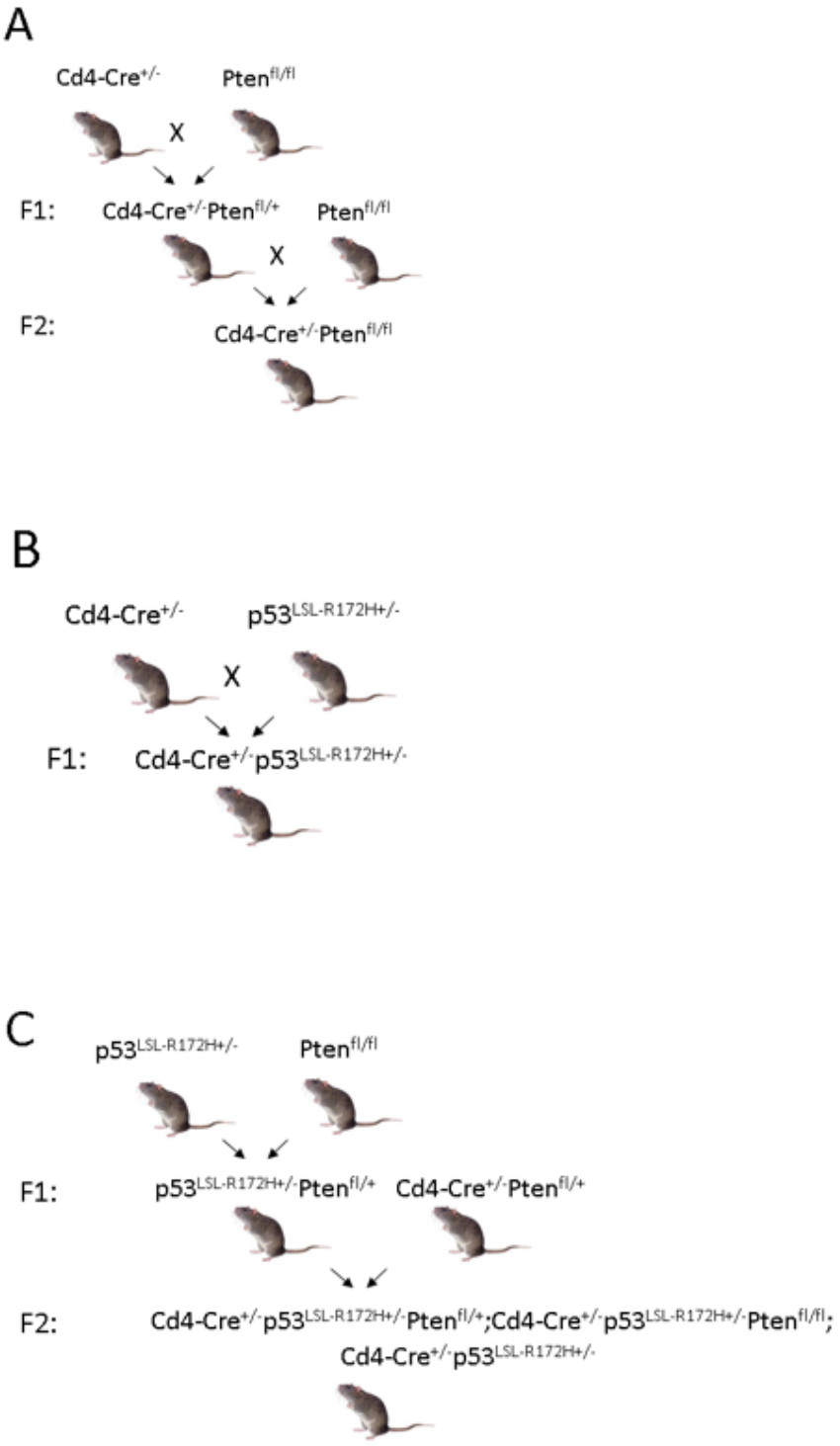

D

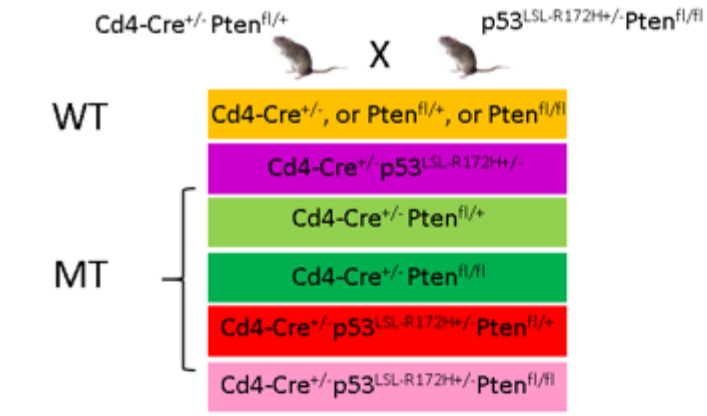
Cd4-Cre+/- Ptenfl/+
X
p53LSL-R172H+/-Ptenfl/fl
WT
Cd4-Cre+/-, or Ptenfl/+, or Ptenfl/fl
Cd4-Cre+/- p53LSL-R172H+/-
MT
Cd4-Cre+/- Ptenfl/+
Cd4-Cre+/- Ptenfl/fl
Cd4-Cre+/- p53LSL-R172H+/- Ptenfl/+
Cd4-Cre+/- p53LSL-R172H+/- Ptenfl/fl

E

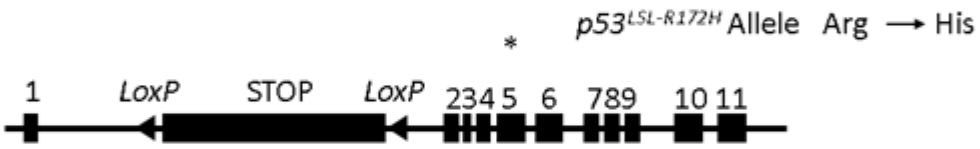
p53LSL-R172H Allele Arg → His
*
1
LoxP
STOP
LoxP
2345
6
789
10 11

F

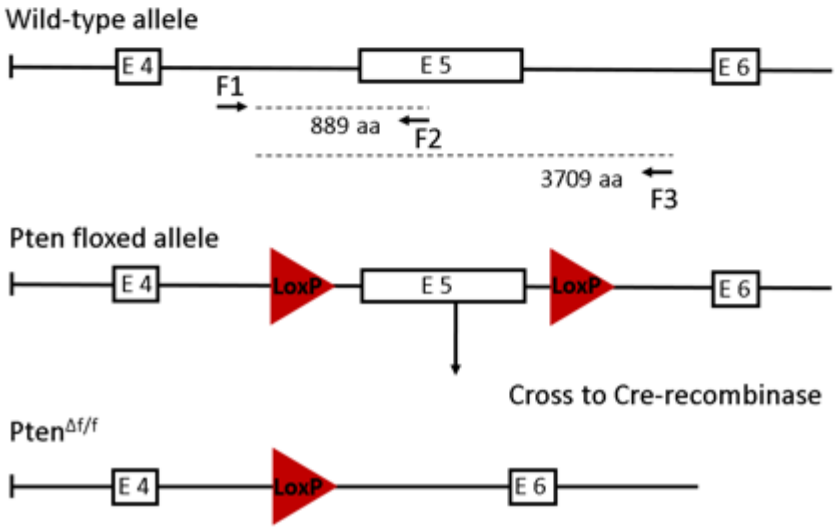
Wild-type allele
E 4
E 5
E 6
F1
889 aa
F2
3709 aa
F3
Pten floxed allele
E 4
LoxP
E 5
LoxP
E 6
Cross to Cre-recombinase
Pten Δf/f
E 4
LoxP
E 6

Figure 11: Strategy for breeding Cd4 specific *p53;Pten* mutant mice

(A) The *Pten*$^{fl/fl}$ mice were crossed with CD4 specific Cre mice to generate heterozygous *Cd4-cre;Pten*$^{fl/+}$ mice in the first generation. (B) Mouse carrying *p53*$^{LSL-R172H/+}$ single mutant allele were crossed with *Pten*$^{fl/fl}$ mice to generate heterozygous *p53*$^{LSL-R172H/+}$;*Pten*$^{fl/+}$ mice. Mice carrying *p53*$^{LSL-R172H/+}$;*Pten*$^{fl/+}$ were crossed with mice harboring *Cd4-cre;Pten*$^{fl/+}$ to generate mutant mice with CD4 T cell-specific deletion of *p53* and/or *Pten*. (C) Genotypes for wild-type and *p53;Pten* mutant mice. (D) (E) Genomic structure of *p53* and *Pten* locus.

A

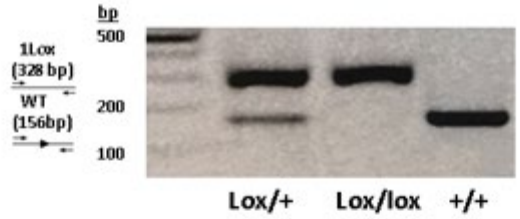

B

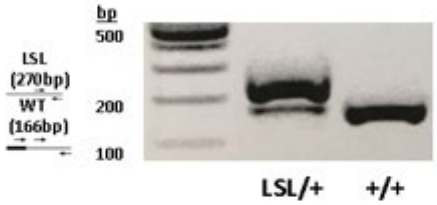

C

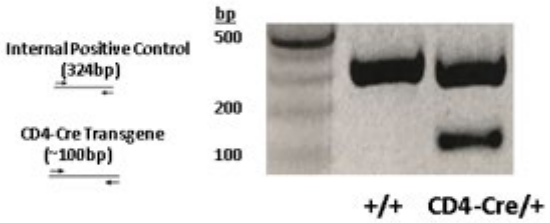

D

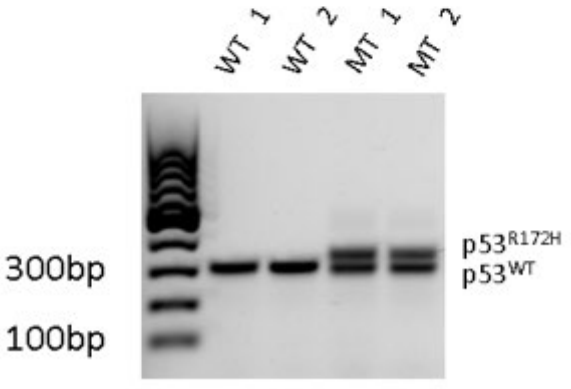

WT band: 290 bp
MT allele: 330 bp

E

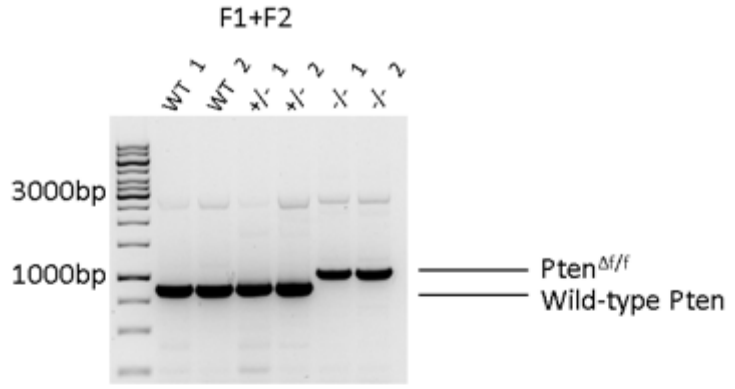

WT band: 889bp

Pten$^{\Delta f/f}$ band > 889bp

F

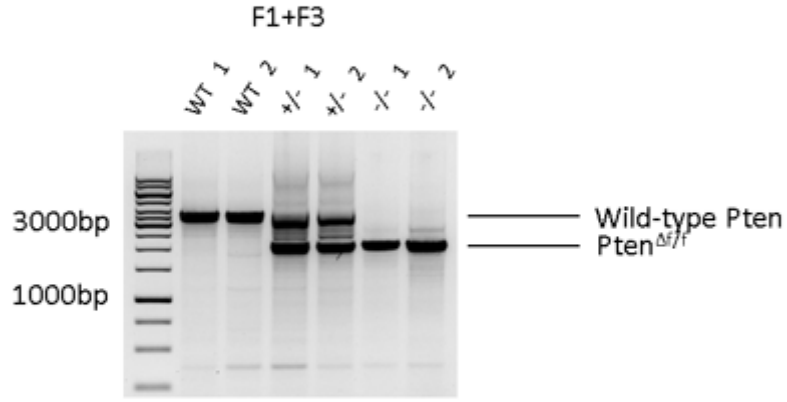

WT band: 3709bp

Pten$^{\Delta f/f}$ band < 3709bp

G

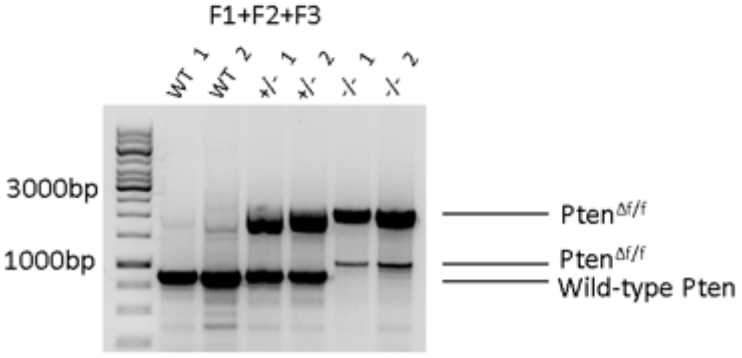

WT band: 889bp

Pten$^{\Delta f/f}$ band #1> 889bp

Pten$^{\Delta f/f}$ band #2 < 3709bp

Figure 12: Conditional inactivation of *p53;Pten* gene

For genotyping, mouse ear DNA was subjected to polymerase chain reaction (PCR) analysis. (A). PCR primers flanking the exon 5 of Pten locus yields a 328bp homozygote band and a 156bp WT band. (B). PCR amplification of conditional mutant *p53* alleles generate a 270bp mutant product and a 166bp control product. (C). PCR amplification of genomic DNA from CD4-Cre transgenic mice yield a ~100bp CD4-Cre transgene product and a 324bp internal positive control product. For DNA recombination, $CD4^+$ T cells were isolated from the spleen of mutant and wild-type mice using a negative selection $CD4^+$ T cell isolation kit. DNA was extracted from isolated $CD4^+$ T cells. (D) To determine the presence of the LSL cassette in *p53*, PCR amplification of conditional mutant *p53* alleles to generate a 270bp mutant band and a 166bp wild-type band. (E) (F) (G) Deletion of the $Pten^{fl/fl}$ allele was detected by polymerase chain reaction (PCR) using genomic DNA. Primers used are forward primer F1 and reverse primer F2 are inside exon 5. Reverse primer F3 is downstream of exon 5. 889bp and 3709bp products indicate wild type *Pten*, and product between 889 to 3709bp indicate $Pten^{\Delta f/f}$.

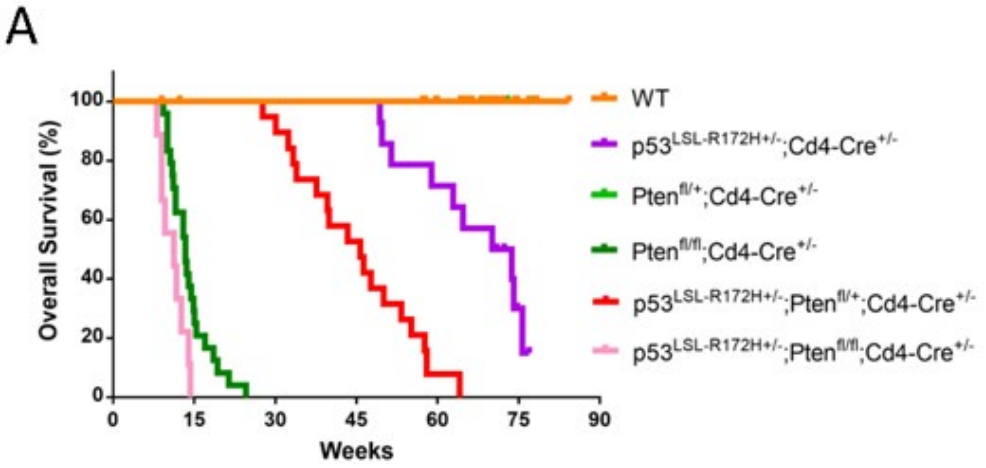
A
Overall Survival (%)
100
80
60
40
20
0
0
15
30
45
60
75
90
Weeks
WT
p53LSL-R172H+/-;Cd4-Cre+/-
Pten fl/+;Cd4-Cre+/-
Pten fl/fl;Cd4-Cre+/-
p53LSL-R172H+/-;Pten fl/+;Cd4-Cre+/-
p53LSL-R172H+/-;Pten fl/fl;Cd4-Cre+/-


B
p53LSL-R172H+/-;Pten fl/fl;Cd4-Cre+/-
Pten fl/fl;Cd4-Cre+/-
p53LSL-R172H+/-;Pten fl/+;Cd4-Cre+/-
p53LSL-R172H+/-; Cd4-Cre+/-
WT


C
Thymus
Spleen
WT
p53LSL-R172H+/-; Pten Fl/Fl;Cd4-Cre+
Spleen
Thymus

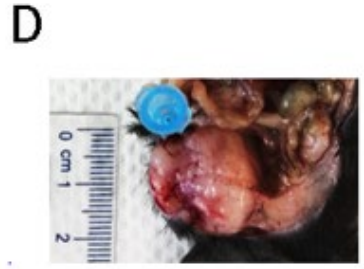
D

E

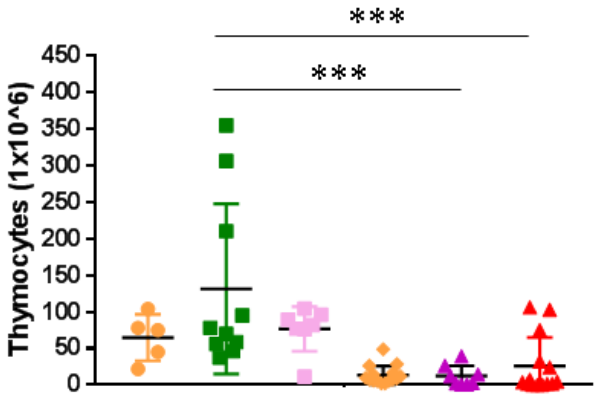
***
***
Thymocytes (1x10^6)
450
400
350
300
250
200
150
100
50
0

F

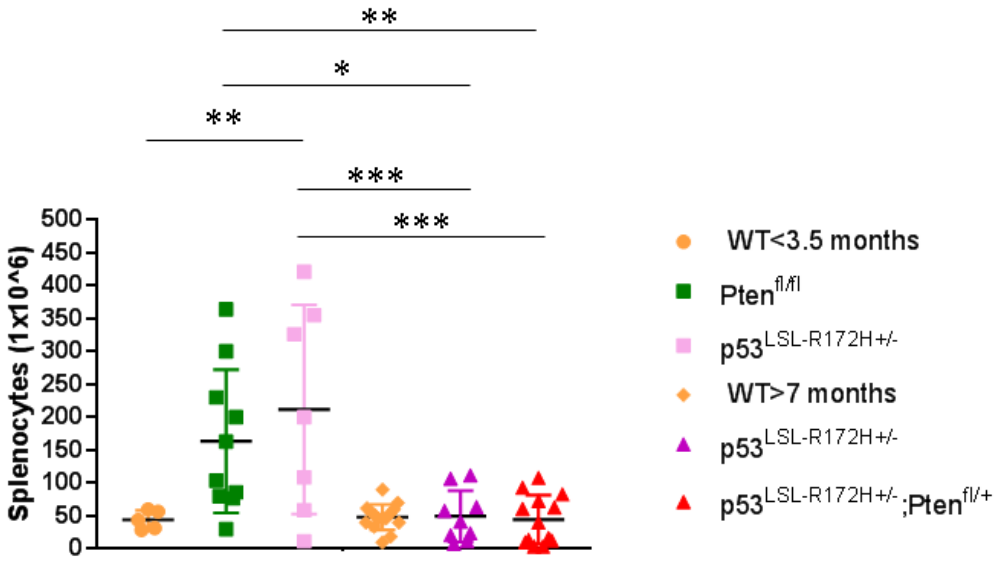
**
*
**
***
***
Splenocytes (1x10^6)
500
450
400
350
300
250
200
150
100
50
0
WT<3.5 months
Pten fl/fl
p53 LSL-R172H+/-
WT>7 months
p53 LSL-R172H+/-
p53 LSL-R172H+/- ;Pten fl/+

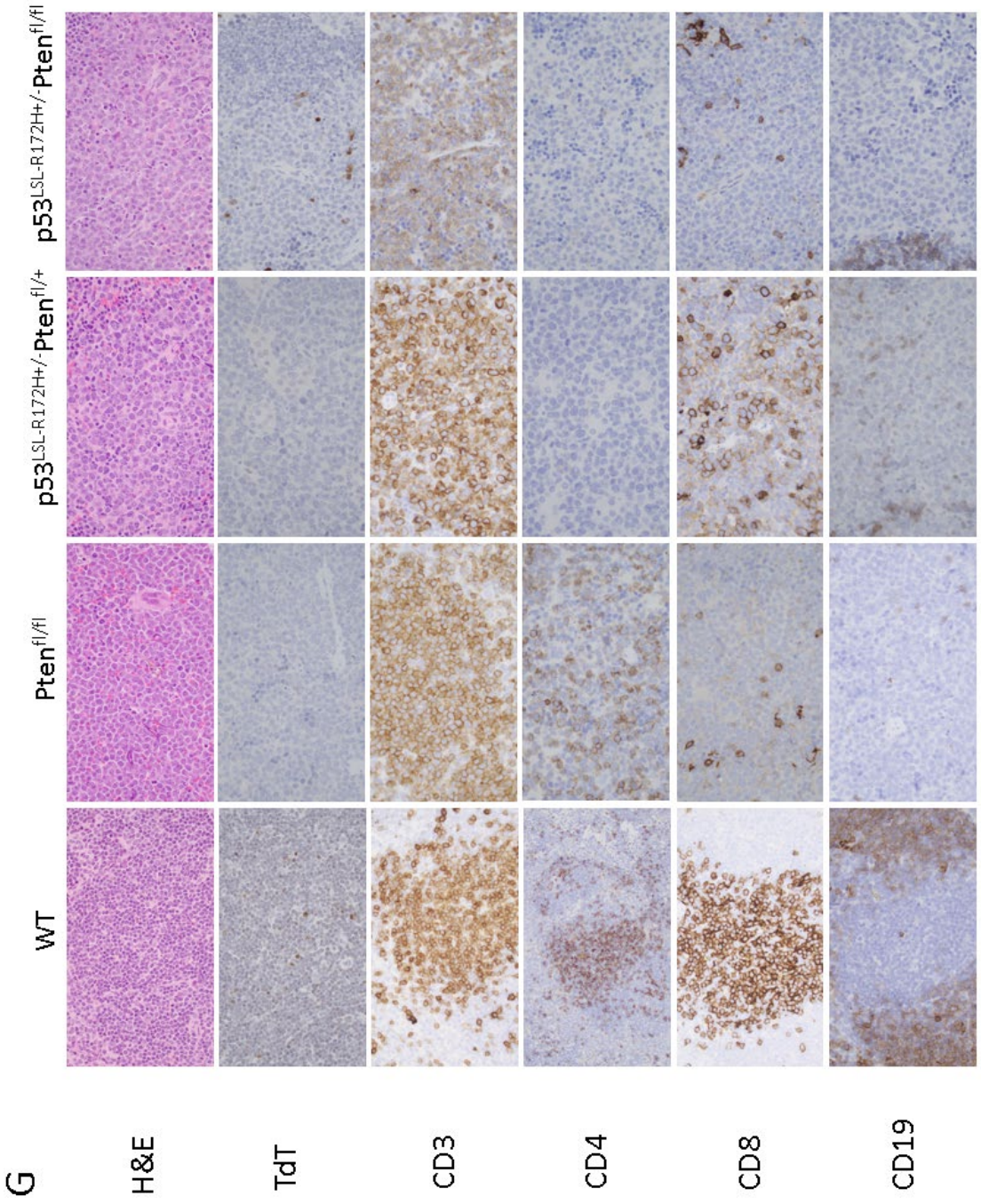
G
WT
Pten fl/fl
p53 LSL-R172H+/- Pten fl/+
p53 LSL-R172H+/- Pten fl/fl
H&E
TdT
CD3
CD4
CD8
CD19

Table 1: Spleen, thymus and body weights of tumor-bearing mice per different genotype

Table 2:

Table 1 Spleen, thymus and body weights of tumor-bearing mice per different genotype

Genotype	N	OS (Weeks)	Body weight (g)			Thymus weight (g)			Spleen weight (g)		
			Mean	S.D.	*P*	Mean	S.D	*P*	Mean	S.D	*P*
WT	10	8.1-15.0	20.5	2.7		0.04	0.01		0.05	0.03	
$p53^{LSL-R172H+/-}$ $Pten^{fl/fl}$	12	8.1-14.3	15.9	2.7	0.0021	0.24	0.11	0.0034	0.56	0.14	<0.0001
$Pten^{fl/fl}$	28	8.3-24.6	17.6	2.7	0.0153	0.25	0.14	0.0080	0.64	0.20	<0.0001
WT	15	33.9-89.1	25.5	2.6		0.04	0.01		0.09	0.02	
$p53^{LSL-R172H+/-}$ $Pten^{fl/+}$	18	27.7-64.1	20.6	4.3	0.0004	0.34	0.39	0.0126	0.26	0.32	0.0184
$p53^{LSL-R172H+/-}$	11	49.3-89.1	27.4	6.9	0.2101	0.19	0.44	0.1434	0.23	0.28	0.0662

Table 2 Pathological heterogeneity of peripheral T-cell lymphoma

Genotypes	Mouse IDs	Disease	Thymus involved	Spleen involved	Liver involved	Phenotype
$p53^{LSL\text{-}R172H+/-}$	#469	Sarcoma(soft tissue)	+	+	+	CD3-,CD4-,CD8-,CD19-,Tdt-
	#360	Negative				
$p53^{LSL\text{-}R172H+/-}$ $Pten^{fl/+}$	#Unlabeled	Heterogeneous, mixed-lineage	+	+	+	CD3-,CD4-,CD8,thymus CD19+, Tdt-,small cells
	#906	Lymphoma	+	+	+	CD3+,CD4-,CD8+++,CD19-,Tdt-
	#366	Plasma cell neoplasms	-	+	+	CD3-,CD4-,CD8-,weird non-specific CD19+,Tdt-
	#420	Immature lymphoma	+	+	+	CD3+,CD4+,CD8+,CD19-, scattered Tdt+
$Pten^{fl/fl}$	#745	Lymphoma	+	+	+	CD3+,CD19-,Tdt-,CD4+,CD8-
	#879	Lymphoma	+	+	+	CD3+,CD19-,Tdt-,CD4+,CD8-
$p53^{LSL\text{-}R172H+/-}$ $Pten^{fl/fl}$	#827	Lymphoma	+	+	+	CD3+,CD4-,CD8-,CD19-,Tdt-
	#1614	Lymphoma	+	+	+	CD3+,CD4-,CD8-,CD19-,Tdt-

Figure 13: Conditional knock out of *p53* and *Pten* in CD4 T cells leads to T-cell malignancies

(A) Kaplan-Meier survival curve comparing survival of *p53* and/or *Pten* deficient mice. (B) Physical alteration of spleen size in *p53* and/or *Pten* deficient tumor-bearing mice compared to wild-type control mice. (C) Enlargement of thymus and spleen have been observed in an 11-week old $p53^{LSL\text{-}R172H+/-}Pten^{fl/fl}$ mouse at lethal disease stage in necropsy. (D) Significant increased in size of the lymph node in $p53^{LSL\cdot R172H/+}$ tumor-bearing mouse. (E) (F) Thymocytes and splenocytes counting after red blood cell lysis of lethal disease stage *p53* and/or *Pten* deficient mice comparing to age-matched wild-type mice. (G) Microscopic H&E and IHC analysis of 4 study cohort genotypes. Sections from the primary and secondary lymphoid organs were immunostained for TdT, CD3, CD4, CD8, and CD19.

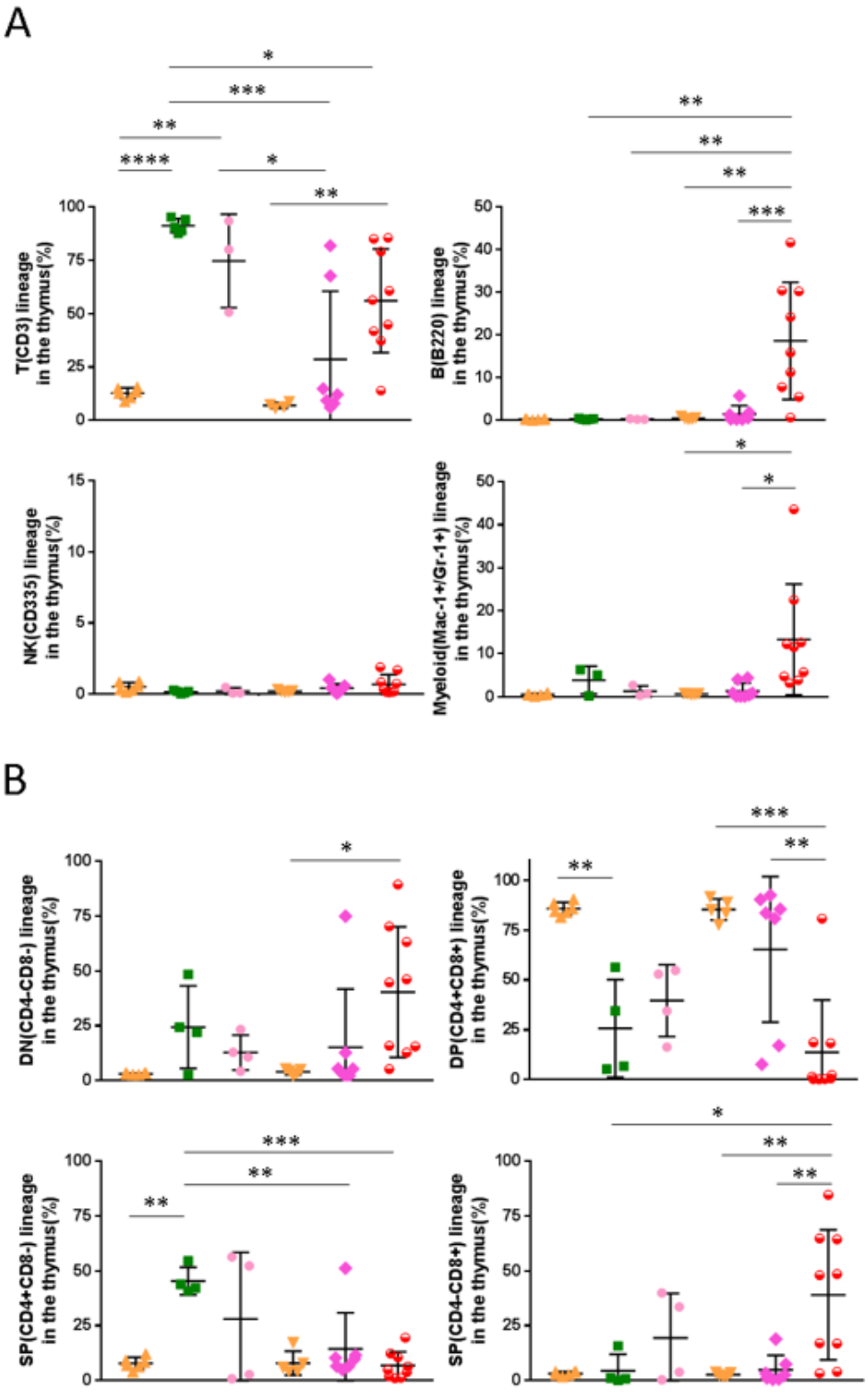
A
T(CD3) lineage in the thymus(%)
B(B220) lineage in the thymus(%)
NK(CD335) lineage in the thymus(%)
Myeloid(Mac-1+/Gr-1+) lineage in the thymus(%)
B
DN(CD4-CD8-) lineage in the thymus(%)
DP(CD4+CD8+) lineage in the thymus(%)
SP(CD4+CD8-) lineage in the thymus(%)
SP(CD4-CD8+) lineage in the thymus(%)

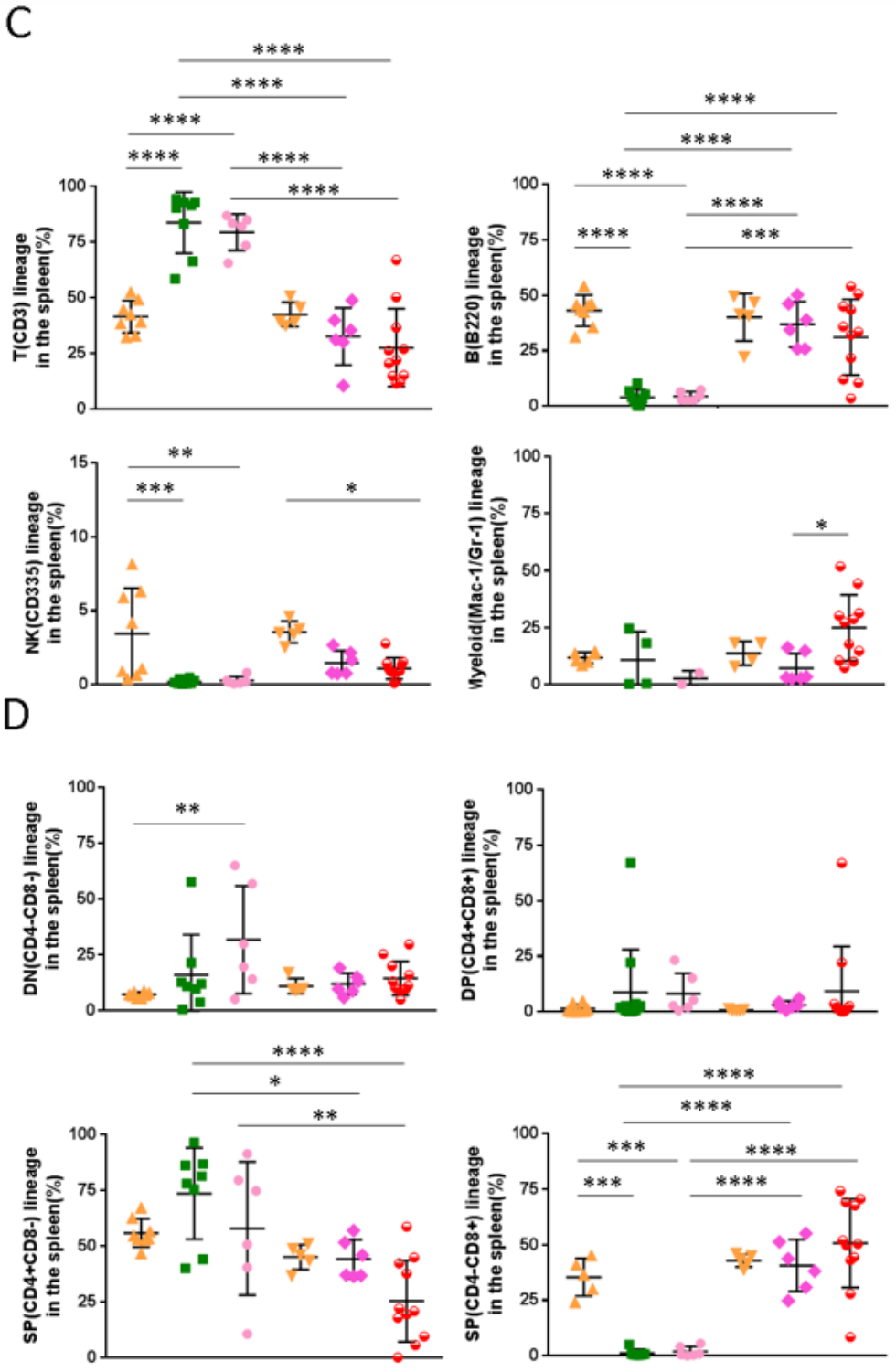
C
T(CD3) lineage in the spleen(%)
B(B220) lineage in the spleen(%)
NK(CD335) lineage in the spleen(%)
Myeloid(Mac-1/Gr-1) lineage in the spleen(%)
D
DN(CD4-CD8-) lineage in the spleen(%)
DP(CD4+CD8+) lineage in the spleen(%)
SP(CD4+CD8-) lineage in the spleen(%)
SP(CD4-CD8+) lineage in the spleen(%)

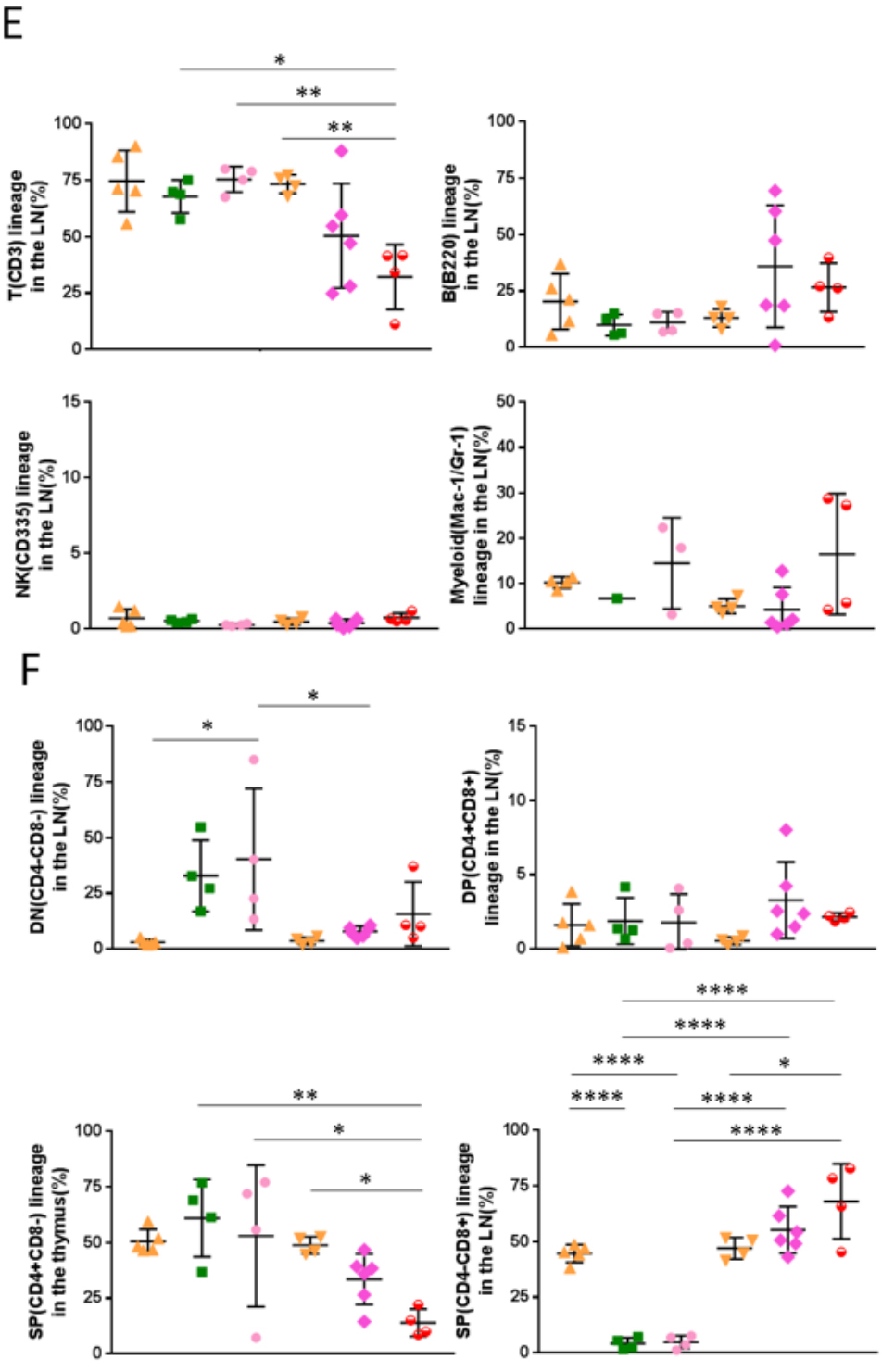
E
T(CD3) lineage in the LN(%)
B(B220) lineage in the LN(%)
NK(CD335) lineage in the LN(%)
Myeloid(Mac-1/Gr-1) lineage in the LN(%)
F
DN(CD4-CD8-) lineage in the LN(%)
DP(CD4+CD8+) lineage in the LN(%)
SP(CD4+CD8-) lineage in the thymus(%)
SP(CD4-CD8+) lineage in the LN(%)

G

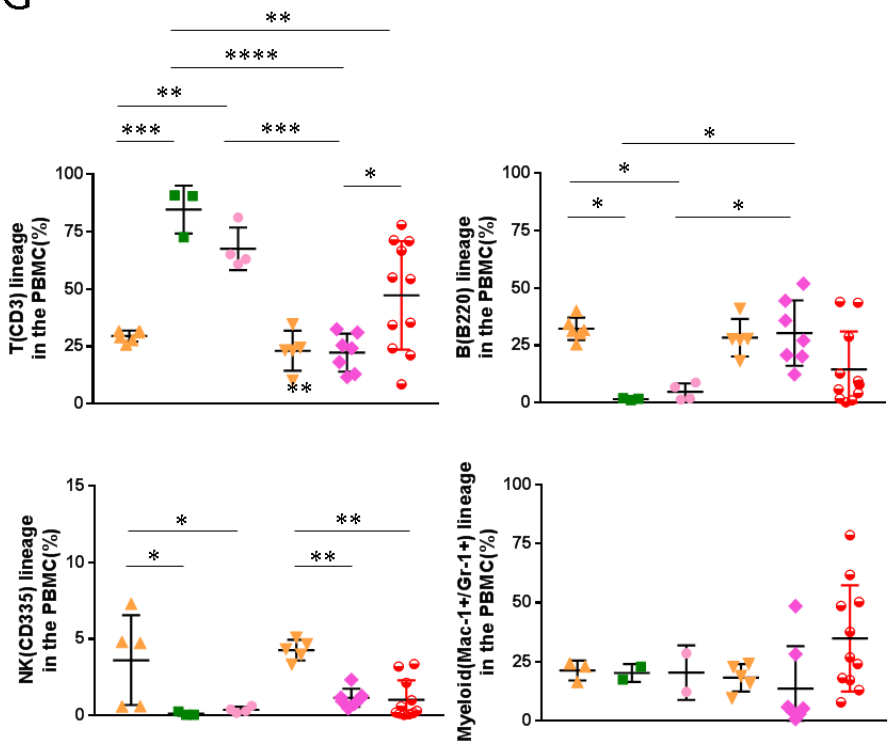
T(CD3) lineage in the PBMC(%)
B(B220) lineage in the PBMC(%)
NK(CD335) lineage in the PBMC(%)
Myeloid(Mac-1+/Gr-1+) lineage in the PBMC(%)

Figure 14: Flowcytometirc analysis of T-, B-, NK- and Myeloid-lineage population obtained from the spleen, thymus, lymph nodes and PBMC of terminally sick of 4 different genotype mice and aged-matched wild-type control mice

(A) (C) (E) (G) FACS analysis of the percentages of $CD3^+$ T cells, $B220^+$ B cells, $CD335^+$ NK cells and $Mac\text{-}1^+/Gr\text{-}1^+$ Macrophages/Granular cells in the spleen, thymus, lymph nodes and PBMC of 4 different genotypes of mice at lethal disease stage compared to age-matched wild-type control mice. (B) (D) (F) FACS analysis of the percentages of DN ($CD4^-CD8^-$) cells, DP($CD4^+CD8^+$) cells, SP ($CD4^+CD8^-$) cells, and SP ($CD4^-CD8^+$) cells in the spleen, thymus, lymph nodes and PBMC of 4 different genotypes of mice at lethal disease stage compared to age-matched wild-type control mice. Data are shown as mean ± SEM. Centerlines indicate the means. *P-value* was calculated using the ordinary one-way ANOVA multiple comparisons. * indicates $P<0.05$, ** indicates $P<0.01$, *** indicates $P<0.001$, **** indicates $P<0.0001$.

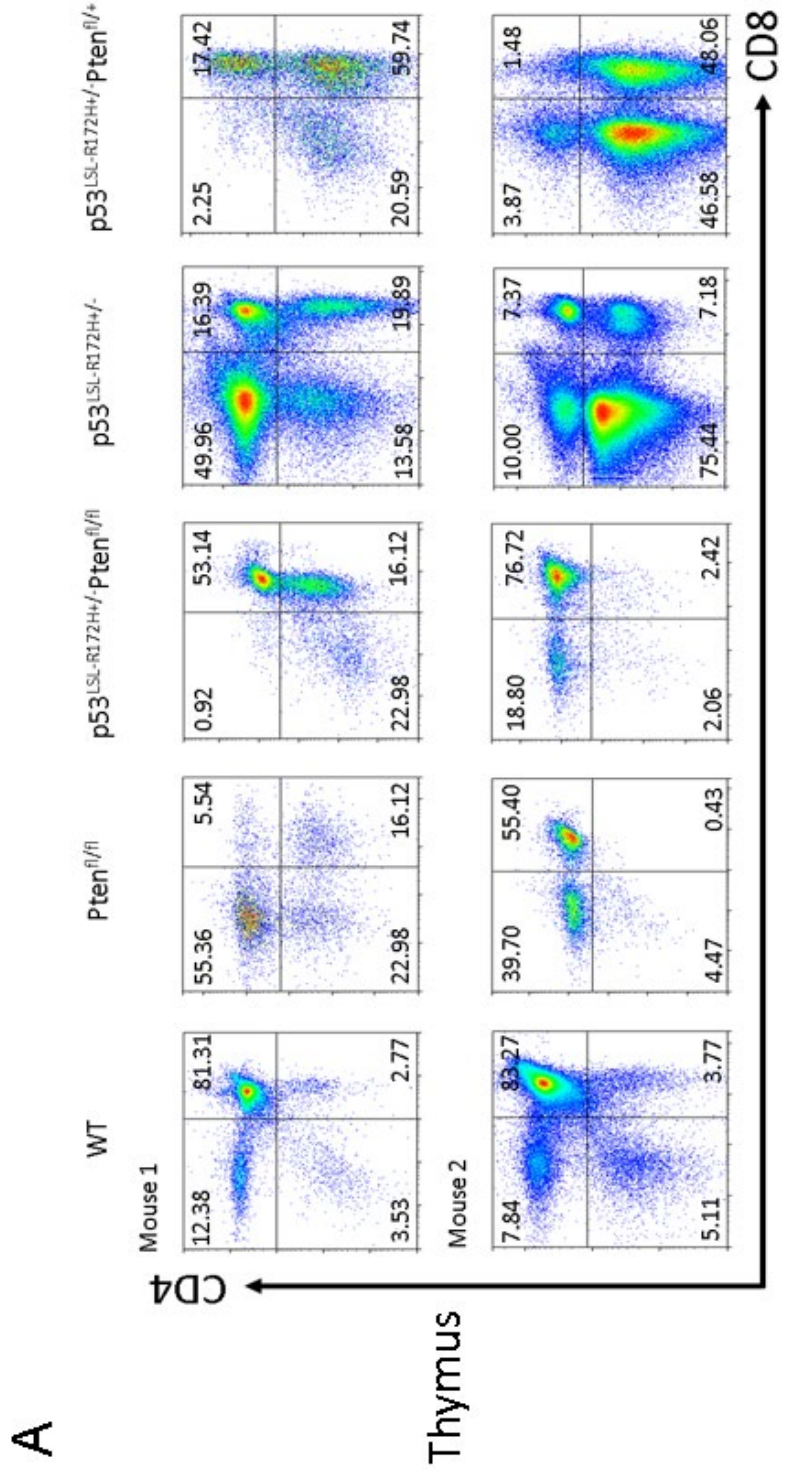
A
Thymus
CD4
CD8
WT
Pten fl/fl
p53 LSL-R172H+/- Pten fl/fl
p53 LSL-R172H+/-
p53 LSL-R172H+/- Pten fl/+
Mouse 1
Mouse 2
12.38
81.31
3.53
2.77
55.36
5.54
22.98
16.12
0.92
53.14
22.98
16.12
49.96
16.39
13.58
19.89
2.25
17.42
20.59
59.74
7.84
83.27
5.11
3.77
39.70
55.40
4.47
0.43
18.80
76.72
2.06
2.42
10.00
7.37
75.44
7.18
3.87
1.48
46.58
48.06

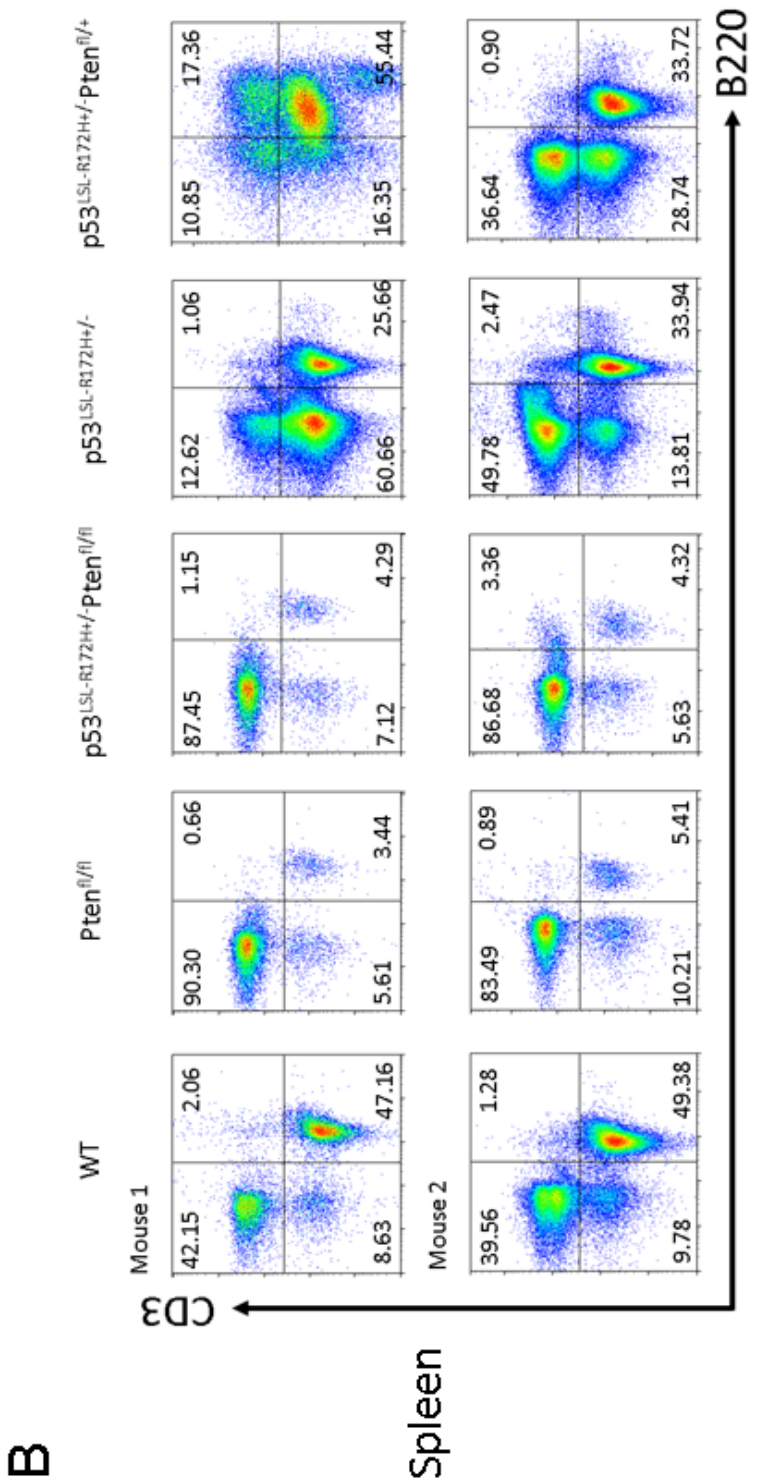
B
Spleen
WT
Pten fl/fl
p53 LSL-R172H+/- Pten fl/fl
p53 LSL-R172H+/-
p53 LSL-R172H+/- Pten fl/+
Mouse 1
Mouse 2
CD3
B220
42.15
2.06
8.63
47.16
90.30
0.66
5.61
3.44
87.45
1.15
7.12
4.29
12.62
1.06
60.66
25.66
10.85
17.36
16.35
55.44
39.56
1.28
9.78
49.38
83.49
0.89
10.21
5.41
86.68
3.36
5.63
4.32
49.78
2.47
13.81
33.94
36.64
0.90
28.74
33.72

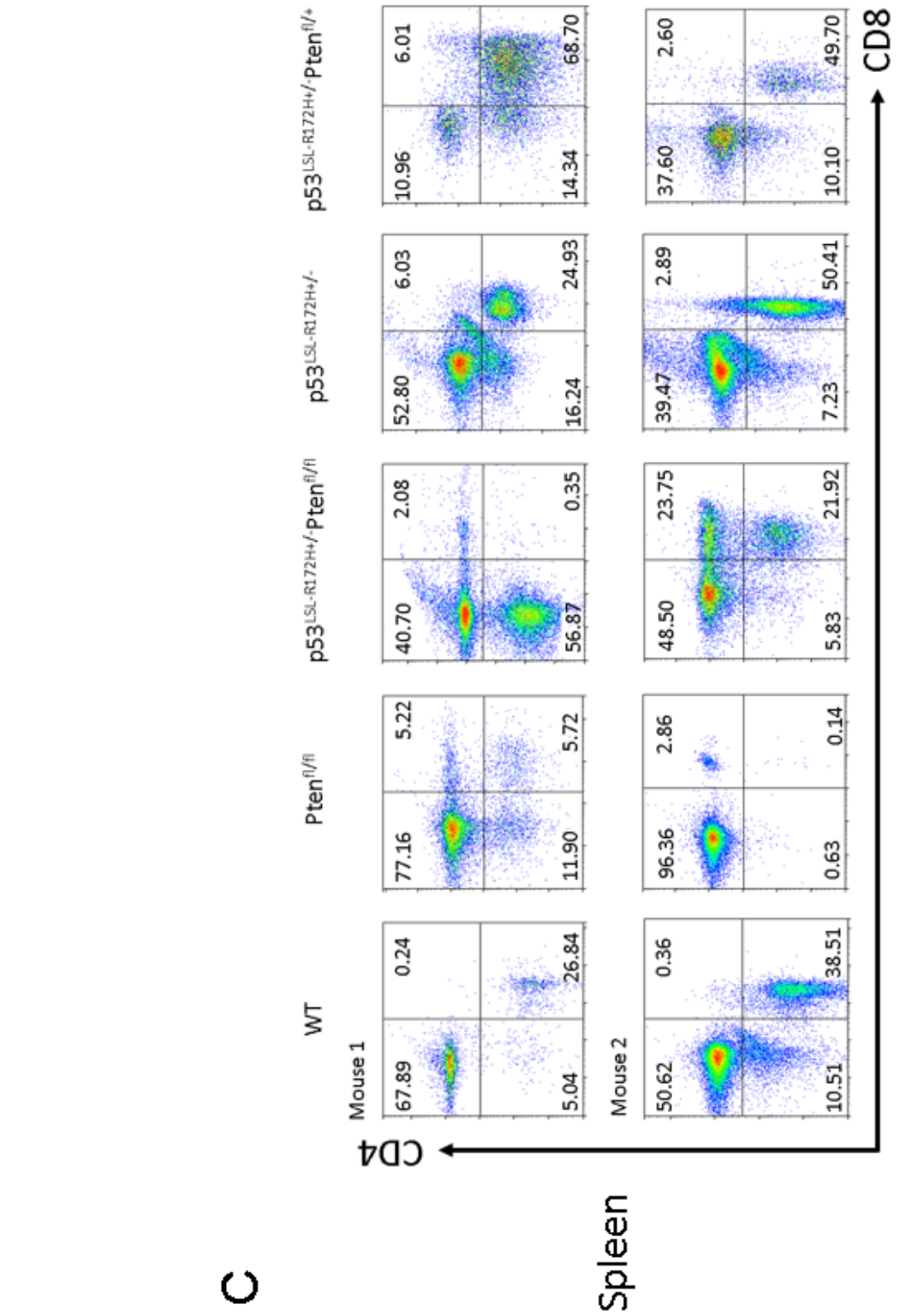
C
Spleen
WT
Pten fl/fl
p53 LSL-R172H+/- Pten fl/fl
p53 LSL-R172H+/-
p53 LSL-R172H+/- Pten fl/+
Mouse 1
Mouse 2
CD4
CD8
67.89
0.24
5.04
26.84
77.16
5.22
11.90
5.72
40.70
2.08
56.87
0.35
52.80
6.03
16.24
24.93
10.96
6.01
14.34
68.70
50.62
0.36
10.51
38.51
96.36
2.86
0.63
0.14
48.50
23.75
5.83
21.92
39.47
2.89
7.23
50.41
37.60
2.60
10.10
49.70

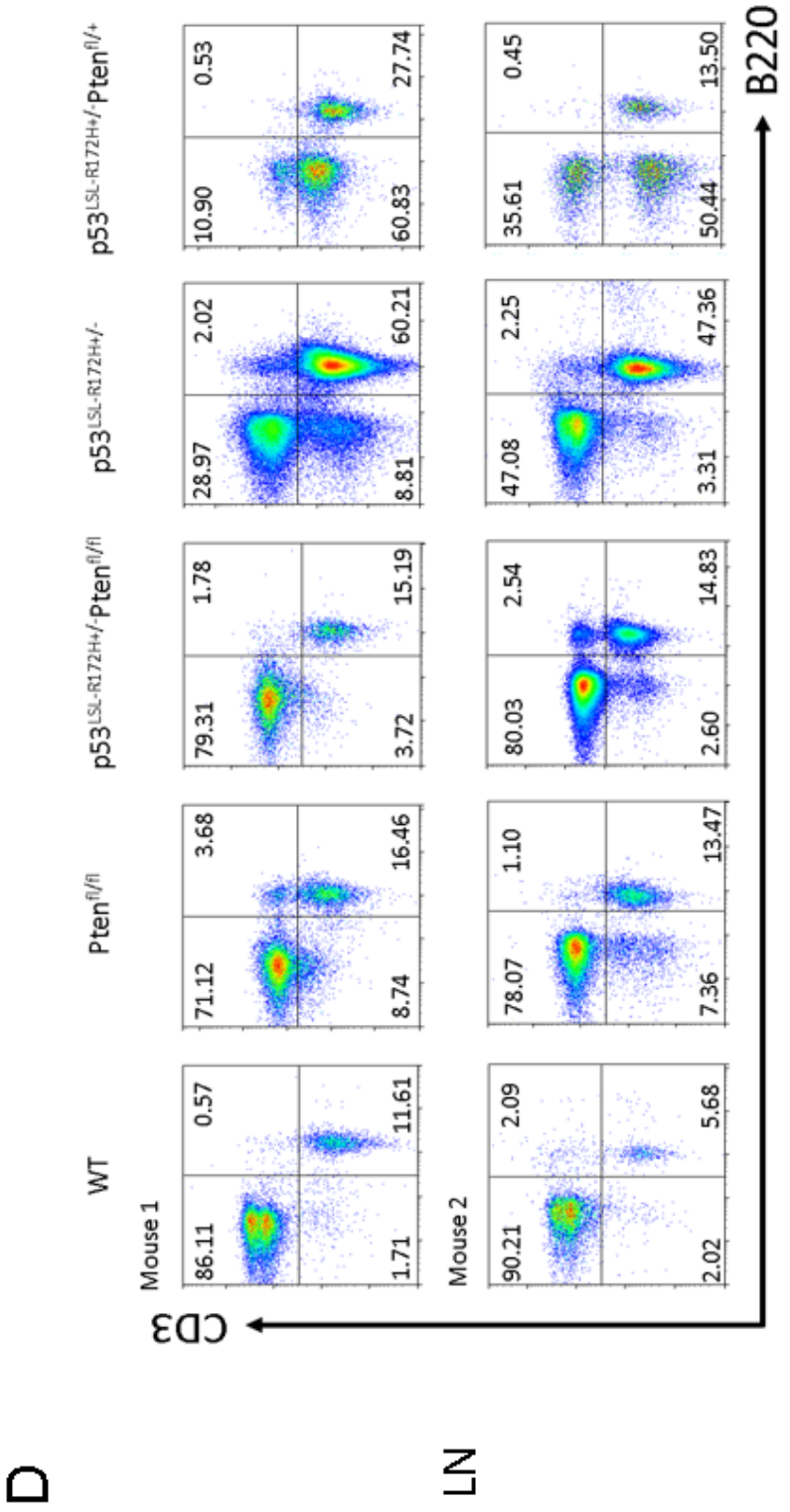
D
LN
WT
Pten fl/fl
p53 LSL-R172H+/- Pten fl/fl
p53 LSL-R172H+/-
p53 LSL-R172H+/- Pten fl/+
Mouse 1
Mouse 2
CD3
B220
86.11
0.57
1.71
11.61
71.12
3.68
8.74
16.46
79.31
1.78
3.72
15.19
28.97
2.02
8.81
60.21
10.90
0.53
60.83
27.74
90.21
2.09
2.02
5.68
78.07
1.10
7.36
13.47
80.03
2.54
2.60
14.83
47.08
2.25
3.31
47.36
35.61
0.45
50.44
13.50

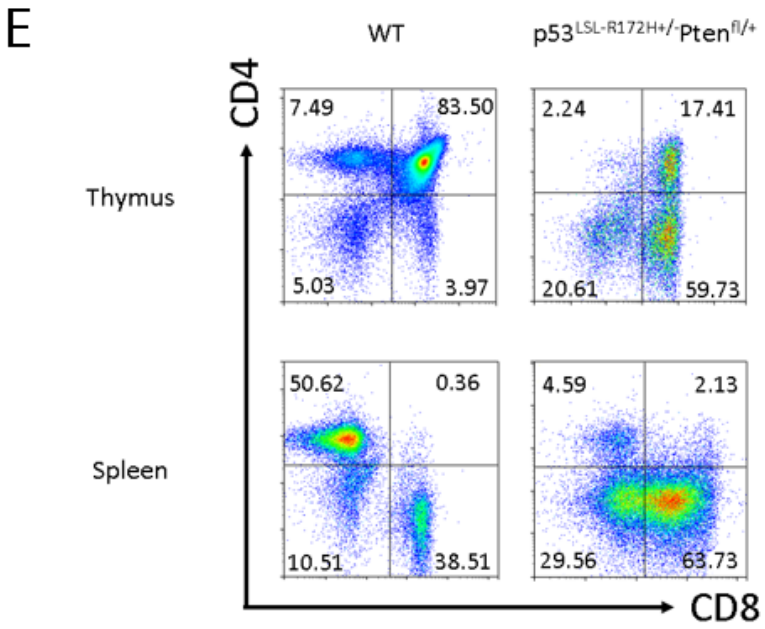
E
WT
p53LSL-R172H+/-Ptenfl/+
CD4
CD8
Thymus
Spleen
7.49
83.50
5.03
3.97
2.24
17.41
20.61
59.73
50.62
0.36
10.51
38.51
4.59
2.13
29.56
63.73

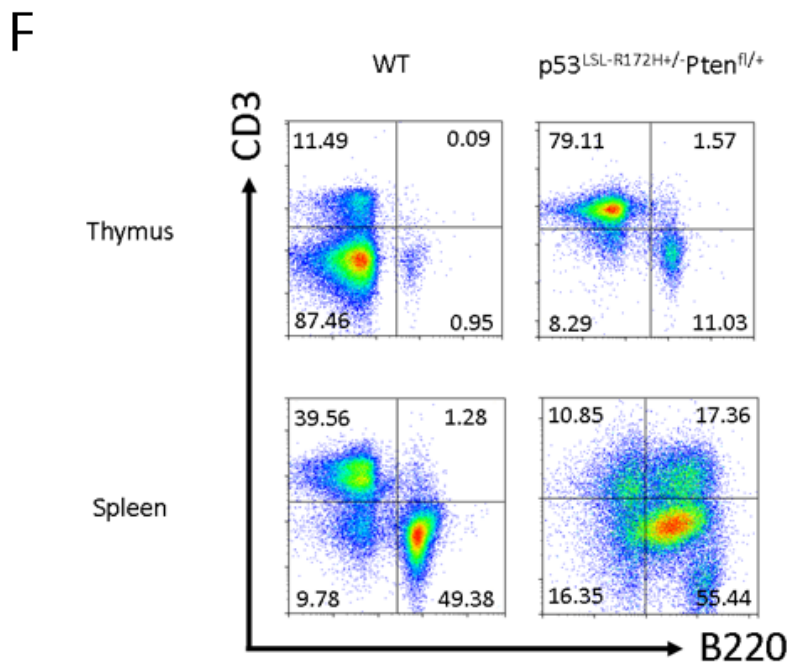
F
WT
p53LSL-R172H+/-Ptenfl/+
CD3
B220
Thymus
Spleen
11.49
0.09
87.46
0.95
79.11
1.57
8.29
11.03
39.56
1.28
9.78
49.38
10.85
17.36
16.35
55.44

G

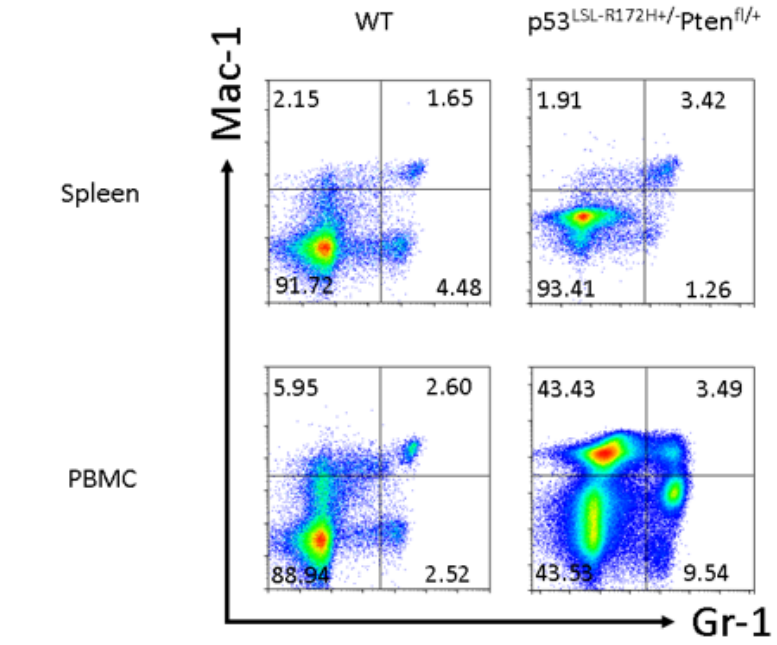
WT
p53LSL-R172H+/-Pten fl/+
Mac-1
Spleen
PBMC
2.15
1.65
91.72
4.48
1.91
3.42
93.41
1.26
5.95
2.60
88.94
2.52
43.43
3.49
43.53
9.54
Gr-1

Figure 15: Loss of *p53* and/or *Pten* in T cells results in a differentiation block at different stage of T cell development

(A) (C) Representative flow cytometry plots showing CD4 vs CD8 expression from two of each of the various genotypes of tumor-bearing mice and age-matched wild-type control mice on the thymus and spleen, respectively. (B) (D) Representative flow cytometry plots showing CD3 vs B220 expression from two of each of the various genotypes of tumor-bearing mice and age-matched wild-type control mice on the spleen and lymph nodes. (E) (F) FACS analysis of CD4 vs CD8, and CD3 vs B220 expression from thymocytes and splenocytes of a representative $p53^{LSL\text{-}R172H+/-}Pten^{fl/+}$ mouse compare to age-matched wild-type control mouse. (G) FACS analysis of Mac-1 vs Gr-1 expression from splenocytes and PBMC of a representative $p53^{LSL\text{-}R172H+/-}Pten^{fl/+}$ mouse compare to age-matched wild-type control mouse.

Chapter 4 Functional cooperation of *p53* and *Pten* on T cell homeostasis *in vitro*

Introduction

Naïve $CD4^+$ T cells proliferate and differentiate in response to signals from the TCR and CD28 costimulatory receptors, and the differentiation pathway can be influenced by a 'third signal' from the environment to result in diverse phenotypic and functional outcomes. In particular, signals from cytokines through the common gamma chain, such as interleukin-2 (IL-2), contribute to signal 3 by promoting the survival and expansion of T cells[174]. Although conventional antigen-specific CD4 T cell activation has been well characterized, unconventional activation of CD4 T cells, known as "bystander" T cells, in the absence of antigen and the downstream functional consequences have been less described[175]. Recently, Watanabe[176] and colleagues provide insight into this process by demonstrating that p53 imposes the checkpoint that prevents the proliferation of bystander T cells exposed to signal 3, in the form of IL-2, and that this checkpoint is lifted by signals delivered through the TCR[174].

p53 is a transcription factor that mainly promotes cell cycle arrest, DNA repair, cellular senescence and apoptosis in stress conditions, and the function of p53 is to

avoid the accumulation of DNA changes which can lead to carcinogenesis. The reversible cell-cycle arrest induced by p53 is mainly mediated by the downstream transcription activation of p21/WAF1[177], which binds to cyclin E/Cdk2 and cyclin D/Cdk4 complexes and further promotes transcription silencing of E2F1 targets through binding to pRb[178-180]. By arresting cells at the G1 phase which allows time for the repair of potentially lethal DNA double-strand breaks before further cell division, *TP53* maintains chromosomal integrity and improves the survival of damaged cells[181]. In some circumstances, *TP53* favors the cell entrance into the G0 phase through transactivation of *p21* which results in irreversible arrest called replicative senescence[182], which also involves the *RB* gene product[183]. Senescent cells have unique features including large cell size, active autophagy, high lysosomal SA-β-gal activity, and secretion of pro-inflammatory cytokines[184]. PTEN manifests its tumor suppressor function by inducing G1-phase cell cycle arrest through decreasing the level of nuclear cyclin D1[185]. Therefore, the functional cross-talk between p53 and PI3K signaling pathways may affect the cell fate between reversible cell cycle arrest and irreversible cellular senescence.

Another prominent outcome of *TP53* activation is apoptosis if DNA damage is abnormally widespread. Although cell apoptosis and the cell cycle are tightly linked, they are controlled by distinct cellular machinery. p53 promotes apoptosis through the induction of pro-apoptotic Bcl-2 family members such as PUMA and NOXA[186], whose action facilitates caspase activation and cell death, whereas *TP53* gain-of-function

(GOF) mutation is usually resistant to a variety of pro-apoptotic signals by suppressing cMyc-induced apoptosis[187], which exacerbate the consequences of *TP53* loss. T cells from either *p53*$^{-/-}$ or *p53*$^{+/515A}$ mice are less apoptotic in response to CD3 stimulation[142,188]. However, no significant difference in the proportion of apoptotic cells between WT and *p53*$^{-/-}$ clones were detected in another study[176]. In contrast, PTEN induces apoptosis through PI3K/AKT-dependent and -independent pathways[189]. Some studies have shown *PTEN* as a downstream transcriptional target of p53 in mediating apoptosis[190], whereas others suggest that PTEN acts upstream of p53 by increasing p53 stability[191]. However, the relationship between the activation of the p53 pathway and the PI3K pathway *in vivo* is extremely complex.

It has become clear that *TP53* and *PTEN* somatic mutations are mutually exclusive and usually does not occur in the same compartment or the same sample[192,193], indicating the genetic alterations indeed occur independently and these two guardians of the genome are functionally distinct in homeostasis and cellular processes. However, functional cross-talk and reciprocal cooperation between p53 signaling and PI3K signaling pathways are necessary for proper actions in the protection of the genome and have been applied to several animal models, such as in triple-negative breast cancer, prostate cancer, and high-grade astrocytomas[131,132,194]. In contrast, the functional cross-talk of *TP53* and *PTEN* in T cells is lacking.

The latest appreciation is not just confined to the understanding of the basic aspects of T cell biology; also, the new insights of cell-of-origin provide a deep

understanding of the pathogenesis of immune-mediated disease and new opportunities for therapy[195]. After engagement of the TCR by the MHC complex, clonal expansion was triggered and naïve $CD4^+$ T cells rapidly undergo programmed differentiation into a variety of effector subsets, including classical Th1 cells and Th2 cells[5,196]. The differentiation process is highly plastic, and the decision is governed by both intrinsic and extrinsic factors that drive specific mechanisms that influence flexibility[195]. It has been well-characterized than exogenous cytokines in the microenvironment bind to the membrane receptors of the cell and activate intracellular signaling pathways which up-regulate the master transcription factor, T-bet for Th1 and GATA3 for Th2, which results in effector cell differentiation[5]. In addition to environmental factors, genetic alterations also contributed to effector subsets differentiation. Upon TCR stimulation, melanoma patient-derived *p53*-KO TCR transgenic $CD8^+$ T cells exhibit increased T-bet expression and correlates to a 2-fold more IFNγ secretion compared with the h3T T cells[197]. In contrast, germline deletion of $p53^{+/-}$ mice down-regulated Th1 response and shift into a Th2 phenotype after gastric helicobacter infection[198]. Strong Th2-type cytokine production and GATA3 expression were also significantly increased 15 days after SRBC-injection in $p53^{-/-}$ mice[199]. PI3K/mTOR signaling is required for enhanced GATA3 translation and Th2 cell differentiation[107]. T cells from $mTOR^{-/-}$ mice failed to differentiate into effector Th1 or Th2 cells under corresponding polarization conditions[106], highlighting the role of mTOR in the development of distinct effector subset of T cells. Furthermore, in the absence

of PI3K/mTOR signaling, a specific defect in Th2 differentiation correlates with down-regulation of GATA3 translation has been detected[107]. Alternatively, Buckler and his colleague demonstrated enhanced activation of the PI3K/mTOR pathway by primary *Pten*-deficiency $CD4^+$ T cells have a Th2 bias after 96 h of TCR stimulation *in vitro* compare to its WT counterpart[108]. These data highlight the possibility of the cooperative role of *p53* and *Pten* in regulation of Th2 differentiation. Collectively, these data strongly support the idea that *p53* and *Pten* plays a critical role in regulating the response of mature T cells in the periphery, especially for the cross-talk between *p53* and *Pten in vitro*.

Results

$p53^{R172H}$ switch $CD4^+$ T cells from arrest into proliferation in the context of *Pten*-deficiency in response to TCR ligation *in vitro*

An effective immune system requires a high degree of antigen specificity in responses of T cells to specific antigen and cytokines. Activated $CD4^+$ T cells express high-affinity IL-2R which comprise α, β, γ chains, and binding if IL-2 to IL-2R contributes to clonal expansion of $CD4^+$ T cells via activation of multiple signaling cascades such as JAK-STAT and PI3K/Akt[200,201]. Therefore, to address the role of *p53* and *Pten* in T cell growth upon Ag-specific stimulation, we stimulated naive $CD4^+$ T cells fresh isolated from 4-week age mice with anti-CD3 mAb/anti-CD28 mAb and 20ng/ml IL-2 in 1%, 5% and 20% fetal bovine serum (FBS) supplied media, respectively. After 2 d resting state, transgenic and wild-type $CD4^+$ T cells started a fast and stable rate of

proliferation in media supplied with 1%, 5% and 20% FBS culture conditions (Figure 16A B C). After this time point, a stark difference in proliferation rates was observed on $CD4^+$ T cells among various genotypes. Although most of the transgenic $CD4^+$ T cells continued to show increased cell growth in the presence of a TCR stimulus, the proliferation rate was inhibited in all of the transgenic compared to wild-type $CD4^+$ T cells in 1% FBS supplied culture media (Figure 16A), especially in $Pten^{fl/fl}$ and $p53^{LSL\text{-}R172H+/\text{-}}Pten^{fl/+}$ $CD4^+$ T cells which showed a drastic growth arrest, suggesting *Pten* acts as an important growth factor in this scenario. The previous reports[145,202] studying the biological effects of loss of *p53* and *Pten* in prostate epithelial cells have shown though complete *Pten*-loss activates the Akt pathway, but also triggers p53-mediated senescence[145]. Consistently, we found that $Pten^{fl/fl}$ primary $CD4^+$ T cells significantly arrested in a growth assay when compared to WT $CD4^+$ T cells in our model (Figure 16A B C), pinpointing the possibility that a p53-mediated senescence response restricts cell growth in *Pten*-null background in our model system. Even though without reaching statistical significance, loss of both *Pten* alleles lead to a lower proliferation compare to a decrease in *Pten* levels by 50% in heterozygous $CD4^+$ T cells in 1%, 5%, and 20% FBS culture conditions, indicating that *Pten* triggers p53-mediated cellular senescence in a copy-dependent manner (Figure 16A B C). However, further experiments are required for validation of our findings, such as β-Gal staining and p53 expression on these cells. A decrease in Pten levels by 50% in heterozygous $CD4^+$ T cells resulted in lowered proliferation compare to WT $CD4^+$ T cells, however,

further loss of *p53* in the context of heterozygous loss of *Pten* switched $CD4^+$ T cells from arrest into proliferation. As showed in Figure 16B and 16C, $p53^{LSL\text{-}R172H+/-}Pten^{fl/+}$ $CD4^+$ T cells have significant growth advantage comparing to $Pten^{fl/+}$ $CD4^+$ T cells, as well as other genotypes especially in 5% and 20% FBS, supplied culture media, indicating $p53^{R172H}$ rendered $CD4^+$ T cells with full proliferative potential in the setting of conditional heterozygous loss of *Pten* (Figure 16B C).

The dose of *Pten* dictates cell growth by regulation of apoptotic cell death

To gain insights into the mechanisms responsible for the differential proliferation rate for the transgenic and wild-type $CD4^+$ T cells in response to TCR signal and cytokine stimulation, we next compared the cellular response of day 10 cultured $CD4^+$ T cells in a serum depletion assay. After 10 d of activation, cell apoptosis was analyzed by staining with early apoptotic marker Annexin V and cell viability dye 7-AAD. Cells that are 7-AAD^+ are considered dead, and Annexin V^+, 7-AAD^- is considered the early stage of apoptosis. Cell cycle progression was measured by DNA content through propidium iodide (PI) staining. As predicted based on the robust cell growth under basal condition (20% FBS) (Figure 16C), transgenic and WT $CD4^+$ T cells showed low levels of cell death, but no significant difference has been detected among 6 genotypes of mice in cell cycle analysis (Figure 16D E), suggesting 20% FBS protected transgenic and WT $CD4^+$ T cells from apoptosis without significantly affecting cell cycle progression. High apoptosis was detected in serum restricted conditions (Figure 16D), which is consistent with a substantial level of DNA degradation (>50%) as indicated by

the appearance of sub-G1/G0 DNA in the cell cycle analysis (Figure 16E).

As expected, *p53*^{R172H} showed the ability to confer on cells an elevated resistance to apoptotic cell death in *p53*$^{LSL\text{-}R172H+/-}$ and *p53*$^{LSL\text{-}R172H+/-}$*Pten*$^{fl/+}$ compared to wild-type CD4^{+} T cells (*P*=0.5498 and 0.2113, respectively) (Figure 16D), indicating *p53*^{R172H} are resistant to bead-coated Ab-induced apoptosis. The statistical significance was not reached due to the fact that apoptotic cell death was marginally affected by the expression of p53 in wild-type CD4^{+} T cells. Indeed, this was found to be the case in another study, in which apoptosis in T cells caused by p53 was observed only when the stimulation was provided by the flat surface-coated Abs and not by bead-coated Abs[203]. However, the exact mechanisms by which p53 is unable to induce apoptosis in bead-coated Abs are unclear, but it is thought to involve the level of MDM2 in regulation of its activity[203].

In contrast, we observed significant increase in apoptotic cell death in *Pten*$^{fl/fl}$ compare to *Pten*$^{fl/+}$ CD4^{+} T cells in all 3 culture conditions (Figure 16D, 1% FBS, *P*=0.0816; 5% FBS, *P*=0.0008; 20% FBS, *P*=0.0001), suggesting *Pten* induces apoptosis in a dose-dependent manner. These observations prompted us to the hypothesis that Pten expression levels constitute discrete biochemical thresholds below which qualitative functional changes occur, contributing to T cell functions and tumor phenotypes. The apparent proliferative deficit in *Pten*-null CD4^{+} T cells is due to the remarkable induction of apoptosis (Figure 16A B C D). Regarding the underlying mechanisms, which is possibly caused by the enhanced expression of wild-type p53-

mediated apoptosis, triggered by complete ablation of *Pten.*

In agreement with this hypothesis, *p53*$^{LSL\text{-}R172H+/-}$*Pten*$^{fl/fl}$ CD4^{+} T cells induced a remarkable proportion of apoptotic cells compare to wild-type CD4^{+} T cells (Figure 16D, 1% FBS, *P*=0.0156; 5% FBS, *P*=0.0004, 20% FBS, *P*=0.0371), as well as compared to other genotypes. Functional impairment of T cell in *Pten*-null background antagonized by the introduction of the anti-apoptotic function of mutp53, suggesting *Pten* is the major survival factor in CD4^{+} T cells. Other than the *Pten*-null background, CD4^{+} T cells from the rest of the genotypes were able to continuously grow after anti-CD3 mAb/anti-CD28 mAb and IL-2 stimulation (Figure 16A B C), indicating cell death was not due to deterioration of the culture conditions, such as such as exhaustion of nutrients. Therefore, our data clearly demonstrate that, unlike previous reports of *Pten*-mediated apoptosis[189], the apoptotic cell death caused by bead-bound stimulation is dependent on complete ablation of *Pten*.

Interestingly, in the presence of limiting concentrations of serum (1%), reduced apoptosis was observed in *p53*$^{LSL\text{-}R172H+/-}$*Pten*$^{fl/+}$ compared to *Pten*$^{fl/+}$ CD4^{+} T cells (*P*=0.1730), in contrast, significantly enhanced apoptosis were detected in *p53*$^{LSL\text{-}R172H+/-}$*Pten*$^{fl/fl}$ as compare to *Pten*$^{fl/+}$ CD4^{+} T cells (*P*=0.0018) (Figure 16D). These observations suggested that apoptosis mediated by heterozygous loss of *Pten* was partially antagonized by the introduction of *p53*^{R172H}, however, the anti-apoptotic function of *p53*^{R172H} can be compromised by a stronger phenotype upon homozygous loss of *Pten*. Collectively, our data strongly suggests the cooperation of *p53* and *Pten*

in regulating the cellular response and biology of mature CD4$^+$ T cells *in vitro*.

$p53^{R172H}$ rendered CD4$^+$ T cell growth advantage in the absence of TCR stimulus

An effective immune system requires antigen-specific signal 1 delivered by T cell receptor (TCR) engagement with cognate antigenic peptides presented by major histocompatibility complexes (MHC) molecules[33], and signal 2 upon the recognition of co-stimulatory signaling[33,204] presented by APCs, as well as antigen-nonspecific signals provided by cytokines[38,174], for full T cell activation. Bystander T cell activation defines T cell activation that is independent of TCR signaling, which has been mainly observed in inflammatory environments, including autoimmunity, cancer, and infection[174,205]. TCR-independent activation during pathogenesis has primarily been observed in CD8$^+$ T cells, while less is known about CD4$^+$ bystander T cell activation. Recently, it has been reported that downregulation of *p53* by TCR signaling prevent CD4$^+$ T cell proliferation to antigen-nonspecific signals, but this inhibition is overcome by antigen-specific TCR signaling, revealing the role of *p53* in the mediation of limiting bystander proliferation of CD4$^+$ T cells in an antigen-independent manner[176]. However, the collaborative role of *p53;Pten* in antigen-nonspecific signal driven CD4$^+$ T cell proliferation is unclear.

To characterize the role of antigen-nonspecific signals (IL-2) during T-cell priming *in vitro*, we depleted TCR stimulation and supplied culture media with 3 different concentrations of IL-2. 20% of FBS were supplied to all the culture conditions. After a 15 d of resting-state upon antigen-independent stimulation, CD4$^+$ T cells start

to proliferate (Figure 16F G H). As compared to normal antigen-specific IL-2-driven T cell proliferation (Figure 16C), growth advantage in *p53*$^{LSL\text{-}R172H+/-}$*Pten*$^{fl/+}$ CD4^{+} T cells has been retained upon antigen-nonspecific IL-2-driven T cell proliferation (Figure 16F G), suggesting the loss of one *Pten* allele or reduction in its expression plays a key role in accelerating cell growth in *p53*^{R172H} CD4^{+} T cells through TCR-dependent and -independent pathways.

In the absence of antigen stimulation, strikingly, *p53*$^{LSL\text{-}R172H+/-}$*Pten*$^{fl/+}$ and *p53*$^{LSL\text{-}R172H+/-}$*Pten*$^{fl/fl}$ CD4^{+} T cells proliferated strongly to lower concentrations of IL-2 at a magnitude of response compared to other genotypes of CD4^{+} T cells (Figure 16F). In particular, antigen-nonspecific IL-2-driven stimulation converts *p53*$^{LSL\text{-}R172H+/-}$*Pten*$^{fl/fl}$ CD4^{+} T cells from growth inhibited to a highly proliferative state by removing TCR stimulation, indicating *p53*^{R172H} rendered CD4^{+} T cell growth advantage in the absence of TCR stimulus. Furthermore, this function is dependent on loss of a *Pten* allele, as shown in Figure 16F and 16G, *p53*$^{LSL\text{-}R172H+/-}$ CD4^{+} T cells remain growth inhibited upon 10ng/ml and 20ng/ml antigen-nonspecific IL-2-driven stimulation.

In the context of *p53*^{R172H}, *p53*$^{LSL\text{-}R172H+/-}$*Pten*$^{fl/+}$ and *p53*$^{LSL\text{-}R172H+/-}$*Pten*$^{fl/fl}$ CD4^{+} T cells arrested growth in a *Pten* dose-dependent manner as compared to p53$^{LSL\text{-}R172H+/-}$ CD4^{+} T cells in the high concentration of IL-2 (40ng/ml) without TCR stimulus (Figure 16H). Similarly, *Pten*$^{fl/fl}$ CD4^{+} T cells have a lower proliferation rate compared to *Pten*$^{fl/+}$ CD4^{+} T cells (Figure 16H). These observations demonstrated that *Pten* expression probably renders CD4^{+} T cells tumor-promoting properties in the settings of high doses

of IL-2 in the absence of TCR stimulus.

We hypothesized that IL-2 signals during priming were required for the acquisition of long-term survival potential by activated CD4$^+$ T cells. We next analyzed the effects of the withdrawal of signals via cytokine stimulation *in vitro* and observed that after obtaining the maximum activation on day 4, CD4$^+$ T cells ceased to proliferate and remained relatively constant over the time course among all 6 genotypes, demonstrated that IL-2 is not required for initial expansion, but is required for the long-term survival of primed T cells *in vitro* (Figure 16I). Hyper-responsiveness to sub-optimal T cell stimulation has been observed in *p53*$^{R172H+/-}$*Pten*$^{fl/fl}$ CD4$^+$ T cells upon TCR stimulation, which is possibly due to the augmented response to TCR signals in the absence of *Pten*. The observation that *p53*$^{R172H+/-}$*Pten*$^{fl/fl}$ CD4$^+$ T cells obtained augmented response to sub-optimal T cell stimulation raised the possibility that *p53;Pten* deficient T cells probably no longer have a stringent requirement for all of the 3 signals to become fully activated (Figure 16I).

Polarization of naïve CD4$^+$ T cells toward the Th2 subset by *p53*$^{LSL\text{-}R172H+/-}$*Pten*$^{fl/+}$ cells

The significance of the association between genes from various genotypes and the functional pathway was calculated by ingenuity pathway analysis (IPA) using a two-tailed Fisher exact test. In this study we identified the top differentially expressed genes of *p53;Pten* mutant CD4$^+$ T cells compared to wild-type CD4$^+$ T cells using the cutoff of $P<0.05$, and the top differentially expressed genes were identified. *Pten* deficiency

skews CD4$^+$ T cells into the Th2 phenotype, as Th2 signaling augments in *Pten*$^{fl/+}$, *Pten*$^{fl/fl}$, *p53*$^{LSL\text{-}R172H+/-}$*Pten*$^{fl/fl}$ and *p53*$^{LSL\text{-}R172H+/-}$*Pten*$^{fl/+}$ CD4$^+$ T cells (Figure 17A). In contrast, *p53*^{R172H} alone did not have intrinsic ability to skew cells towards Th2 differentiation, as both IL-6 and PI3K signaling are significantly downregulated in these cells.

To determine whether the cooperation between *p53* and *Pten* affects Th cell subset polarization, we first examined the effect of *p53;Pten* deficiency on Th1 and Th2 cell differentiation in the absence of exogenous polarizing cytokines *in vitro*. After a 10 d culturing, we phenotyped them according to their differential expression of Gata3 and T-bet, as both markers correlate with lineage specificity. Protein expression of p53 and Pten were also examined on these cells. High expression of p53 in *p53*$^{LSL\text{-}R172H+/-}$, *p53*$^{LSL\text{-}R172H+/-}$*Pten*$^{fl/+}$ and *p53*$^{LSL\text{-}R172H+/-}$Pten$^{fl/fl}$ and drastically decreased expression of Pten in *Pten*$^{fl/+}$, *Pten*$^{fl/fl}$, and *p53*$^{LSL\text{-}R172H+/-}$*Pten*$^{fl/+}$ transgenic comparing to wild-type CD4$^+$ T cells have been detected, which further confirmed increased expression of p53 and loss of function of Pten in protein level (Figure 17B C). However, Gata3 and T-bet protein expression were either decreased or remained normal in transgenic CD4$^+$ T cells compared to wild-type CD4$^+$ T cells (Figure 17B C), suggesting *p53;Pten* deficient CD4$^+$ T cells do not intrinsic mediate Th1 or Th2 cell differentiation without stimulation of exogenous polarization cytokines *in vitro*.

To better mimic the *in vivo* conditions, we proceeded to stimulate naïve CD4$^+$ T cells from C57BL/6 mice under exogenous Th1 and Th2 polarizing conditions,

respectively. After 96 hrs of the priming, we examined the protein expression of Gata3 and T-bet for $CD4^+$ T cells in each culture condition (Figure 17D E). As we expected, $p53^{LSL\text{-}R172H+/-}Pten^{fl/+}$ $CD4^+$ T cells skew more to the Th2 phenotype compared to other genotypes (Figure 17D E). It should be noted that the T cells from C57BL/6 mice preferentially produce Th1 cytokines with high IFN and low interleukin IL-4, whereas those from BALB/c mice favor Th2 cytokine production with low IFN and high IL-4 due to the genetically programmed biases[206]. Even though this effect was not significant, the potential influence of high Gata3 protein level can results in a huge impact on Th2-associated transcripts and cytokine expression, based on the fact that Gata3 orchestrates the regulatory gene network for a Th2 subtype differentiation. In contrast, all genotypes of *p53;Pten*-deficient $CD4^+$ T cells have less potential to skew to Th1 phenotype compare to wild-type with stimulation of Th1 conditions (Figure 17D E). This further confirmed our hypothesis that *p53;Pten* deficiency skews $CD4^+$ T cells into a Th2 phenotype, but not Th1 phenotype. Though micro-environmental factors in the tissues are thought to provide additional cues that drive T helper cell differentiation, our data provide evidence that genetic background could be more important in the effects of T cell differentiation in lymphoid malignancies.

Adoptive transfer of tumor-primed, non-activated $CD4^+$ T cells

Due to the fact that peripheral T cell lymphoma originates from mature post-thymic T cells, we next carried out adoptive transfer studies to evaluate if the phenotype of mature $CD4^+$ T cells with *p53;Pten* deficiency can give rise to PTCL-

GATA3 in genetically compatible hosts. $CD4^+$ T cells were negatively isolated from the spleen of 4 weeks of age mice, yielding between 1-6 million of the initial cell number. The $CD4^+$ subset purity was examined by flow cytometric analysis. $CD4^+CD45.2^+$ splenocytes were obtained from individual *Pten*$^{fl/fl}$, *p53*$^{LSL\text{-}R172H+/-}$*Pten*$^{fl/fl}$, *p53*$^{LSL\text{-}R172H+/-}$ *Pten*$^{fl/+}$ and *p53*$^{LSL\text{-}R172H+/-}$ mice and adoptively transferred, via either tail or retro-orbital intravenously injection, to $CD45.1^+$ sublethally (6 Gy) irradiated host mice (Figure 18A). By taking advantage of specific antibodies to CD45.2 and CD45.1, for donor and host respectively, to unambiguously distinguish donor and host cells, we next examined the ability of donor $CD4^+$ T cells to persist after intravenous injection into sub-lethal irradiated host mice. The steady-state engraftment of $CD45.2^+$ cells was routinely detected in PBMC obtained through maxillary bleeding 2 weeks post-adoptive transfer (Figure 18B). In addition, donor $CD4^+$ T cells had no detectable efficacy below 1 X 10^6 cells transfer, which probably was the result of a limited density of cells in the infused population for engraftment.

We next examined the ability of $CD4^+$ T cells to persist after intravenous injection into host mice. As we expected, there was a stable increase in the percentage of donor T cells in the blood of recipient mice receiving *Pten*$^{fl/fl}$ and *p53*$^{LSL\text{-}R172H+/-}$*Pten*$^{fl/fl}$ donor $CD4^+$ T cells (Figure 18B C). In contrast, there was a significant decrease in the percentage of donor T cells in the blood of recipient mice having received *p53*$^{LSL\text{-}R172H+/-}$ donor $CD4^+$ T cells and remained the level of at approximately 5% engraftment until it fell below the level of detection (Figure 18C). These results indicate the superior

engraftment ability of *Pten*$^{fl/fl}$ and *p53*$^{LSL\text{-}R172H+/-}$*Pten*$^{fl/fl}$ donor CD4$^+$ T cells as compared to *p53*$^{LSL\text{-}R172H+/-}$ donor CD4$^+$ T cells, which possibly reflects the preferential expansion and survival ability of *Pten*-null cells *in vivo*.

Tumors grew robustly in *Pten*$^{fl/fl}$ CD4$^+$ T cells transplanted mice due to the fact that it reached to fatal illness 3.4 months post-engrafted. In contrast, there was a 3 fold increase in the number of splenocytes of *Pten*$^{fl/fl}$ CD4$^+$ T cells transplanted mice as compared to wild-type control mice (Figure 18D). Flow cytometric analysis of cell composition for *Pten*$^{fl/fl}$ donor CD4$^+$ T cells transplanted tumor-bearing mice shows a significantly high percentage of SP CD8$^+$ T homed to the thymus and spleen of the transplanted mice, indicating that the *Pten*-null CD4$^+$ T cells can markedly augment CD8$^+$ T cell responses in the host mice (Figure 18E).

Discussion

Deletion of chromosome 10q encompassing *PTEN* in human cancer typically affects one allele, whereas the other copy is retained[145,207], suggesting that dosage is important determinant of its biological consequences[145,208]. The most common *TP53* configuration involves a missense mutation together with a segmental 17p deletion of the wild-type *TP53* allele. *TP53* mutation may also act in a dominant-negative manner to inhibit wild-type *TP53* function in lymphoid malignancies[81,209]. Both *TP53* and *PTEN* are known as the guardian of the genome, although they are functionally distinct, reciprocal cooperation has been proposed. Recent advances in whole genome-sequencing analyses reveal that *TP53* and *PTEN* are often co-deleted in highly

aggressive types of cancers, which associated with the worst survival outcome for patients in particular subtypes[210]. Importantly, tracking the clonal origin of PTCL-GATA3 through patient samples collected from multiple institutions at the time of death identified that a significant number of primary PTCL-GATA3 carrying mutant *TP53* and *PTEN* deletion. However, the molecular basis of cooperation between *TP53* and *PTEN* in $CD4^+$ T cells is unknown. For this reason, we studied the consequences of both heterozygous and homozygous deletion of *p53* and *Pten* in mouse $CD4^+$ T cells. As the splenic and lymphoid compartments at 4-weeks age *p53;Pten* mice are grossly normal, containing appropriate numbers and ratios of lymphoid and myeloid cell populations and $CD4^+$ T cells isolated from these mice are phenotypically and functionally naïve[108], we used fresh isolated splenic $CD4^+$ T cells from 4-weeks old C57BL/6 mice to perform all the *in vitro* studies.

To characterize the T-cell biology of *p53;Pten* deficient mice, we performed cell proliferation, cell apoptosis, and cell cycle analysis on fresh isolated 4 weeks age $CD4^+$ T cells. The physiologic stimuli which activate T cells include antigen-specific stimuli delivered through TCR, recognition of costimulatory ligands and integration of Ag-nonspecific signals provided by cytokines. In the presence of conventional T cell activation, $CD4^+$ T cells of 6 genotypes gave strong IL-2-dependent proliferative responses, which leads to the creation of clonal expansion and ultimately, memory. The canonical function of *PTEN* is to put a ‘brake’ on cell proliferation and survival and loss of *PTEN* is expected to abolish these mechanisms. However, as demonstrated by

recent studies[145,211], loss of *Pten* activated p53-mediated senescence, whereas loss of *p53* caused immortalization of mouse embryonic fibroblasts (MEFs) as the cells bypassed senescence, suggesting rather than further promoting cancer progression, complete loss of *PTEN* is potently tumor suppressive and much less tumorigenic than the heterozygous loss of *PTEN*[94]. In addition, inhibition of PTEN expression in U1242 cells harboring a gain-of-function mutation of $p53^{R175H}$ leads to a significant inhibition *in vivo* xenograft growth, but exerts the opposite effects in wt-p53 cells[212], indicating the molecular biology of *PTEN* is determined by *p53* status. The ablation of *Pten* in $CD4^+$ T cells led to lower proliferation and a significant increase in cell death was observed in our model system. In this circumstance, complete loss of *Pten* could induce *p53* activity in response to cellular stress, initiating a cascade of events that results in the block of cell division. Another possibility for the deficient proliferation and high cell apoptosis in $p53^{LSL\text{-}R172H+/-}Pten^{fl/fl}$ and $Pten^{fl/fl}$ $CD4^+$ T cells could be associated with the dysfunction of T cells. As indicated in our mouse model, $p53^{LSL\text{-}R172H+/-}Pten^{fl/fl}$ and $Pten^{fl/fl}$ tumor-bearing mice had a considerably shorter latency compared to other genotypes, and the abnormality of cellular composition can be detected as early as 6 weeks age mice in both of these two genotypes. Therefore, the transformation of T-cell malignancy could not be excluded from mice at 4-5 weeks age in the context of homozygous loss of *Pten* with or without *p53* mutation.

Of note, the expansion of Ag-specific $CD4^+$ T cells drastically increased with heterozygous deficiency of *p53* and *Pten*, comparing to either $p53^{LSL\text{-}R172H+/-}$ or $Pten^{fl/+}$

CD4$^+$ T cells. Regarding the underlying mechanisms, this could be due to the stabilization of mutp53 by further mono-allelic loss of *Pten* which maximizes the proliferation rate of *p53*$^{LSL\text{-}R172H+/-}$ CD4$^+$ T cells. Therefore, our findings indicate that loss of *Pten* enhanced mutp53 activity which requires *Pten* to be below the heterozygosity threshold and is in a copy-dependent manner *in vitro* because even though mutp53 can augment cell proliferation both *in vitro*[213] and *in vivo*[214], this effect has not been found in *Pten*-null background in our model system.

To distinguish an intrinsic capacity of proliferation and survival of *p53;Pten* transgenic CD4$^+$ T cells from contributions of survival factors, we analyzed the growth effects of the withdrawal of signals via TCR and cytokines. At lower IL-2 doses, *p53*$^{LSL\text{-}R172H+/-}$*Pten*$^{fl/fl}$ and *p53*$^{LSL\text{-}R172H+/-}$*Pten*$^{fl/+}$ CD4$^+$ T cells behave similarly to what is seen at normal IL-2 doses, with a significantly higher proliferation rate compared to other genotypes. Notably, removing TCR switches *p53*$^{LSL\text{-}R172H+/-}$*Pten*$^{fl/fl}$ CD4$^+$ T cells from growth arrest to a highly proliferative state. This was supported by the previous finding that antigen stimulation was not required for IL-2 responsiveness in p53$^{-/-}$ T cells[176]. In contrast, cells of all 6 genotypes grow at high IL-2 doses. Regarding the underlying mechanisms, which probably due to higher JAK/STATs signals maintained in the absence of TCR stimulation further promote survival and proliferation of CD4$^+$ T cells, especially in the absence of normally required environmental and cellular cues. The observation that *p53*$^{LSL\text{-}R172H+/-}$*Pten*$^{fl/fl}$ CD4$^+$ T cells obtained augmented response to sub-optimal T cell stimulation raised the possibility that p53; Pten deficient cells

probably no longer have a stringent requirement for all of the 3 signals to become fully activated.

Upon receiving low doses (Anti-CD3 0.1 μg/ml, anti-CD28 5 μg/ml) of TCR signals, the enhanced phosphorylation of molecules downstream of PI3K such as Akt, GSK3β and p70 S6 kinase has been observed in $CD4^+$ T cells deficient of *Pten* in order to utilize PI3K activity to positively transduce survival and proliferation signals[108,215]. Consistently, hyper-responsiveness to sub-optimal T cell stimulation has been observed in $p53^{LSL\text{-}R172H+/-}Pten^{fl/fl}$ $CD4^+$ T cells upon TCR stimulation, which is possibly due to the augmented response to TCR signals in the absence of *Pten*. Collectively, these data demonstrated that IL-2 is not required for initial activation, but is required for the long-term survival and expansion of primed T cells *in vitro*.

To derive biological meaning from the pre-neoplasm $CD4^+$ T cells of 6 genotypes of mice differentially expressed genes were analyzed for enrichment of functional annotation using Ingenuity Pathway Analysis (IPA). Previous studies[107,108] shown the induction of Th2 responses of $CD4^+$ T cells *in vivo* is dependent on PI3K signature. Consistently, Th2 signature was upregulated in both *Pten*-null background mice, whereas Th1 signaling was downregulated relative to wild-type control mice in our model system ($P< 0.05$).

Priming of naïve $CD4^+$ T cells both *in vivo* and *in vitro* can lead to proliferating cells that produce IL-2, but neither IL-4 nor INF-y. These cells maintain a flexible and plastic state and can be differentiated into different subsets depending on the nature

of the secondary challenge. In contrast to signature cytokines, we considered both intrinsic and extrinsic factors to drive different cell fates. $CD4^+$ T cells that do not express PTEN produce elevated levels of classic Th2 cytokines even in the absence of CD28 signals based on the fact that its production of approximately 5-10 fold more IL-4 and IL-10 than WT T cells in response to TCR stimulation[108]. Another independent study has demonstrated impairment of IL-4 production in the absence of PI3K/mTOR signaling, and that this defect correlates with a failure to upregulate GATA3-translation[107].

However, functional plasticity and response to immunomodulatory factors of *p53* and further collaboration with *Pten* remain poorly defined. Thus, we set up two different polarization conditions that allow us to separately study the role of *p53* and/or *Pten* in the immune system, especially adaptive immunity. Apart from TCR stimulation and co-stimulation of CD28 on naive $CD4^+$ T cells, 6 genotypes of cells were cultured in either Th1 or Th2 polarized conditions with additional cytokine supplied. In contrast to other studies, we showed that homozygous loss of *Pten* was not promoting Th2-response. GATA3 expression was reduced slightly in both $Pten^{fl/fl}$ and $p53^{LSL\text{-}R172H+/-}$ $Pten^{fl/+}$ cells. This result is surprising given that the induction of Th2 responses *in vivo* has been shown to be dependent on PI3K signaling and *Pten* loss activates PI3K-mTOR-AKT pathway. This might be due to the fact that early transformation could have occurred despite that the morphology of these mice is grossly normal. However, *p53* mutant with or without heterozygous loss of *Pten* showed modestly increased GATA3

expression. Even though the increase in GATA3 expression in these two genotypes is not significant different compared to wild-type mice, our data suggest a potential influence of *p53* mutation in the Th2 phenotype differentiation based on the fact that C57BL/6 mice are prototypical Th1 mouse strains. Thus, our study suggests *p53* mutation may contribute to the Th2 phenotype and one copy loss of the *Pten* allele facilitates its differentiation. In contrast, all genotypes also successfully polarized into the Th1 phenotype but have lower expression of T-bet compare to wild-type mice, suggesting *p53* and/or *Pten* deficiency are not the driving force skewing towards Th1 lineage differentiation.

To address the effect of ablation of *p53* and *Pten* in mature $CD4^+$ T cells *in vivo*, 1-6 $X10^{\wedge 6}$ $CD4^+$ T cells carrying Cre were injected into sub-lethally irradiated recipient mice for engraftment. By taking advantage of allotype-specific antibodies to CD45 to precisely identify rare $CD45.2^+$ T cells in a $CD45.1^+$ environment, we next examined the ability of donor $CD4^+$ T cells to persist after intravenous injection into sub-lethal irradiated host mice. Tumor cells were prevalent in the blood and peripheral tissues, residing predominantly in the spleen where they are capable of extensive proliferation and differentiation on antigen reencounter. The engraftment of the $CD4^+$ T cells derived from $Pten^{fl/fl}$ and $p53^{LSL\text{-}R172H+/-}Pten^{fl/fl}$ in the blood remained steady at above 50% of mononuclear cells, whereas $CD4^+$ T cells derived from $p53^{LSL\text{-}R172H+/-}$ and $p53^{LSL\text{-}R172H+/-}Pten^{fl/+}$ remained at approximately 10% or below the level of detection, indicating cell-intrinsic programming by genetic alterations affects the differential engraftment fitness

after adoptive transfer. Complete loss of *Pten* gave rise to superior engraftment fitness compare to other genotypes of tumor-primed $CD4^+$ T cells, suggesting that the cell-intrinsic characteristics that enable survival are a general property conferred by complete loss of *Pten*. In contrast, mice inoculated with *p53* single mutant cells did not exhibit sustained increasing engraftment of $CD4^+$ T cells in the periphery. The engrafted donor $CD4^+$ T cells spontaneously regressed in $p53^{LSL\text{-}R172H+/-}$ donor $CD4^+$ T cells transplanted host, suggesting that their disappearance was probably due to cell-intrinsic characteristics which possess inflammatory lesion instead of malignant disease. The possibility for the superior engraftment of *Pten*-null $CD4^+$ T cells can be reflected in the preferential expansion or survival of these cells. In addition, the low success rate of engraftment of $p53^{LSL\text{-}R172H+/-}Pten^{fl/+}$ mice probably was the result of a limited density of cells in the infused population. Another potential mechanism by which *in vivo* engraftment of $CD4^+$ T cells derived from $Pten^{fl/fl}$ and $p53^{LSL\text{-}R172H+/-}Pten^{fl/fl}$ mice are superior to $CD4^+$ T cells derived from $p53^{LSL\text{-}R172H+/-}$ and $p53^{LSL\text{-}R172H+/-}Pten^{fl/+}$ mice was that the alteration of cell surface expression markers on the cells due to genetic ablation of *Pten*.

Using forward and sides scatter profiles to gate on the $CD3^+$ T cell population, we found that the proportion of $CD8^+$ T cells was significantly higher than $CD4^+$ T cells in the spleen and PBMC of the recipient mice. Although $CD8^+$ T cells were depleted prior to the initiation of transfer, it was possible that the residual $CD8^+$ T cells from the $CD4^+$ T cells took over the dominance of growth advantage during engraftment due to

the more rapid intrinsic proliferation rate of murine $CD8^+$ T cells compared to $CD4^+$ T cells[216]. As shown previously, 3-week-old PTEN-deficient mature T cells are unable to undergo a malignant transformation when placed into either *Rag1*$^{-/-}$ or sub-lethally irradiated host mice but are sufficient for the development of autoimmunity[161]. In contrast, adoptive transfer from 4-week-old mice into sub-lethally irradiated recipient mice led to lymphoma development in 3.4 months in our model system, indicating mature $CD4^+$ T cells of 4-week-old *Pten*-null mice successfully undergo a malignant transformation in the periphery.

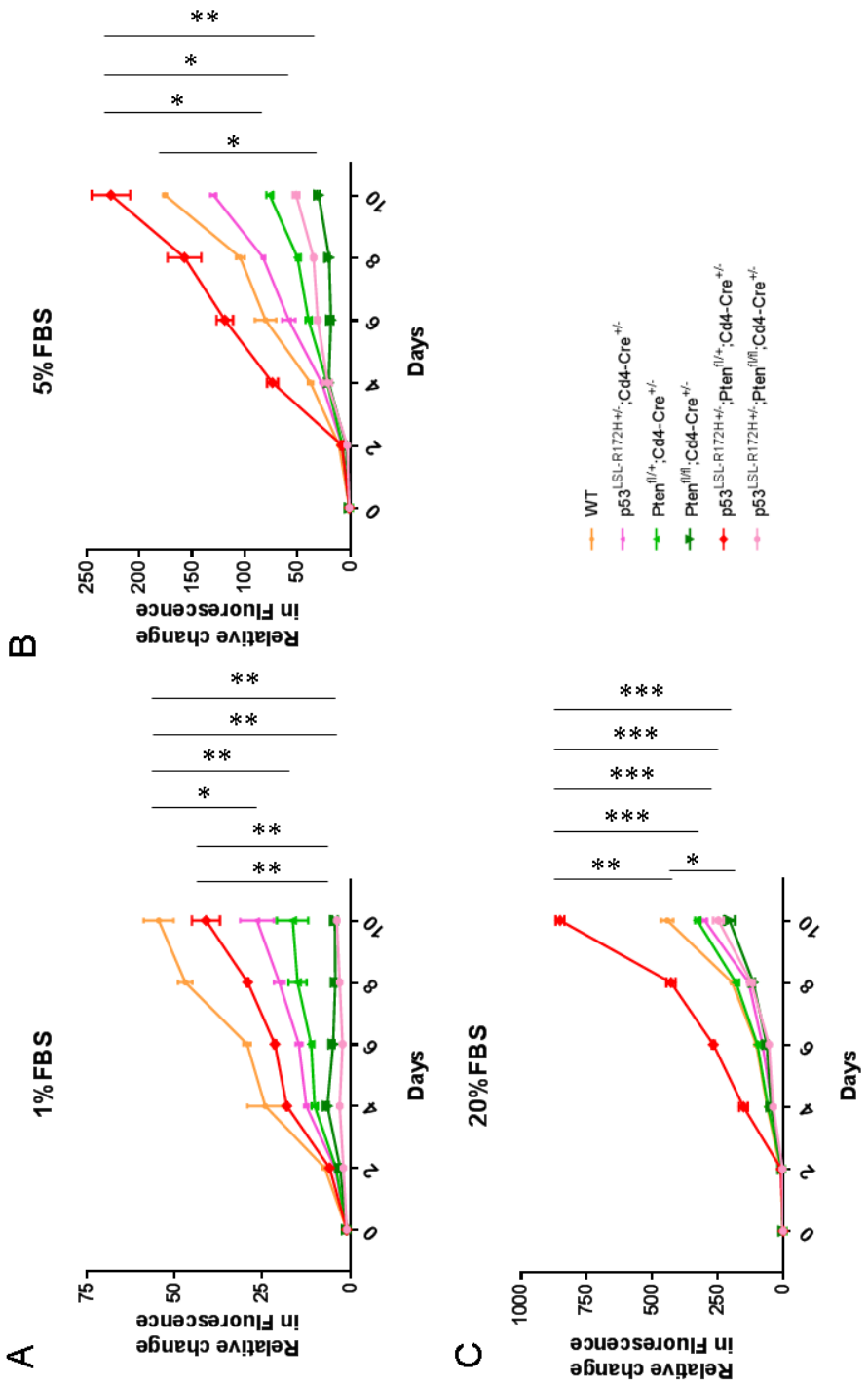
A
1% FBS
Relative change in Fluorescence
Days
B
5% FBS
Relative change in Fluorescence
Days
C
20% FBS
Relative change in Fluorescence
Days
WT
p53LSL-R172H+/-;Cd4-Cre+/-
Pten fl/+;Cd4-Cre+/-
Pten fl/fl;Cd4-Cre+/-
p53LSL-R172H+/-;Pten fl/+;Cd4-Cre+/-
p53LSL-R172H+/-;Pten fl/fl;Cd4-Cre+/-

D

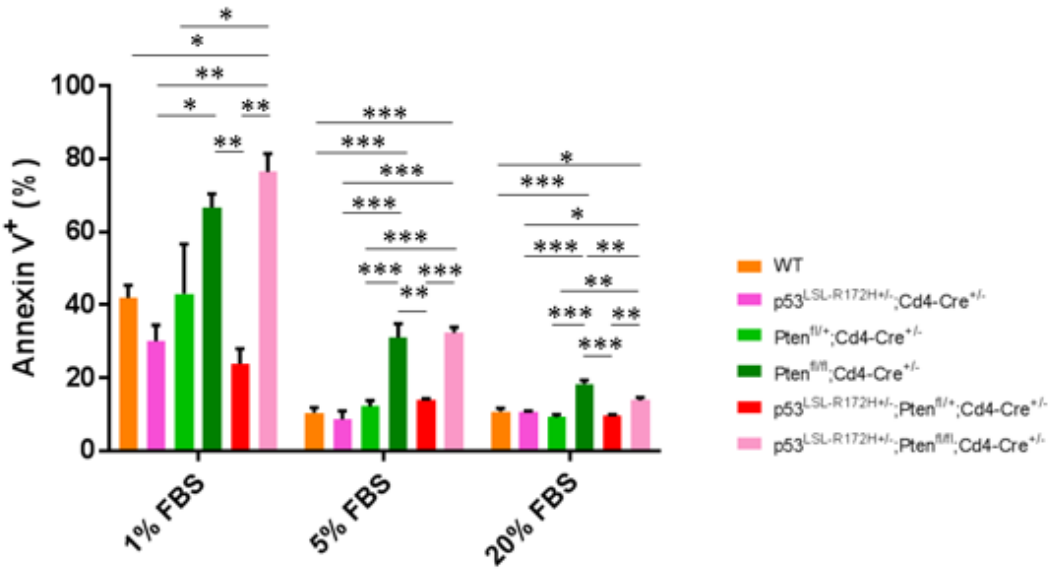
Annexin V+ (%)
100
80
60
40
20
0
1% FBS
5% FBS
20% FBS
WT
p53LSL-R172H+/-;Cd4-Cre+/-
Pten fl/+;Cd4-Cre+/-
Pten fl/fl;Cd4-Cre+/-
p53LSL-R172H+/-;Pten fl/+;Cd4-Cre+/-
p53LSL-R172H+/-;Pten fl/fl;Cd4-Cre+/-

E

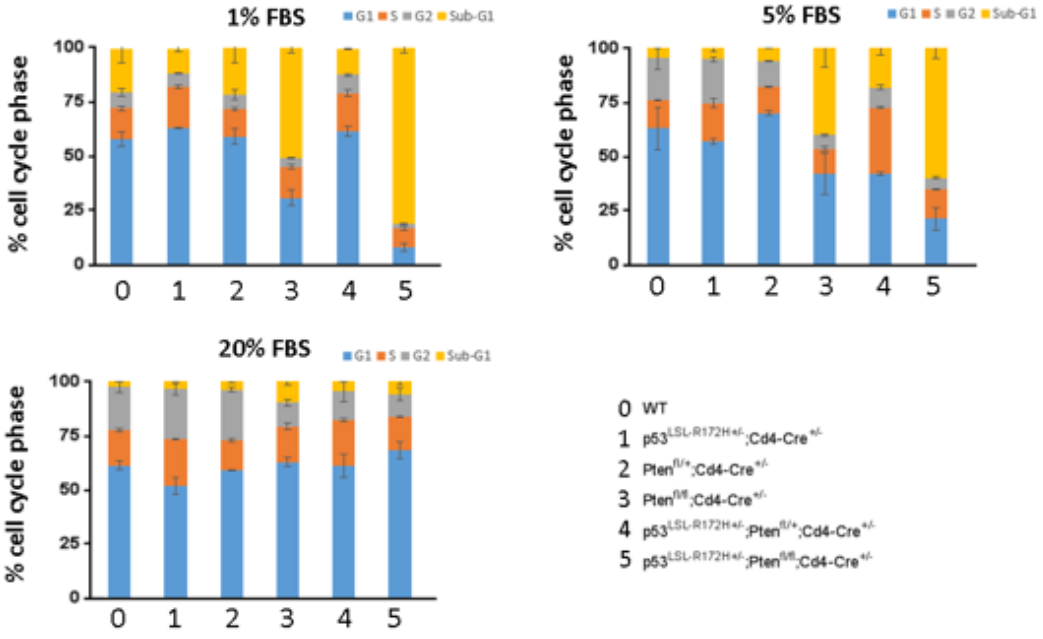
1% FBS
5% FBS
20% FBS
G1 S G2 Sub-G1
% cell cycle phase
100
75
50
25
0
0 1 2 3 4 5
0 WT
1 p53LSL-R172H+/-;Cd4-Cre+/-
2 Pten fl/+;Cd4-Cre+/-
3 Pten fl/fl;Cd4-Cre+/-
4 p53LSL-R172H+/-;Pten fl/+;Cd4-Cre+/-
5 p53LSL-R172H+/-;Pten fl/fl;Cd4-Cre+/-

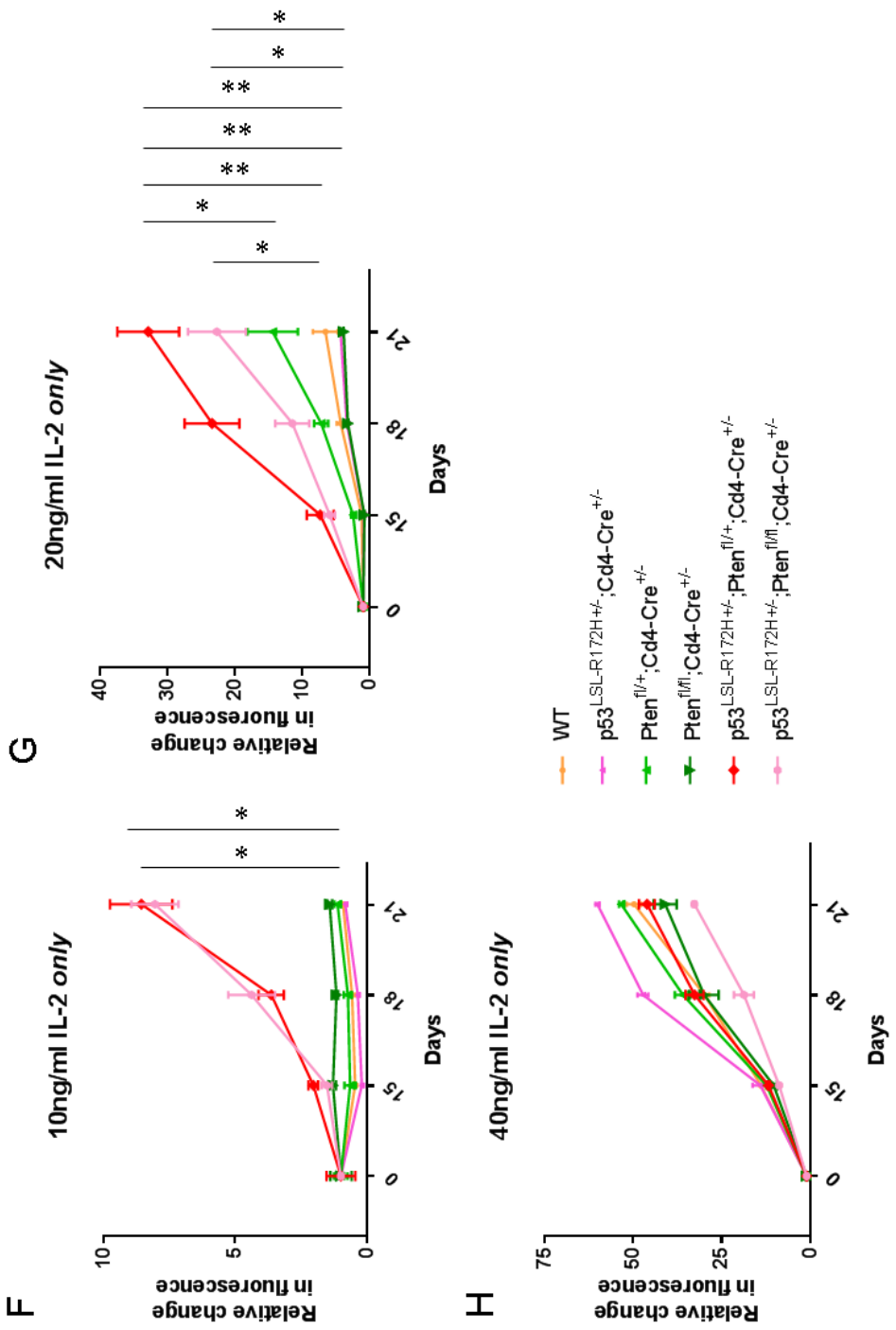
F
10ng/ml IL-2 only
Relative change in fluorescence
Days
G
20ng/ml IL-2 only
Relative change in fluorescence
Days
H
40ng/ml IL-2 only
Relative change in fluorescence
Days
WT
p53LSL-R172H+/-;Cd4-Cre+/-
Pten fl/+;Cd4-Cre+/-
Pten fl/fl;Cd4-Cre+/-
p53LSL-R172H+/-;Pten fl/+;Cd4-Cre+/-
p53LSL-R172H+/-;Pten fl/fl;Cd4-Cre+/-

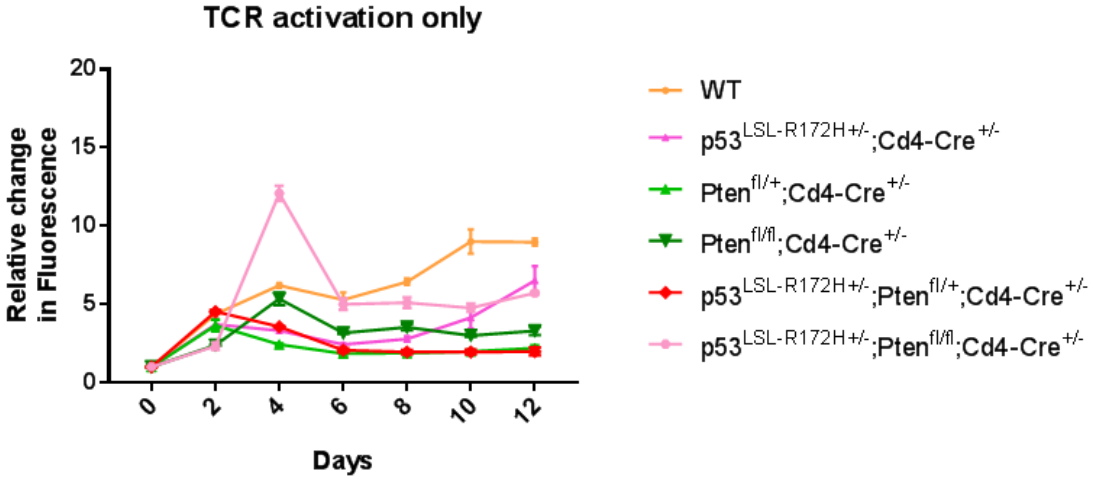
TCR activation only
Relative change in Fluorescence
20
15
10
5
0
0
2
4
6
8
10
12
Days
WT
p53LSL-R172H+/-;Cd4-Cre+/-
Pten fl/+;Cd4-Cre+/-
Pten fl/fl;Cd4-Cre+/-
p53LSL-R172H+/-;Pten fl/+;Cd4-Cre+/-
p53LSL-R172H+/-;Pten fl/fl;Cd4-Cre+/-

Figure 16: *P53* and/or *Pten* have effects on $CD4^+$ T cell proliferation and survival

(A) (B) (C) Serum depletion assay on $CD4^+$ T cells isolated from spleen of 4-5 week-age mice. Culture media contains 1640RPMI, 0.1% 2-ME, Dynabeads® magnetic beads, mouse IL-2 (20ng/ml) and supplied with 1% FBS, 5% FBS and 20% FBS, respectively. (D) Levels of cell apoptosis from different dosage of FBS were determined by Annexin V and 7-AAD staining on day 15 culturing. (E) Cell cycle distribution of CD4 T cells through 50μg/ml propidium indide (PI) staining on day 15 culturing. (F) (G) (H) Cell proliferation assay upon Ag-independent stimulation. Culture media contains 1640RPMI, 0.1% 2-ME, 20% FBS, and supplied with 10, 20 and 40 ng/ml mouse IL-2, respectively. (I) Cell proliferation assay upon Ag-dependent stimulation withdrawal IL-2. Culture media contains 1640RPMI, 0.1% 2-ME, 20% FBS, and Dynabeads® magnetic beads. For all the culture conditions, 1 x 10^6 cells/ml were seeded into a 48-

well tissue culture plate with 500ul media to start culturing immediately after CD4 T cells were isolated from spleen. Cell proliferation from each experiments was measured at the indicated time points by PrestoBlue™ Cell Viability Reagent in a 384-well plate according to the manufacture's protocol. Cells were then incubated at 37°C, 5% CO_2 for 2 hrs prior to reading out fluorescence. Error bars are SD of biological duplicates.

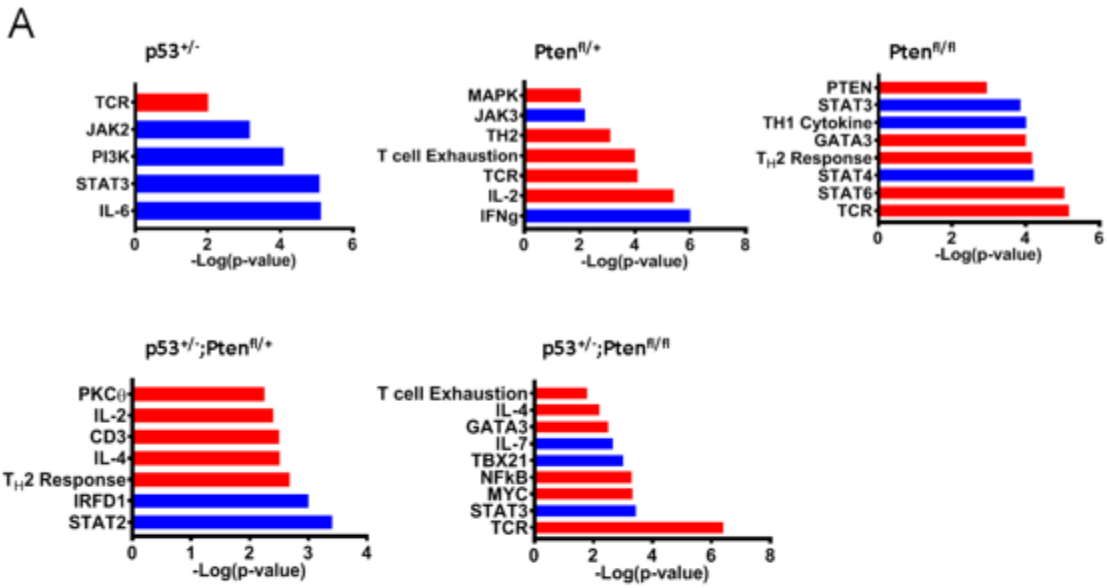
A
p53+/-
TCR
JAK2
PI3K
STAT3
IL-6
0 2 4 6
-Log(p-value)
Pten fl/+
MAPK
JAK3
TH2
T cell Exhaustion
TCR
IL-2
IFNg
0 2 4 6 8
-Log(p-value)
Pten fl/fl
PTEN
STAT3
TH1 Cytokine
GATA3
TH2 Response
STAT4
STAT6
TCR
0 2 4 6
-Log(p-value)
p53+/-;Pten fl/+
PKCθ
IL-2
CD3
IL-4
TH2 Response
IRFD1
STAT2
0 1 2 3 4
-Log(p-value)
p53+/-;Pten fl/fl
T cell Exhaustion
IL-4
GATA3
IL-7
TBX21
NFkB
MYC
STAT3
TCR
0 2 4 6 8
-Log(p-value)

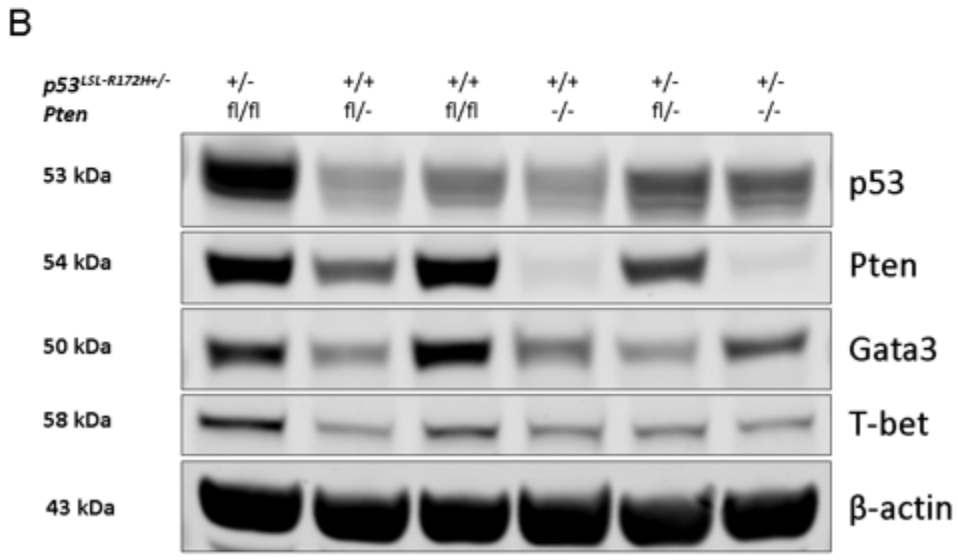
B
p53LSL-R172H+/-
Pten
+/- +/+ +/+ +/+ +/- +/-
fl/fl fl/- fl/fl -/- fl/- -/-
53 kDa
p53
54 kDa
Pten
50 kDa
Gata3
58 kDa
T-bet
43 kDa
β-actin

C

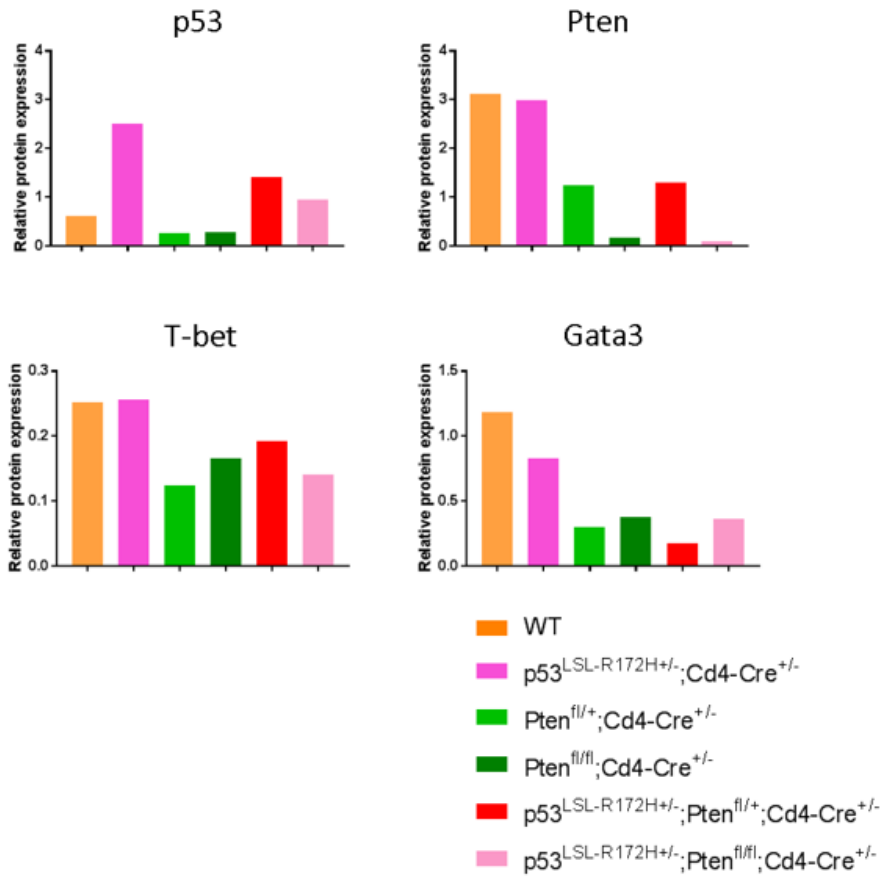
p53
Pten
T-bet
Gata3
Relative protein expression
WT
p53LSL-R172H+/-;Cd4-Cre+/-
Ptenfl/+;Cd4-Cre+/-
Ptenfl/fl;Cd4-Cre+/-
p53LSL-R172H+/-;Ptenfl/+;Cd4-Cre+/-
p53LSL-R172H+/-;Ptenfl/fl;Cd4-Cre+/-

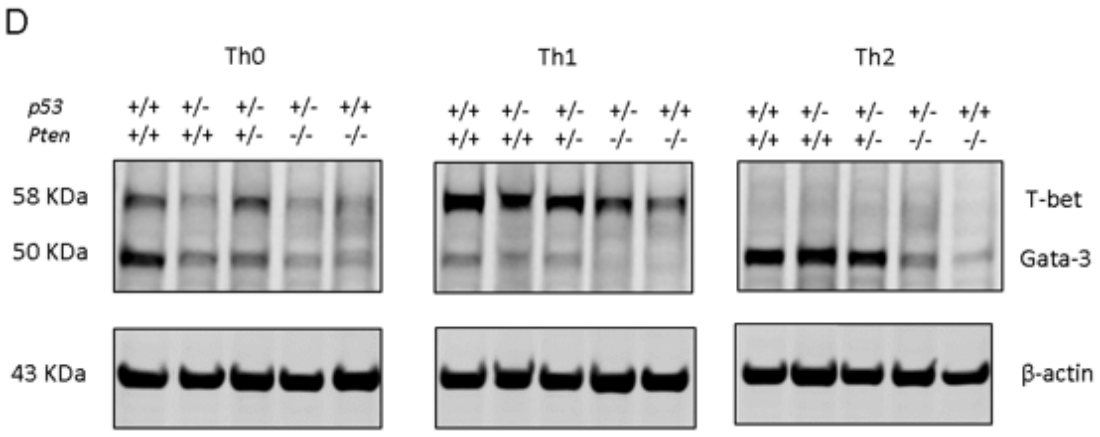
D
Th0
Th1
Th2
p53
Pten
+/+ +/- +/- +/- +/+
+/+ +/+ +/- -/- -/-
58 KDa
50 KDa
43 KDa
T-bet
Gata-3
β-actin

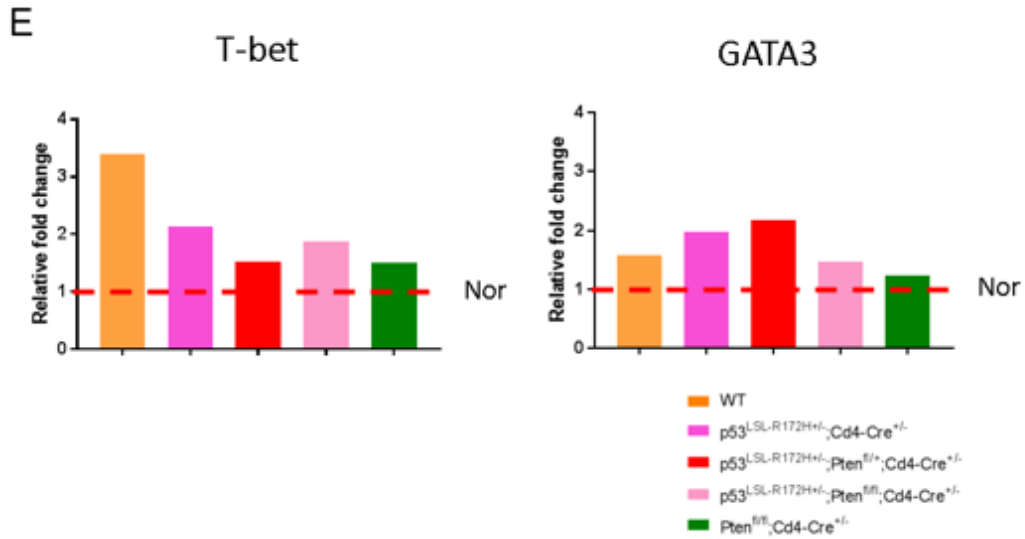
E
T-bet
GATA3
Relative fold change
0
1
2
3
4
Nor
WT
p53LSL-R172H+/-;Cd4-Cre+/-
p53LSL-R172H+/-;Pten fl/+;Cd4-Cre+/-
p53LSL-R172H+/-;Pten fl/fl;Cd4-Cre+/-
Pten fl/fl;Cd4-Cre+/-

Figure 17: Effect of the *p53;Pten* transgene on Th cell differentiation

(A) Ingenuity pathway analysis of mRNA-seq data. IPA identified pathways that were significantly upregulated (P<0.05) or downregulated (P<0.05) in MT $CD4^+$ T cells compare to WT $CD4^+$ T cells. (B) Detection of p53, Pten, Gata3 and T-bet proteins in $CD4^+$ T cell differentiation in the absence of exogenous polarizing cytokines. The specificity of p53, Pten, Gata3 and T-bet were tested by Western blot using cell lysates of *p53;Pten* transgenic and wild-type $CD4^+$ T cells for a 10-day culturing. Cells were stimulated with anti-CD3/CD28 beads and 20ng/ml IL-2, and supplied with 20% FBS, 1% PS and 0.1% ME. Proteins were separated by SDS-PAGE. (C) Levels of p53, Pten, T-bet and Gata3 in 6 genotype of mice $CD4^+$ T cells are presented as protein relative to β-actin comparing within the same genotypes. (D) Western blot detection of Gata3 and T-bet proteins in $CD4^+$ T cell differentiation under polarizing conditions. In both

culture condition, cells were stimulated with anti-CD3/CD28 beads and 20ng/ml IL-2, and supplied with 20% FBS, 1% PS and 0.1% ME. For Th1, supplement the culture media with 20ng/ml rmIL-12, and 10μg/ml anti-rmIL-4. For Th2, supplement the culture media with 100ng/ml rmIL-4, 10μg/ml anti-rmIFNγ and 10μg/ml anti-rmIL-12. New medium with neutralizing antibodies (no cytokines) were added after 48 hrs culturing. After 96 hrs of differentiation, the cells were collected and lysed for protein analysis. (E) Levels of T-bet and Gata3 in transgenic and wild-type $CD4^+$ T cells are presented as protein relative to β-actin.

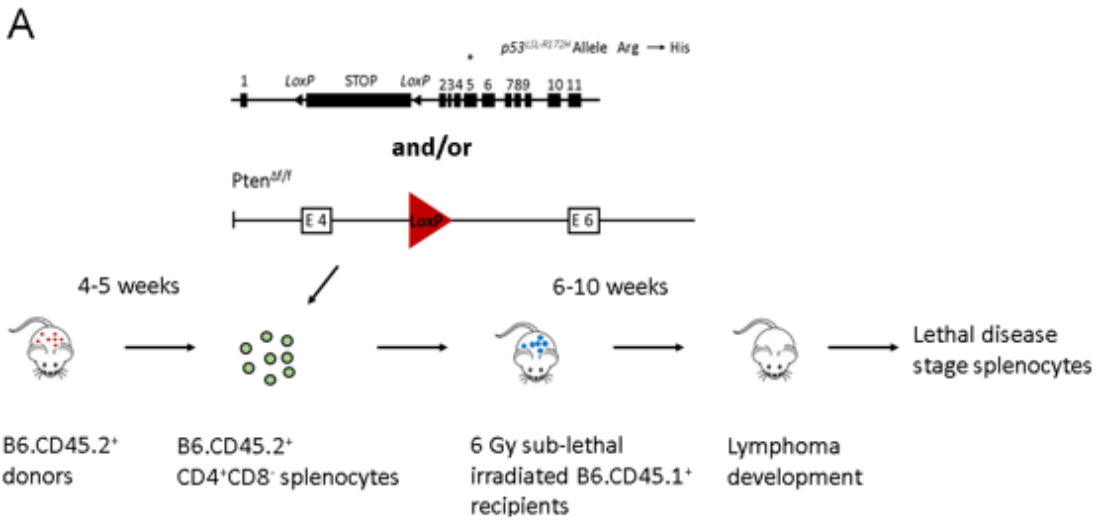
A
p53 Allele Arg → His
1 LoxP STOP LoxP 2 3 4 5 6 7 8 9 10 11
and/or
Pten
E 4
LoxP
E 6
4-5 weeks
6-10 weeks
Lethal disease stage splenocytes
B6.CD45.2+ donors
B6.CD45.2+ CD4+CD8- splenocytes
6 Gy sub-lethal irradiated B6.CD45.1+ recipients
Lymphoma development

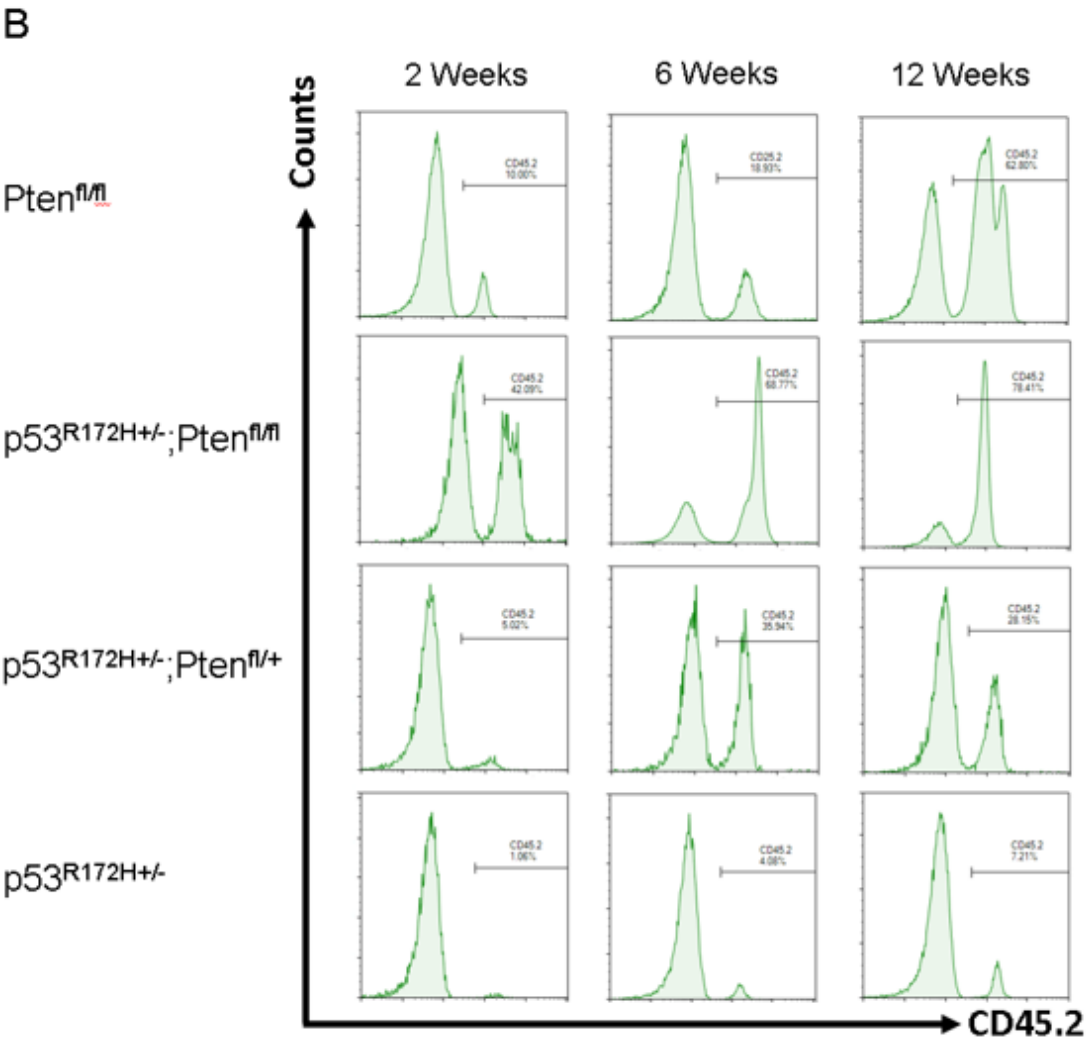
B
2 Weeks
6 Weeks
12 Weeks
Counts
Pten
p53R172H+/-;Ptenfl/fl
p53R172H+/-;Ptenfl/+
p53R172H+/-
CD45.2

C

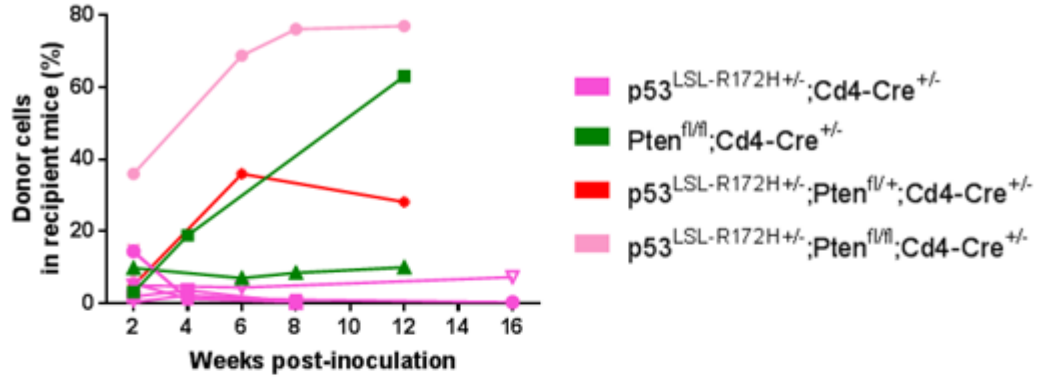
Donor cells in recipient mice (%)
80
60
40
20
0
2
4
6
8
10
12
14
16
Weeks post-inoculation
p53LSL-R172H+/-;Cd4-Cre+/-
Ptenfl/fl;Cd4-Cre+/-
p53LSL-R172H+/-;Ptenfl/+;Cd4-Cre+/-
p53LSL-R172H+/-;Ptenfl/fl;Cd4-Cre+/-

D

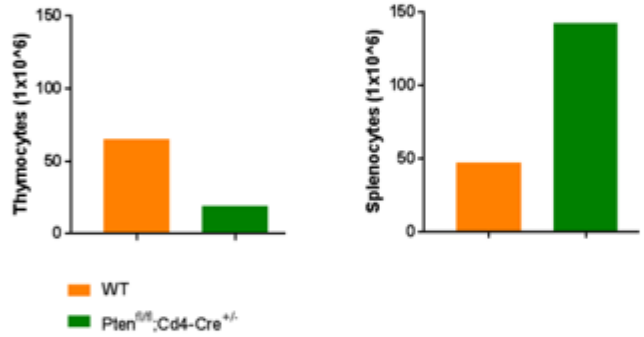
Thymocytes (1x10^6)
150
100
50
0
Splenocytes (1x10^6)
150
100
50
0
WT
Ptenfl/fl;Cd4-Cre+/-

E

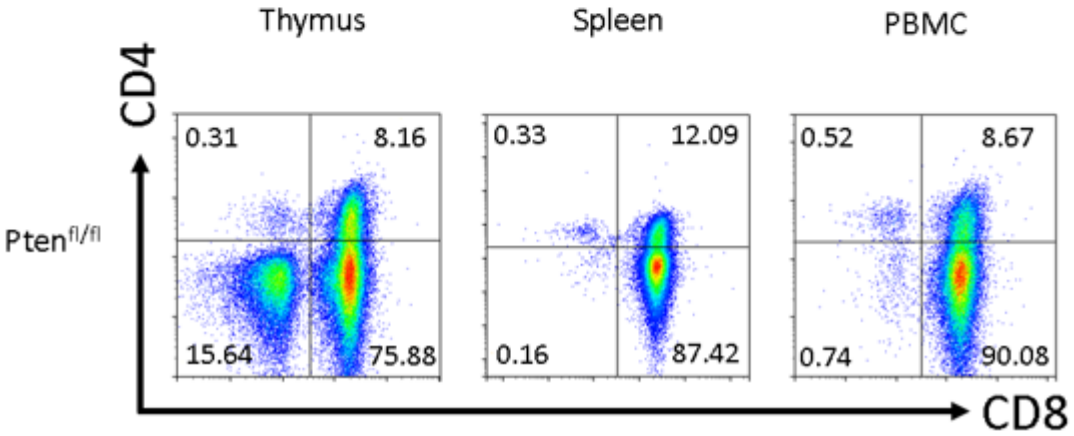
Thymus
Spleen
PBMC
CD4
Ptenfl/fl
0.31
8.16
15.64
75.88
0.33
12.09
0.16
87.42
0.52
8.67
0.74
90.08
CD8

Figure 18: Adoptive transfer of *Pten*$^{fl/fl}$ or *53*$^{LSL\text{-}R172H+/-}$-*Pten*$^{fl/fl}$ CD4^{+} T cells give rise to T-cell malignancy in host mice

(A) Schematic display of the experimental procedure used to generate mature T-cell lymphoma mouse model. The experimental approach relied on the adoptive transfer of CD4^{+} T cell obtained from spleen of 4 weeks old *p53*$^{LSL\text{-}R172H+/-}$, *Pten*$^{fl/fl}$, *p53*$^{LSL\text{-}R172H+/-}$ *Pten*$^{fl/+}$, and *p53*$^{LSL\text{-}R172H+/-}$*Pten*$^{fl/fl}$ mice congenic for CD45.2^{+}. Donor CD4^{+} T cells were fresh isolated with the assistance of the EasySep^{TM} Mouse CD4^{+} T Cell Isolation Kit and 1-6 x 10^{6} cells were transferred to wild-type non-transgenic CD45.1^{+} host mice that had been conditioned with 6 Gy sub-lethal irradiation 18-20 hrs before the cell transfer. I.V. injection were performed through tail or retro-orbital vein. Neoplasms arising in *p53;Pten* deficient cells were analyzed by flow cytometry. (B) (C) (D) Line graphs tracking down in the peripheral blood *in vivo* for the CD45.2^{+} T cell engraftment. The percent of transferred cells were detected by flow cytometry in blood of recipient mice. (E) (F) Thymocytes and splenocytes counting after red blood cell lysis of recipient mice at lethal disease stage comparing to age-matched wild-type mice. (G) Flow cytometric analysis of recipient mice thymus, spleen, and PBMC. The percentage of CD4^{+} and CD8^{+} T cells in the thymus, spleen, and PBMC of recipient mice receiving donor CD4^{+} T cells from *Pten*$^{fl/fl}$ mouse. The cells were surface stained with anti-CD3^{+}, CD4^{+} and CD8^{+} antibodies and analyzed by flow cytometry. Thymocytes are gated on the whole cell population. Splenocytes and PBMC were gated on the CD3^{+} T cell

population.

Chapter 5 Major conclusions and future directions

This dissertation describes the exciting discovery of mutations and deletions of the two most well-known tumor suppressor genes *TP53* and *PTEN* and their role in peripheral T-cell lymphomas *in vivo*. The pathogenesis of PTCL-GATA3 is unknown. The pathological diagnosis of this subgroup of diseases remains challenging.

We described a method in Chapter 2 for the underlying mechanism for the distinct expression pattern identified in GEP in molecular subtypes of PTCL-GATA3 and PTCL-TBX21. PTCL-GATA3 and PTCL-TBX21 are both characterized by structural abnormalities along with numerical changes, whereas PTCL-GATA3 is more frequently involved in genomic imbalance. *TP53* mutation along with heterozygous loss of *PTEN* is a unique characteristic in PTCL-GATA3 compared to other subtypes of PTCLs. The patients carrying *TP53;PTEN*-deficiency have the worst prognosis compared to other subtypes with a normal level of these tumor suppressors.

Currently, there is no PTCL-NOS human cell line available, which makes it challenging for investigating the pathogenesis of this disease. To determine the impact of *TP53* mutation in combination with *PTEN* loss, in Chapter 3, we developed a transgenic mouse model with CD4 T cell-specific conditional expression of $p53^{LSL\text{-}R172H+/-}$, a hot spot mutation identified in PTCL-GATA3, accompany with deletion of *Pten*.

We provide information that *p53* and *Pten* are critical for regulating T cell selection signals in the thymus. Mutp53 and heterozygous loss of *Pten* cooperatively commit T cells to the CD8-lineage differentiation, while the biallelic loss of *Pten* skews T cells to the CD4-linage differentiation. Our data demonstrate that cell-intrinsic programming by genetic alterations of *p53* and *Pten* impart dictate lineage fate choice of T cell differentiation. Moreover, our mouse genetic studies suggest that mono-allelic deletion of *Pten* in $CD4^+$ T cells gave rise to primarily splenomegaly but is not sufficient to cause tumorigenesis, whereas the biallelic deletion of *Pten* gave rise to $CD4^+$ T cell lymphoma, suggesting *Pten* deficiency contributes to lymphomagenesis in a dose-dependent manner. In contrast, mutp53 in $CD4^+$ T cells results in T cell malignancies with a low penetrance after a long latency. The low penetrance of the malignancy in $p53^{LSL\text{-}R172H+/-}$ mice strongly suggests that additional events have to occur for his pathological transition to occur. However, combined deficiency of *p53* and heterozygous loss of *Pten* revealed additional phenotypes, such as commitment of T cells to the $CD8^+$ T cell lymphoma transformation, further providing conclusive genetic support for the notion that *PTEN* is haploinsufficient in tumor suppression and that its dose is a key determinant in cancer progression. Our results demonstrate that *p53* mutation and *Pten* loss in T cells affect specific phenotypes in T-cell lymphomagenesis, and one copy loss alone are not sufficient to drive lymphomagenesis in the mouse $CD4^+$ T cells, in the specific genetic context of C57BL/6 strain.

In Chapter 4, we performed functional studies to further characterize the role of

p53;Pten in T cell biology. Cell growth requires both proliferation signals and survival signals. Our *in vitro* study showed that mutp53 drives a distinct growth advantage in the context of heterozygous loss of of *Pten* on $CD4^+$ T cells in an Ag-specific and non-specific manner. By identifying the underlying mechanisms, we found that *Pten* inhibits apoptosis in the presence of TCR activation. *p53*-mediated cellular senescence response likely restricts cell proliferation and induces cell apoptosis after the biallelic loss of *Pten*. Much of the current understanding of T helper cell lineage fate decisions are derived from studies in extrinsic factors that drive specific mechanisms to influence naïve $CD4^+$ T cell differentiation. However, our study explored the intrinsic mechanisms through which genetic alteration of *p53* and *Pten* cooperate effectively to polarize naïve $CD4^+$ T cells towards to Th2 phenotype, further providing a rational mechanistic basis for the new insights of cell-of-origin in the pathogenesis of PTCL-GATA3. Furthermore, a key finding of the adoptive transfer study was that $CD4^+$ T cells derived from *Pten*-null mice exhibit superior engraftment in host mice. Although the ability of the engraftment of donor $CD4^+$ T cells is markedly different among different genotypes, our data demonstrated that engraftment fitness is a general trait common to all $CD4^+$ T cells derived from *p53;Pten* deficiency.

Future directions

Identification of the blockage stage in T-cell development

Expression of PTEN and TP53 imposes a requirement for growth at various stages of development have been demonstrated by previous studies, we further

demonstrate that *Pten* plays a role in regulating lineage fate decisions.

Upon acute loss of *p53* and *Pten*, *Pten*-null mice gave rise to $CD4^+$ T cell lymphoma but the phenotype switched to DN T cell lymphoma when accompanying a *p53* mutation. In our model system, mutp53 was expressed and *Pten* expression was abolished when developing DN thymocytes started to express Cre at very late DN but before the DP stage. Besides, as it has become clear that *PTEN*-mediated regulation of PI3K signaling in the thymus and transformation took place after β-selection upon ablation of *PTEN*. Therefore, these observations indicate that the accumulation of DN cells in $p53^{LSL\text{-}R172H+/-}Pten^{fl/fl}$ mice is likely due to the blockage between DN4 and ISP stage mediated by mutp53. The second block is probably in a narrow window of thymic differentiation prior to the DP stage and focused on the ISP stage, due to a high proportion of $CD8^+$ T cells has been detected in the thymus of mutp53 mice. Therefore, to determine more precisely at which stage of thymocyte development the block occurred in these mice, DN thymocytes will be analyzed for the expression of CD44, CD25, and surface TCRβ expression, which define distinct immature thymocyte populations.

After DP stage, the third node of transformation occurs which is mediated by the complete loss of *Pten* and possibly due to the appropriate binding affinity to pMHC II molecules by DP cells, which skews DP to $CD4^+$ SP and further differentiate to a Th2 phenotype, as a considerable increase in $CD4^+$ T cells has been detected in $Pten^{fl/fl}$ mice which highly express of GATA3. In contrast, the forth node of transformation

occurs when mutp53 skews DP to $CD8^+$ SP cells, as a significant amount of mature $CD8^+$ SP cells were detected in the peripheral lymphoid organs in the long-term deficiency of mutp53 tumor-bearing mice.

How does *p53;Pten* influence T-cell activation signaling?

It is well-documented that BCR signaling is an important driver of B-cell lymphoma growth and survival, and represents the therapeutic target. Compelling evidence also indicates the pathogenic role of TCR signaling in human T cell transformation. Therefore, additional experiments will be required to determine which dysregulated signals contribute to disease progression in our mouse model.

Our transcriptome analyses high-lighted different altered pathways associated with pre-neoplasm T-cell lymphoma, including the TCR signaling pathway. In an effort to identify primary abnormalities that are central to the pathogenesis of PTCLs, we will study antigen-dependent TCR/CD3-mediated signaling events (Signal 1) in the different mouse lines, including the basal and induced TCR signaling activity of proximal protein tyrosine kinases and substrates, such as PLCγ, LCK, ZAP-70, LAT, and ITK protein levels, as well T cell co-stimulation signaling (Signal 2) activity such as ERK, Akt, mTORC1/2, S6, and 4E-BP-1.

In the context of the T-cell lymphoproliferative disorders, any cytokine/chemokine that directly promotes the growth/survival of a malignant T cell may be considered to have “signal 3” activity[217]. Bystander T cell activation reveals a

role for T cell function that is independent of TCR signaling via the JAK/STAT pathway upon cytokine activation, such as in the form of IL-2. Therefore, we will also investigate the mechanism by which p53; Pten deficiency affects antigen-independent bystander T cell activation by focus on key components of the JAK/STAT signaling pathway such as (i) cytokine receptor expression, (ii) JAK activation, and (iii) the activation of cytokine-specific STAT molecules, such as the Th2 biased response of JAK3 and STAT6. Given the fact that the vast majority of the T cells present in secondary lymphoid organs are not specific for antigens derived from an offending pathogen, data from the study of antigen-independent T cell activation signaling will provide a molecular insight into the characteristic hyperactivity of such cells and whether these defects are probably central to the pathogenesis of the disease.

The mechanisms of growth inhibition by *Pten* ablation: *p53*-mediated senescence or apoptosis?

In Chapter 4, when we investigated the molecular basis of cooperation between *p53* mutation and loss of *Pten* by using mature $CD4^+$ T cells freshly isolated from the spleen of 6 genotypes of mice, we observed complete ablation in *Pten* expression plays a key role in TCR induced apoptotic cell death and was accompanied by growth arrest. This provided a rationale to explore the mechanisms through which genetic alteration of *Pten* induces apoptosis in peripheral T cells during the effector phase.

Considerable controversy exists as to the effects of *Pten* on cell proliferation

and viability. *Pten*-null MEFs exhibited the distinctive morphology of senescent cells and were positive for B-galactosidase, a hallmark of senescent cells. The increased *p53* activity initiates cellular senescence in suppression of *Pten*-deficient tumorigenesis which is a fail-safe response to oppose tumorigenesis *in vitro*. *Phlpp1*$^{-/-}$ and *Pten*$^{+/-}$; *Phlpp*1$^{-/-}$ primary MEFs arrested in growth assay, but the arrest can be removed when *p53* was inactivated due to the escape from senescence[202]. However, in our mouse model, the emergence of GOF *p53*$^{LSL\text{-}R172H}$ mutation not only exerts dominant-negative effects over co-expressed wild-type p53 alleles by forming mixed tetramers that are incapable of DNA binding and transactivation but also acquires additional activities which not present in the original wild-type p53 allele and contributes to tumor progression[143].

First, the acute loss of *Pten* below the heterozygosity threshold may elicit a strong cellular senescence response by full activation of *p53* signaling. Therefore, it is worth assessing the expression of senescence-associated β-galactosidase (SA- β-Gal) on *Pten*-null cells. Second, *p53* stimulates a wide network of signals that act through two major apoptotic pathways if the DNA damage is strong enough, which includes the activation of a caspase cascade and the shifts of the balance in the Bcl-2 family towards the pro-apoptotic members. However, mutp53 confer cells an elevated resistance to a variety of pro-apoptotic signals. To investigate the cooperative effects of mutp53 and loss of *Pten* in CD4^{+} T cell apoptosis, we will examine the protein expression of caspase-3, caspase-9, PUMA, NOXA, Bcl-2, Bcl-x, Mdm-2 and p-21

upon TCR stimulation, with or withdraw IL-2.

Study of the cooperative effects of tumor-primed CD4$^+$ T cells with the microenvironment

In our adoptive cell transfer study, we showed that mature CD4$^+$ T cells in the periphery of 4-week-old *Pten*$^{fl/fl}$ and *p53*$^{LSL\text{-}R172H+/-}$*Pten*$^{fl/fl}$ mice undergo a malignant transformation when placed into sub-lethally irradiated congenic hosts, which demonstrated that cell-intrinsic programming by genetic alterations impart affects the differential engraftment fitness. So far, the primary recipient mice engrafted with *Pten*$^{fl/fl}$ and *p53*$^{LSL\text{-}R172H+/-}$*Pten*$^{fl/fl}$ CD4$^+$ SP T cells developed T cell malignancy approximately at 3 months latency post-inoculation. However, *p53*$^{LSL\text{-}R172H+/-}$ and *p53*$^{LSL\text{-}R172H+/-}$*Pten*$^{fl/+}$ transplanted mice have not shown signs of malignant transformation. *p53;Pten* deficient CD4$^+$ T cells from 4 weeks old mice are prone to malignant transformation by the virtue of loss of tumor-suppressor function, but tumor onset was unpredictable. These observations support the hypothesis that the cell-intrinsic genetic programming of these distinct genotypes of CD4$^+$ T cells may dictate divergent fates including the ability to survive *in vivo* after adoptive transfer and the tumor phenotype in the host. Therefore, it provides a strong rationale to keep monitoring mature T-cell lymphomagenesis in genetically compatible hosts from *p53*$^{LSL\text{-}R172H+/-}$*Pten*$^{fl/+}$ donor-derived transplants.

To study the impact of the microenvironment in tumorigenesis of mature T-cell malignancies as well as the diversity and phenotype of the long-term engrafted

populations, we will monitor tumor generation and differentiation by taking advantage of specific antibodies to CD45.2 and CD45.1, respectively, to distinguish donor and host cells, we used flow cytometry analysis to evaluate the cell composition of $CD45.2^{+}$ tumors. Expression of surface molecule CD3, CD4, CD8, and intracellular GATA3, IL-4, INFγ, and T-bet will be evaluated from both of the donor and recipient mice of $p53^{LSL\text{-}R172H+/-}Pten^{fl/+}$ donor-derived transplants.

Novel therapeutic targets for bystander malignant T cells in PTCLs

T-cell lymphomas have been treated with the first-line therapy using CHOP regimen designed for aggressive diffuse large B-cell lymphomas. Even though the cases in the PTCL-NOS category show extreme cytological and phenotypic heterogeneity, recurrent genetic abnormalities of combined *p53* mutation and *Pten* deletion took part in the process of lymphomagenesis in PTCL-GATA3 in human and mice which can represent the targets for therapies. Correlation of the tissue culture data with tumorigenesis *in vivo*, we showed the synergistic effect of augment of *p53* signaling and *Pten* loss contributes to maximum growth advantages on mature T cells, given a strong rationale for targeting mutp53 and PI3K-AKT-mTOR signaling pathway, due to the fact that *p53* mutation combined with *Pten* deletion is most likely the driver genetic alterations involved in bystander T cell activation in T-cell lymphomagenesis. The oncogenic GOF missense mutant p53 proteins (mutp53) obtained its GOF largely by inhibition of activity of p53 family members p63 and p73 through interactions with mutant *p53*[218,219]. Besides, activation of the PI3K-AKT-mTOR signaling pathway

contributes to PI3K-driven Akt proliferation of T cells downstream of CD28 co-stimulatory signals. Therefore, the investigation of the clinical efficacy for the synergistic combination of targeting mutp53 and PI3K-AKT-mTOR signaling pathways is critical.

Two classes of drugs were developed to target mutp53 protein. On one hand, numerous compounds were identified to destabilize highly accumulated GOF p53 mutants. Inhibition of the HSP90/HDAC6 axis extends the overall survival of *p53*^{R175H} mice by 30-59% mice *in vivo*[220]. Mouse xenografts confirmed the allele-specific higher response of p53^{R175H} tumors to Chetomin, an Hsp40 inhibitor, by decreased tumor volume and weight, however, it failed to inhibit p53^{R273H} or p53-null tumors[221]. On the other hand, by reversing the oncogenic properties of mutp53 to wild-type-like p53 activity, drugs such as PRIMA-1 and APR-246 re-established wtp53-like transcriptional activity with increased expression of p53 target genes, Puma, Noxa and Bax. However, these drugs are mostly at the level of *in vitro* cell-based testing or in Phase Ib/II study.

Duvelisib (IPI-145), an oral inhibitor of phosphatidylinositol 3-kinase (PI3K)-δ/γ isoforms, demonstrated clinical activity and a favorable safety profile in patients with CTCL and PTCL[222].The delta isoform is one of four catalytic isoforms (p110 α, β, γ, and δ) that differ in their tissue expression, with PI3Kδ being highly expressed in lymphoid cells[223], which activates downstream AKT and mTOR and exerts pleiotropic effects on cell metabolism, migration, proliferation, survival, and differentiation. In addition, currently in Phase II clinical trials, dual PI3K/mTOR inhibitors such as NVP

BEZ235 (Dactolisib), BEZ235 GDC-0980 (Apitolisib, RG7422) PF-04691502 and PF-05212384 (Gedatolisib, PKI-587) have exhibited significant clinical efficacy in several types of cancer including lymphoma.

Although *TP53* and *PTEN* are functionally distinct, reciprocal cooperation has been proposed, as PTEN is thought to regulate TP53 stability, and *TP53* to enhance *PTEN* transcription[190,224]. Our study suggests that the pathogenesis of PTCLs requires both GOF mutp53 signaling and activation of PI3K signaling pathways, suggesting the possibility of inhibition of disease progression by a selective therapy targeting both mutp53 signaling pathways and PI3K enzymatic activity in these PTCLs.

Chapter 6 Materials and methods

Patient samples

In this study, 27 patient samples were classified as PTCL-GATA3, including 18 fresh frozen (FF) and 9 formalin-fixed paraffin-embedded (FFPE) cases. 21 patient samples were classified as PTCL-TBX21, including 18 fresh frozen (FF) and 3 formalin-fixed paraffin-embedded (FFPE) cases. Patient tissues were collected from the University of Nebraska Medical Center (UNMC) and the International Peripheral T-cell Lymphoma

(IPTCL) Consortium comprises specimens from Kurume University School of Medicine, Fukuoka, Japan; Division of Medical Oncology, National Cancer Centre Singapore, Singapore; University of Wuerzburg and Comprehensive Cancer Center Mainfranken, Wuerzburg, Germany; Département de Pathologie, Université Paris-Est, Hôpital Henri-Mondor, INSERM U955, Créteil, France during the year 2006-2015. All of the FFPE cases were from Milan/Bologna University School of Medicine, Bologna. All patients had signed informed consent as part of the clinical documentation and this study was conducted under the supervision of the University of Nebraska Medical Center Institutional Review Board.

DNA copy number analysis

The extraction and purification of DNA were previously performed using AllPrep DNA/RNA Mini Kit (Qiagen) on FF specimen and AllPrep DNA/RNA FFPE Kit (Qiagen) on FFPE cases. All patients DNA were quantified by Qubit™ dsDNA BR Assay Kit (Cat. Q32853) and 80ng DNA per sample was required for DNA library preparation using OncoScan® FFPE Assay Kit according to the manufacturer's instruction. CEL files were generated and scanned by Affymetrix GeneChip Command Console® (AGCC) 4.0 Software, which includes "AT" and "GC" arrays. CEL files were then converted into OSCHP files by OncoScan Console 1.3 Software, which runs TuScan analysis algorithm to determine copy number variations. Using a reference model file (RMF), the algorithm identifies the normal diploid regions, computes Log2 ratios and B allele frequency (BAF), and output copy number segmentation in OSCHP Files visualized

for interpretation in Nexus Copy Number™ Software (BioDiscovery, El Segundo, CA, USA). Genomic alterations were analyzed by the SNP-FASST2 algorithm with gain and loss threshold set at a log2 ratio of 0.06 and -0.06. Copy number variations (CNVs) were identified by comparing the coverage depth of individual capture intervals and supported by a significant deviation of the B allele frequency from the genome-wide average.

Mice breeding and maintaining

The *Pten*$^{fl/fl}$ mouse (B6.129S4-Ptentm1Hwu/J, Stock No: 006440) and CD4 specific Cre mouse (B6.Cg-Tg(Cd4-cre)1Cwi/BfluJ, Stock No: 022071) were purchased from The Jackson Laboratory. The *p53*$^{LSL\cdot R172H/+}$ mouse was generously provided by Dr. Surinder K. Batra. *Pten*$^{fl/fl}$ mice were crossed with CD4-Cre mice to generate mice with CD4 T-specific deletion of *Pten. Pten*$^{fl/fl}$ mice were crossed with *p53*$^{LSL\text{-}R172H/+}$ mice to generate *p53*$^{LSL\text{-}R172H/+}$;*Pten*$^{fl/+}$ mice. Mice carrying *p53*$^{LSL\text{-}R172H/+}$;*Pten*$^{fl/+}$ mice were crossed with mice harboring CD4-Cre;*Pten*$^{fl/+}$ to generate mutant mice with CD4 T specific deletion of *Pten* and/or *p53*. All mice were maintained under specific pathogen-free conditions in a barrier facility and all animal studies were approved by the University of Nebraska Medical Center (UNMC) Institutional Animal Care and Use Committee (IACUC).

PCR genotyping and deletion analysis

For genotyping, mouse-ear DNA was subjected to polymerase chain reaction (PCR) analysis with the following primers. PCR primers flanking the exon 5 of *Pten* locus

yields a 328bp homozygote band and a 156bp wild-type band. Forward: 5'-CAAGCACTCTGCGAACTGAG-3', Reverse: 5'-GCATCTTGCCTTCAAAAACTT-3'. Deletion of the *Pten*$^{fl/fl}$ allele was detected by polymerase chain reaction (PCR) on purified CD4^{+} T cells from mouse spleen using the following primers: Forward: 5'-ACTCAAGGCAGGGATGAGC-3', Reverse 1: 5'-AATCTAGGGCCTCTTGTG-3', Reverse 2: 5'-GCTTGATATCGAATTCCTGCAGC-3', where wild-type allele results in an 889bp product and *Pten*$^{fl/fl}$ deletion generates a product either >889bp (F+R1) or <3709bp (F+R2). To determine the presence of the LSL cassette in *p53*, PCR amplification of conditional mutant *p53* alleles on mouse-ear DNA using the following primers to generate a 270bp mutant band and a 166bp wild-type band. Forward: 5'-CTTGGAGACATAGCCACACTG-3'; Reverse 1: 5'-AGCTAGCCACCATGGCTTGAGTAAGTCTGCA-3', Reverse 2: 5'-TTACACATCCAGCCTCTGTGG-3'. For *p53*^{R172H} recombination detection, the following primers were used on purified CD4^{+} T cells from mouse spleen to yield a wild-type band of 290 bp and mutant allele of 330 bp: Forward: 5'-AGCCTGCCTAGCTTCCTCAGG-3', Reverse 5'-CTTGGAGACATAGCCACACTG-3'.

Histology and immunohistochemistry (IHC)

The spleen, thymus, lymph nodes, liver, and kidney were collected and fixed by 4% paraformaldehyde overnight followed by 70% ethanol for 72 hours until the tissues were processed. Mice lymphoid organs were then paraffin-embedded and sectioned into 5μm for hematoxylin and eosin (H&E) or immunohistochemistry (IHC) staining.

FFPE sections were prepared for staining using standard protocols for xylene and alcohol gradient for deparaffination. Antigen retrieval was performed in the pressure cooker (95°C for 30 min) using citrate buffer to remove aldehyde links formed during the initial fixation of tissues. Slides were incubated with primary antibodies, including anti-CD3 (MA1-90582, Invitrogen) at 1:100 dilution, anti-CD4 (ab183685, Abcam) at 1:800 dilution, anti-CD8 (4SM15, Invitrogen) at 1:100 dilution, anti-CD19 (D4V4B, Cell Signaling Technology) at 1:800 dilution, anti-TdT (338A-74, Cell Marque) at 1:100 dilution. All slides were examined by the Department of Pathology and Microbiology, UNMC.

RNA-Sequencing (RNA-Seq)

Total RNA was extracted using AllPrep DNA/RNA Mini Kit (Qiagen) from purified 4 weeks of age $CD4^+$ T cells of the spleen from wild-type, $p53^{LSL\text{-}R172H/+}$, $Pten^{fl/+}$, $Pten^{fl/fl}$, $p53^{LSL\text{-}R172H/+}$;$Pten^{fl/+}$, $p53^{LSL\text{-}R172H/+}$;$Pten^{fl/fl}$ mice. Library preparation was performed with 150ng of total RNA using TruSeq RNA Library Prep Kit v2 (illumina®) and sequenced on a NextSeq 500 sequencer to obtain 20 million, 75 base pair paired-end reads. RNA-seq reads were aligned to mm10 using the STAR RNA-seq aligner (v2.5.3). Gene counts were derived from the number of uniquely aligned unambiguous reads by HTSeq (v0.9.1). Transcriptional profiling was carried out on BRB-Array tools. The Ingenuity Pathway Analysis (IPA) was used for identifying gene sets and pathways that distinguished among different genotypes.

Naïve $CD4^+$ T cell isolation and culturing

The harvested spleen was disrupted and homogenized with the plunger of a 3ml syringe against a 70-μM cell strainer into a 50ml tube. Raise the strainer with 10 ml of cold RPMI with 4% FBS through the mesh, count for viable cell numbers using a 0.4% Trypan blue solution, and centrifuge at 1000 x rpm for 5 min at RT. Re-suspend the splenocytes in EasySep™ Buffer (Catalog #20144) at concentration of 1X10^8 cells/ml. Total $CD4^+$ T cells from mice spleen were isolated by negative selection with magnetic beads using EasySep™ Mouse $CD4^+$ T Cell Isolation Kit (Catalog # 19852, STEMCELL™ TECHNOLOGIES) according to manufactory's instruction. Purity was determined by flow cytometry and ranged between 90-97%. Fresh isolated primary $CD4^+$ T cells from 4-week age mice were plated in duplicates at a density of 1x10^6 cells/ml in 48-well plates for all the *in vitro* experiments. Cells were cultured in RPMI 1640 media supplemented with 20% FBS, 1% penicillin/streptomycin, 0.1% β-Mercaptoethanol, 20ng/ml mouse recombinant IL-2 (Cat # 78081, STEMCELL™) and Dynabeads® Mouse T-Activator CD3/CD28 (Cat #11452D, Gibco™) for a bead-to-cell ratio of 1:1. Cells were cultured at 37°C in a humidified incubator with 5% CO_2 for certain periods before they were collected for analysis.

T cell proliferation assay

For determination of growth curves by using the reducing power of living cells to quantitatively measure the proliferation of cells, the PrestoBlue® Cell Viability Reagent (Catalog # A13261, Invitrogen) was mixed with the cell medium in a 1:10 ratio and 4ul of the solution were dispensed into the 384-well plate containing the cells seeded.

Followed by 2 hours incubation at 37°C, fluorescence was measured using 560-nm excitation and 590-nm emission filters by Infinite® 200 PRO plate reader. Duplicate wells were analyzed for each condition, and results were expressed as mean ± SD with the data shown representative of 2 replicated experiments.

Cell cycle analysis

For cell-cycle analysis, cells were collected at indicated time points after seeded. Then cells were fixed in cold 70% ethanol, treated with 0.2mg/ml RNase and stained with 50ug/ml Propidium iodide (PI) for 30 min in 37°C water bath. Cell-cycle profile was determined using the NovoCyte™ flow cytometer (ACEA Biosciences) and percentages of DNA content G0/G1, S, and G2/M phase cells were assessed by NovoCyte™ software (ACEA Biosciences).

Cell apoptosis analysis

Annexin V-APC and 7-AAD staining were used to detect and quantify apoptosis by flow cytometry. Cells were harvested at indicated time points after seeded, washed twice with cold 1XPBS and resuspended in 1X Binding Buffer (10mM HEPES/NaOH (pH 7.4), 140mM NaCl, 2.5mM $CaCl_2$) at a density of $1X10^6$ cells/ml containing APC-conjugated Annexin V (Cat # 561012, BD Pharmingen™) and 7-AAD (Cat # 559925, BD Pharmingen™). Cells were then incubated for 15 min at RT in the dark and processed for FACS within 1 hr of staining.

Flow cytometric analysis

For the phenotypic analysis of lymphoid and myeloid cells, cell suspensions derived from mouse spleen, thymus, lymph nodes, and peripheral blood were re-suspend with 5 ml of red blood cells (RBCs) using RBC lysis buffer for mouse (J62150, Alfa Aesar) and incubate 5 min at RT. Nucleated cell pellets were then re-suspended in 5ml of FACS staining buffer (1 X PBS, 0.5% BSA, 2mM EDTA) and counted for viable cell numbers using a 0.4% Trypan blue solution. Cells were then aliquoted at a density of 1X10^6 cells/ml and incubated with the indicated antibodies for 30mins at 4°C. Antibodies against the following molecules conjugates the indicated fluorochromes were utilized: FITC anti-CD3 (Cat # 561798, BD Pharmingen™), APC anti-CD45R/B220 (Cat # 553092, BD Pharmingen™), PE anti-CD335 (Cat # 560757, BD Pharmingen™), PE anti-CD4 (Cat # 557308, BD Pharmingen™), APC anti-CD8α (Cat # 553035, BD Pharmingen™), FITC anti-CD11b (Cat # 101205, BioLegend®), APC anti-Gr-1 (Cat # 108412, BioLegend®). All of the cytofluorimetric analysis of the surface markers were performed gating on viable (Cat # 13-0865, Ghost Dye™ Red 780) cells were performed using NovoCyte™ software (ACEA Biosciences).

In vitro T helper cell differentiation

Naïve $CD4^+$ T cells were purified from spleens of 4- to 5-week-old 6 genotypes of mice by negative selection and magnetic separation as described above. Purity was determined by flow cytometry and ranged between 90-97%. Fresh isolated and purified naïve $CD4^+$ T cells were plated in duplicates at a density of $1x10^{\wedge 6}$ cells/ml in 48-well plates and activated by 20ng/ml mouse IL-2 and Dynabeads® Mouse T-Activator

CD3/CD28 for a bead-to-cell ratio of 1:1. Th1 and Th2 differentiation conditions were set up by supplement the culture media with cytokines and blocking antibodies accordingly. Dissolve 5 x $10^{\wedge 5}$ naïve $CD4^{+}$ T cells with 500 ul of Th1-polarized media supplemented with mouse recombinant IL-12 (20ng/ml, Cat # 78028.1), anti-IL4 antibodies (10,000ngml, Cat # 504122). Th2-polarized media supplemented with mouse recombinant IL-4 (100ng/ml, Cat # 78047.1), anti-mouse IFN-γ (10,000ng/ml, Cat # 505834), anti-mouse IL-12 antibodies (10,000ng/ml, Cat #505308). Plates were incubated at 37°C with 5% CO2 for 96 hr before protein expression analysis. After the initial 48 hr culture, the addition of fresh media containing mouse recombinant IL-2 and neutralizing antibodies were added. All of the polarization cytokine antibodies were purchased from STEMCELL™ and the neutralizing antibodies were from BioLegend®.

Western Blot

For western blot analysis, cells were washed twice in 1 X PBS and lysed on ice using Pierce™ RIPA Buffer (Prod # 89900, Thermo Scientific™) supplemented with Halt™ Protease and Phosphatase Inhibitor Cocktail (Prod # 1861281, Thermo Scientific™). Protein extracts obtained from mouse cells were clarified and concentrations were measured with Pierce™ Coomassie (Bradford) Protein Assay Kit (Cat # 23200, Thermo Scientific™). 30 µg of protein extracts were separated on Bolt™ 4-12% Bis-Tris Plus Gels (Cat # NW04125BOX, Invitrogen™), transferred to a nitrocellulose membrane (Cat # 1620115, BIO-RAD) and blotted with antibodies raised against p53 (32532, Cell Signaling), Pten (9188, Cell Signaling), GATA3 (sc-268, SANTA CRUZ),

T-bet (ab91109, Abcam). To reduce non-specific signal membranes were blocked in Odyssey® blocking buffer in TBS (927-50000, LI-COR). Membranes were incubated with indicated primary antibodies overnight at 4°C, washed in TBST (10 mmol/L Tris, pH 8.0, 150 mmol/L NaCl, 0.5% Tween 20) buffer and probed against mouse or rabbit IgGs (IRDye® 800CW, LI-COR) at room temperature for 1 hr. The detection of bands was carried out upon then Odyssey infrared imaging system (LI-COR, Biosciences).

Adoptive transfer experiments

6-11-week-old recipient mice (B6.SJL-Ptprca Pepcb/BoyJ, C57BL/6, Stock No: 002014 | B6 Cd45.1, Jackson's Laboratory) were exposed to 6 Gy gamma-ray sublethal whole-body irradiation (WBI) using a RS-2000 Irradiator (LEVEL 3, 3 minutes, dose rate: 2.0 Gy/min) 18-20 hours prior to adoptive cell transfer (ACT). In water sulfamethoxazole/trimethoprim has been administrated to the recipient mice 7 days prior and 14 days post sublethal WBI. To construct a dose rate of 95mg/kg/24 hours, 3.3ml of sulfamethoxazole/trimethoprim oral suspension stock was added to 250ml drinking water. $CD4^+$ donor cells from the spleen of $p53^{LSL\cdot R172H/+}$, $Pten^{fl/fl}$, $p53^{LSL\cdot R172H/+}$;$Pten^{fl/+}$, $p53^{LSL\cdot R172H/+}$;$Pten^{fl/fl}$ 4-5-week-old male or female mice were purified by EasySep™ Mouse $CD4^+$ T Cell Isolation Kit (Catalog # 19852, STEMCELL™ TECHNOLOGIES) as described above. Recipient mice received 1-3x10^6 CD4-enriched cells in 200ul sterile 1 X PBS by intravenous tail vein or retro-orbital injection. For tail vein injection. For tail vein injection, the recipient mice were warmed up with a heated lamp for 5mins to achieve vasodilation for tail vein injection.

Spray the tail with the sterile alcohol prep pad to visualize the lateral tail vein and rotate the tail ¼ turn for easier injection. At the distal portion of the tail, insert the needle parallel to the vein 2 to 5 mm into the lumen. Inject tumor cells in the lateral tail vein with a 1 ml-syringe with a 28G1/2 needle (329461, BD). Inject the cell suspension slowly. The cell suspension should flow easily if needle is properly located. Withdraw the needle and apply pressure to prevent bleeding. Alternatively, the retro-orbital injection was performed instead of tail veil injection for adoptive cell transfer, especially when the tail vein injection is challenging. The retro-orbital injection was performed under inhalant anesthetic by isoflurane 4% for induction and 2.5% for maintenance. $CD4^+$ T cells were administered slowly into the medial canthus through a 28G1/2 (329461, BD) needle insertion. Withdraw the needle and apply pressure to prevent bleeding.

Survival analysis

The animal survival analysis was determined by Kaplan-Meier analysis. The statistical test was performed with the log-rank test. Statistical analysis was performed by using ANOVA multiple comparison of GraphPad Prism 7.04. *P* values were considered significantly different among groups, with * $p<0.05$, ** $p<0.001$, *** $p<0.0001$, unless otherwise indicated in the figure.

Chapter 7 Bibliography

1. Zhu J, Paul WE. CD4 T cells: fates, functions, and faults. *Blood.* 2008;112(5):1557-1569.

2. Zhang N, Bevan MJ. CD8(+) T cells: foot soldiers of the immune system. *Immunity.*

2011;35(2):161-168.

3. Swann JB, Smyth MJ. Immune surveillance of tumors. *J Clin Invest.* 2007;117(5):1137-1146.

4. Vivier E, Artis D, Colonna M, et al. Innate Lymphoid Cells: 10 Years On. *Cell.* 2018;174(5):1054-1066.

5. Murphy KM, Reiner SL. The lineage decisions of helper T cells. *Nat Rev Immunol.* 2002;2(12):933-944.

6. Craft JE. Follicular helper T cells in immunity and systemic autoimmunity. *Nat Rev Rheumatol.* 2012;8(6):337-347.

7. Dang EV, Barbi J, Yang HY, et al. Control of T(H)17/T(reg) balance by hypoxia-inducible factor 1. *Cell.* 2011;146(5):772-784.

8. Eyerich S, Eyerich K, Pennino D, et al. Th22 cells represent a distinct human T cell subset involved in epidermal immunity and remodeling. *J Clin Invest.* 2009;119(12):3573-3585.

9. Dardalhon V, Awasthi A, Kwon H, et al. IL-4 inhibits TGF-beta-induced Foxp3+ T cells and, together with TGF-beta, generates IL-9+ IL-10+ Foxp3(-) effector T cells. *Nat Immunol.* 2008;9(12):1347-1355.

10. Dobrzanski MJ, Reome JB, Hollenbaugh JA, Dutton RW. Tc1 and Tc2 effector cell therapy elicit long-term tumor immunity by contrasting mechanisms that result in complementary endogenous type 1 antitumor responses. *J Immunol.* 2004;172(3):1380-1390.

11. Birnbaum ME, Mendoza JL, Sethi DK, et al. Deconstructing the peptide-MHC specificity of T cell recognition. *Cell.* 2014;157(5):1073-1087.

12. Groettrup M, Ungewiss K, Azogui O, et al. A novel disulfide-linked heterodimer on pre-T cells consists of the T cell receptor beta chain and a 33 kd glycoprotein. *Cell.* 1993;75(2):283-294.

13. Starr TK, Jameson SC, Hogquist KA. Positive and negative selection of T cells. *Annual review of immunology.* 2003;21:139-176.

14. Mahe E, Pugh T, Kamel-Reid S. T cell clonality assessment: past, present and future. *J Clin Pathol.* 2018;71(3):195-200.

15. Bertness V, Kirsch I, Hollis G, Johnson B, Bunn PA, Jr. T-cell receptor gene rearrangements as clinical markers of human T-cell lymphomas. *N Engl J Med.* 1985;313(9):534-538.

16. Hodges E, Krishna MT, Pickard C, Smith JL. Diagnostic role of tests for T cell receptor (TCR) genes. *J Clin Pathol.* 2003;56(1):1-11.

17. Max EE, Seidman JG, Leder P. Sequences of five potential recombination sites encoded close to an immunoglobulin kappa constant region gene. *Proc Natl Acad Sci U S A.* 1979;76(7):3450-

3454.

18. Fugmann SD, Lee AI, Shockett PE, Villey IJ, Schatz DG. The RAG proteins and V(D)J recombination: complexes, ends, and transposition. *Annu Rev Immunol.* 2000;18:495-527.

19. Jung D, Alt FW. Unraveling V(D)J recombination; insights into gene regulation. *Cell.* 2004;116(2):299-311.

20. Alt FW, Oltz EM, Young F, Gorman J, Taccioli G, Chen J. VDJ recombination. *Immunol Today.* 1992;13(8):306-314.

21. Malu S, Malshetty V, Francis D, Cortes P. Role of non-homologous end joining in V(D)J recombination. *Immunol Res.* 2012;54(1-3):233-246.

22. Attaf M, Huseby E, Sewell AK. alphabeta T cell receptors as predictors of health and disease. *Cell Mol Immunol.* 2015;12(4):391-399.

23. Ostuni R, Piccolo V, Barozzi I, et al. Latent enhancers activated by stimulation in differentiated cells. *Cell.* 2013;152(1-2):157-171.

24. Rothenberg EV. The chromatin landscape and transcription factors in T cell programming. *Trends Immunol.* 2014;35(5):195-204.

25. Laslo P, Spooner CJ, Warmflash A, et al. Multilineage transcriptional priming and determination of alternate hematopoietic cell fates. *Cell.* 2006;126(4):755-766.

26. Gangenahalli GU, Gupta P, Saluja D, et al. Stem cell fate specification: role of master regulatory switch transcription factor PU.1 in differential hematopoiesis. *Stem Cells Dev.* 2005;14(2):140-152.

27. Hendriks RW, Nawijn MC, Engel JD, van Doorninck H, Grosveld F, Karis A. Expression of the transcription factor GATA-3 is required for the development of the earliest T cell progenitors and correlates with stages of cellular proliferation in the thymus. *Eur J Immunol.* 1999;29(6):1912-1918.

28. Pai SY, Truitt ML, Ting CN, Leiden JM, Glimcher LH, Ho IC. Critical roles for transcription factor GATA-3 in thymocyte development. *Immunity.* 2003;19(6):863-875.

29. Woolf E, Xiao C, Fainaru O, et al. Runx3 and Runx1 are required for CD8 T cell development during thymopoiesis. *Proc Natl Acad Sci U S A.* 2003;100(13):7731-7736.

30. Huppa JB, Davis MM. T-cell-antigen recognition and the immunological synapse. *Nat Rev Immunol.* 2003;3(12):973-983.

31. Birnbaum ME, Berry R, Hsiao YS, et al. Molecular architecture of the alphabeta T cell receptor-CD3 complex. *Proc Natl Acad Sci U S A.* 2014;111(49):17576-17581.

32. Gaud G, Lesourne R, Love PE. Regulatory mechanisms in T cell receptor signalling. *Nat Rev Immunol.* 2018;18(8):485-497.

33. Smith-Garvin JE, Koretzky GA, Jordan MS. T cell activation. *Annu Rev Immunol.* 2009;27:591-619.

34. Esensten JH, Helou YA, Chopra G, Weiss A, Bluestone JA. CD28 Costimulation: From Mechanism to Therapy. *Immunity.* 2016;44(5):973-988.

35. Linsley PS, Ledbetter JA. The role of the CD28 receptor during T cell responses to antigen. *Annu Rev Immunol.* 1993;11:191-212.

36. Dennehy KM, Elias F, Na SY, Fischer KD, Hunig T, Luhder F. Mitogenic CD28 signals require the exchange factor Vav1 to enhance TCR signaling at the SLP-76-Vav-Itk signalosome. *J Immunol.* 2007;178(3):1363-1371.

37. Geltz NR, Augustine JA. The p85 and p110 subunits of phosphatidylinositol 3-kinase-alpha are substrates, in vitro, for a constitutively associated protein tyrosine kinase in platelets. *Blood.* 1998;91(3):930-939.

38. Curtsinger JM, Mescher MF. Inflammatory cytokines as a third signal for T cell activation. *Curr Opin Immunol.* 2010;22(3):333-340.

39. Murphy E, Shibuya K, Hosken N, et al. Reversibility of T helper 1 and 2 populations is lost after long-term stimulation. *J Exp Med.* 1996;183(3):901-913.

40. Lexberg MH, Taubner A, Albrecht I, et al. IFN-gamma and IL-12 synergize to convert in vivo generated Th17 into Th1/Th17 cells. *Eur J Immunol.* 2010;40(11):3017-3027.

41. Harbour SN, Maynard CL, Zindl CL, Schoeb TR, Weaver CT. Th17 cells give rise to Th1 cells that are required for the pathogenesis of colitis. *Proc Natl Acad Sci U S A.* 2015;112(22):7061-7066.

42. Panzer M, Sitte S, Wirth S, Drexler I, Sparwasser T, Voehringer D. Rapid in vivo conversion of effector T cells into Th2 cells during helminth infection. *J Immunol.* 2012;188(2):615-623.

43. Li MO, Sanjabi S, Flavell RA. Transforming growth factor-beta controls development, homeostasis, and tolerance of T cells by regulatory T cell-dependent and -independent mechanisms. *Immunity.* 2006;25(3):455-471.

44. Voo KS, Wang YH, Santori FR, et al. Identification of IL-17-producing FOXP3+ regulatory T cells in humans. *Proc Natl Acad Sci U S A.* 2009;106(12):4793-4798.

45. Cheson BD, Fisher RI, Barrington SF, et al. Recommendations for initial evaluation, staging, and response assessment of Hodgkin and non-Hodgkin lymphoma: the Lugano classification. *J Clin Oncol.* 2014;32(27):3059-3068.

46. Shankland KR, Armitage JO, Hancock BW. Non-Hodgkin lymphoma. *Lancet.*

2012;380(9844):848-857.

47. Swerdlow SH, Campo E, Pileri SA, et al. The 2016 revision of the World Health Organization classification of lymphoid neoplasms. *Blood.* 2016;127(20):2375-2390.

48. Foss FM, Zinzani PL, Vose JM, Gascoyne RD, Rosen ST, Tobinai K. Peripheral T-cell lymphoma. *Blood.* 2011;117(25):6756-6767.

49. Sandell RF, Boddicker RL, Feldman AL. Genetic Landscape and Classification of Peripheral T Cell Lymphomas. *Curr Oncol Rep.* 2017;19(4):28.

50. Lage LA, Cabral TC, Costa Rde O, et al. Primary nodal peripheral T-cell lymphomas: diagnosis and therapeutic considerations. *Rev Bras Hematol Hemoter.* 2015;37(4):277-284.

51. Broccoli A, Zinzani PL. Peripheral T-cell lymphoma, not otherwise specified. *Blood.* 2017;129(9):1103-1112.

52. Lunning MA, Vose JM. Angioimmunoblastic T-cell lymphoma: the many-faced lymphoma. *Blood.* 2017;129(9):1095-1102.

53. Zinzani PL. ALCL: is it now a curable disease? *Blood.* 2017;130(25):2691-2692.

54. Di Sabatino A, Biagi F, Gobbi PG, Corazza GR. How I treat enteropathy-associated T-cell lymphoma. *Blood.* 2012;119(11):2458-2468.

55. Kojima M, Matsushita H. Hepatosplenic T-cell lymphoma appearing in the peripheral blood. *Blood.* 2013;122(7):1103.

56. Willemze R, Jansen PM, Cerroni L, et al. Subcutaneous panniculitis-like T-cell lymphoma: definition, classification, and prognostic factors: an EORTC Cutaneous Lymphoma Group Study of 83 cases. *Blood.* 2008;111(2):838-845.

57. Vose J, Armitage J, Weisenburger D, International TCLP. International peripheral T-cell and natural killer/T-cell lymphoma study: pathology findings and clinical outcomes. *J Clin Oncol.* 2008;26(25):4124-4130.

58. Rudiger T, Weisenburger DD, Anderson JR, et al. Peripheral T-cell lymphoma (excluding anaplastic large-cell lymphoma): results from the Non-Hodgkin's Lymphoma Classification Project. *Ann Oncol.* 2002;13(1):140-149.

59. Gorczyca W, Weisberger J, Liu Z, et al. An approach to diagnosis of T-cell lymphoproliferative disorders by flow cytometry. *Cytometry.* 2002;50(3):177-190.

60. Geissinger E, Odenwald T, Lee SS, et al. Nodal peripheral T-cell lymphomas and, in particular, their lymphoepithelioid (Lennert's) variant are often derived from CD8(+) cytotoxic T-cells. *Virchows Arch.* 2004;445(4):334-343.

61. Weisenburger DD, Savage KJ, Harris NL, et al. Peripheral T-cell lymphoma, not otherwise specified: a report of 340 cases from the International Peripheral T-cell Lymphoma Project. *Blood.* 2011;117(12):3402-3408.

62. Bellei M, Federico M. The outcome of peripheral T-cell lymphoma patients failing first-line therapy: a report from the prospective International T-Cell Project. *Haematologica.* 2019;104(4):e178.

63. Schmitz N, Trumper L, Ziepert M, et al. Treatment and prognosis of mature T-cell and NK-cell lymphoma: an analysis of patients with T-cell lymphoma treated in studies of the German High-Grade Non-Hodgkin Lymphoma Study Group. *Blood.* 2010;116(18):3418-3425.

64. Alizadeh AA, Eisen MB, Davis RE, et al. Distinct types of diffuse large B-cell lymphoma identified by gene expression profiling. *Nature.* 2000;403(6769):503-511.

65. Scott DW, Wright GW, Williams PM, et al. Determining cell-of-origin subtypes of diffuse large B-cell lymphoma using gene expression in formalin-fixed paraffin-embedded tissue. *Blood.* 2014;123(8):1214-1217.

66. de Leval L, Rickman DS, Thielen C, et al. The gene expression profile of nodal peripheral T-cell lymphoma demonstrates a molecular link between angioimmunoblastic T-cell lymphoma (AITL) and follicular helper T (TFH) cells. *Blood.* 2007;109(11):4952-4963.

67. Iqbal J, Wright G, Wang C, et al. Gene expression signatures delineate biological and prognostic subgroups in peripheral T-cell lymphoma. *Blood.* 2014;123(19):2915-2923.

68. Wang T, Feldman AL, Wada DA, et al. GATA-3 expression identifies a high-risk subset of PTCL, NOS with distinct molecular and clinical features. *Blood.* 2014;123(19):3007-3015.

69. Tsuchiya T, Ohshima K, Karube K, et al. Th1, Th2, and activated T-cell marker and clinical prognosis in peripheral T-cell lymphoma, unspecified: comparison with AILD, ALCL, lymphoblastic lymphoma, and ATLL. *Blood.* 2004;103(1):236-241.

70. Abate F, da Silva-Almeida AC, Zairis S, et al. Activating mutations and translocations in the guanine exchange factor VAV1 in peripheral T-cell lymphomas. *Proc Natl Acad Sci U S A.* 2017;114(4):764-769.

71. Boddicker RL, Razidlo GL, Dasari S, et al. Integrated mate-pair and RNA sequencing identifies novel, targetable gene fusions in peripheral T-cell lymphoma. *Blood.* 2016;128(9):1234-1245.

72. Kong YY, Fischer KD, Bachmann MF, et al. Vav regulates peptide-specific apoptosis in thymocytes. *J Exp Med.* 1998;188(11):2099-2111.

73. Watatani Y, Sato Y, Miyoshi H, et al. Molecular heterogeneity in peripheral T-cell lymphoma, not otherwise specified revealed by comprehensive genetic profiling. *Leukemia.* 2019.

74. Schatz JH, Horwitz SM, Teruya-Feldstein J, et al. Targeted mutational profiling of peripheral T-cell lymphoma not otherwise specified highlights new mechanisms in a heterogeneous pathogenesis. *Leukemia.* 2015;29(1):237-241.

75. Couronne L, Bastard C, Bernard OA. TET2 and DNMT3A mutations in human T-cell lymphoma. *N Engl J Med.* 2012;366(1):95-96.

76. Ji MM, Huang YH, Huang JY, et al. Histone modifier gene mutations in peripheral T-cell lymphoma not otherwise specified. *Haematologica.* 2018;103(4):679-687.

77. Wang C, McKeithan TW, Gong Q, et al. IDH2R172 mutations define a unique subgroup of patients with angioimmunoblastic T-cell lymphoma. *Blood.* 2015;126(15):1741-1752.

78. Laptenko O, Prives C. Transcriptional regulation by p53: one protein, many possibilities. *Cell Death Differ.* 2006;13(6):951-961.

79. Levine AJ. p53, the cellular gatekeeper for growth and division. *Cell.* 1997;88(3):323-331.

80. Rivlin N, Brosh R, Oren M, Rotter V. Mutations in the p53 Tumor Suppressor Gene: Important Milestones at the Various Steps of Tumorigenesis. *Genes Cancer.* 2011;2(4):466-474.

81. Xu-Monette ZY, Medeiros LJ, Li Y, et al. Dysfunction of the TP53 tumor suppressor gene in lymphoid malignancies. *Blood.* 2012;119(16):3668-3683.

82. Moll UM, Petrenko O. The MDM2-p53 interaction. *Mol Cancer Res.* 2003;1(14):1001-1008.

83. Nguyen L, Papenhausen P, Shao H. The Role of c-MYC in B-Cell Lymphomas: Diagnostic and Molecular Aspects. *Genes (Basel).* 2017;8(4).

84. Nelson M, Horsman DE, Weisenburger DD, et al. Cytogenetic abnormalities and clinical correlations in peripheral T-cell lymphoma. *Br J Haematol.* 2008;141(4):461-469.

85. Wineinger NE, Kennedy RE, Erickson SW, Wojczynski MK, Bruder CE, Tiwari HK. Statistical issues in the analysis of DNA Copy Number Variations. *Int J Comput Biol Drug Des.* 2008;1(4):368-395.

86. Hartmann S, Gesk S, Scholtysik R, et al. High resolution SNP array genomic profiling of peripheral T cell lymphomas, not otherwise specified, identifies a subgroup with chromosomal aberrations affecting the REL locus. *Br J Haematol.* 2010;148(3):402-412.

87. Thorns C, Bastian B, Pinkel D, et al. Chromosomal aberrations in angioimmunoblastic T-cell lymphoma and peripheral T-cell lymphoma unspecified: A matrix-based CGH approach. *Genes Chromosomes Cancer.* 2007;46(1):37-44.

88. Zettl A, Rudiger T, Konrad MA, et al. Genomic profiling of peripheral T-cell lymphoma, unspecified, and anaplastic large T-cell lymphoma delineates novel recurrent chromosomal alterations. *Am J Pathol.* 2004;164(5):1837-1848.

89. Lenz G, Wright GW, Emre NC, et al. Molecular subtypes of diffuse large B-cell lymphoma arise by distinct genetic pathways. *Proc Natl Acad Sci U S A.* 2008;105(36):13520-13525.

90. Pfeifer M, Grau M, Lenze D, et al. PTEN loss defines a PI3K/AKT pathway-dependent germinal center subtype of diffuse large B-cell lymphoma. *Proc Natl Acad Sci U S A.* 2013;110(30):12420-12425.

91. Schlegelberger B, Himmler A, Godde E, Grote W, Feller AC, Lennert K. Cytogenetic findings in peripheral T-cell lymphomas as a basis for distinguishing low-grade and high-grade lymphomas. *Blood.* 1994;83(2):505-511.

92. Lepretre S, Buchonnet G, Stamatoullas A, et al. Chromosome abnormalities in peripheral T-cell lymphoma. *Cancer Genet Cytogenet.* 2000;117(1):71-79.

93. Li J, Yen C, Liaw D, et al. PTEN, a putative protein tyrosine phosphatase gene mutated in human brain, breast, and prostate cancer. *Science.* 1997;275(5308):1943-1947.

94. Song MS, Salmena L, Pandolfi PP. The functions and regulation of the PTEN tumour suppressor. *Nat Rev Mol Cell Biol.* 2012;13(5):283-296.

95. Zuurbier L, Petricoin EF, 3rd, Vuerhard MJ, et al. The significance of PTEN and AKT aberrations in pediatric T-cell acute lymphoblastic leukemia. *Haematologica.* 2012;97(9):1405-1413.

96. Eng C. PTEN: one gene, many syndromes. *Hum Mutat.* 2003;22(3):183-198.

97. Yin Y, Shen WH. PTEN: a new guardian of the genome. *Oncogene.* 2008;27(41):5443-5453.

98. Sabattini E, Bacci F, Sagramoso C, Pileri SA. WHO classification of tumours of haematopoietic and lymphoid tissues in 2008: an overview. *Pathologica.* 2010;102(3):83-87.

99. Savage KJ, Ferreri AJ, Zinzani PL, Pileri SA. Peripheral T-cell lymphoma--not otherwise specified. *Crit Rev Oncol Hematol.* 2011;79(3):321-329.

100. Piekarz RL, Frye R, Prince HM, et al. Phase 2 trial of romidepsin in patients with peripheral T-cell lymphoma. *Blood.* 2011;117(22):5827-5834.

101. Horwitz SM, Advani RH, Bartlett NL, et al. Objective responses in relapsed T-cell lymphomas with single-agent brentuximab vedotin. *Blood.* 2014;123(20):3095-3100.

102. Enblad G, Hagberg H, Erlanson M, et al. A pilot study of alemtuzumab (anti-CD52 monoclonal antibody) therapy for patients with relapsed or chemotherapy-refractory peripheral T-cell lymphomas. *Blood.* 2004;103(8):2920-2924.

103. Iqbal J, Weisenburger DD, Greiner TC, et al. Molecular signatures to improve diagnosis in peripheral T-cell lymphoma and prognostication in angioimmunoblastic T-cell lymphoma. *Blood.*115(5):1026-1036.

104. Tindemans I, Serafini N, Di Santo JP, Hendriks RW. GATA-3 function in innate and adaptive immunity. *Immunity.* 2014;41(2):191-206.

105. Szabo SJ, Kim ST, Costa GL, Zhang X, Fathman CG, Glimcher LH. A novel transcription factor, T-bet, directs Th1 lineage commitment. *Cell.* 2000;100(6):655-669.

106. Delgoffe GM, Kole TP, Zheng Y, et al. The mTOR kinase differentially regulates effector and regulatory T cell lineage commitment. *Immunity.* 2009;30(6):832-844.

107. Cook KD, Miller J. TCR-dependent translational control of GATA-3 enhances Th2 differentiation. *J Immunol.* 2010;185(6):3209-3216.

108. Buckler JL, Liu X, Turka LA. Regulation of T-cell responses by PTEN. *Immunol Rev.* 2008;224:239-248.

109. Baysan M, Woolard K, Cam MC, et al. Detailed longitudinal sampling of glioma stem cells in situ reveals Chr7 gain and Chr10 loss as repeated events in primary tumor formation and recurrence. *Int J Cancer.* 2017;141(10):2002-2013.

110. Wessels PH, Twijnstra A, Kessels AG, et al. Gain of chromosome 7, as detected by in situ hybridization, strongly correlates with shorter survival in astrocytoma grade 2. *Genes Chromosomes Cancer.* 2002;33(3):279-284.

111. Buishand FO, Cardin E, Hu Y, Ried T. Trichostatin A preferentially reverses the upregulation of gene-expression levels induced by gain of chromosome 7 in colorectal cancer cell lines. *Genes Chromosomes Cancer.* 2018;57(1):35-41.

112. Roth JJ, Fierst TM, Waanders AJ, Yimei L, Biegel JA, Santi M. Whole Chromosome 7 Gain Predicts Higher Risk of Recurrence in Pediatric Pilocytic Astrocytomas Independently From KIAA1549-BRAF Fusion Status. *J Neuropathol Exp Neurol.* 2016;75(4):306-315.

113. Alers JC, Rochat J, Krijtenburg PJ, et al. Identification of genetic markers for prostatic cancer progression. *Lab Invest.* 2000;80(6):931-942.

114. El Gammal AT, Bruchmann M, Zustin J, et al. Chromosome 8p deletions and 8q gains are associated with tumor progression and poor prognosis in prostate cancer. *Clin Cancer Res.* 2010;16(1):56-64.

115. Kang JU. Chromosome 8q as the most frequent target for amplification in early gastric carcinoma. *Oncol Lett.* 2014;7(4):1139-1143.

116. Klatte T, Kroeger N, Rampersaud EN, et al. Gain of chromosome 8q is associated with metastases and poor survival of patients with clear cell renal cell carcinoma. *Cancer.* 2012;118(23):5777-5782.

117. Alpermann T, Haferlach C, Eder C, et al. AML with gain of chromosome 8 as the sole

chromosomal abnormality (+8sole) is associated with a specific molecular mutation pattern including ASXL1 mutations in 46.8% of the patients. *Leuk Res.* 2015;39(3):265-272.

118. Salido M, Baro C, Oscier D, et al. Cytogenetic aberrations and their prognostic value in a series of 330 splenic marginal zone B-cell lymphomas: a multicenter study of the Splenic B-Cell Lymphoma Group. *Blood.* 2010;116(9):1479-1488.

119. Ding BB, Yu JJ, Yu RY, et al. Constitutively activated STAT3 promotes cell proliferation and survival in the activated B-cell subtype of diffuse large B-cell lymphomas. *Blood.* 2008;111(3):1515-1523.

120. Kataoka K, Iwanaga M, Yasunaga JI, et al. Prognostic relevance of integrated genetic profiling in adult T-cell leukemia/lymphoma. *Blood.* 2018;131(2):215-225.

121. Martinez-Climent JA, Vizcarra E, Sanchez D, et al. Loss of a novel tumor suppressor gene locus at chromosome 8p is associated with leukemic mantle cell lymphoma. *Blood.* 2001;98(12):3479-3482.

122. Vasmatzis G, Johnson SH, Knudson RA, et al. Genome-wide analysis reveals recurrent structural abnormalities of TP63 and other p53-related genes in peripheral T-cell lymphomas. *Blood.* 2012;120(11):2280-2289.

123. Petitjean A, Achatz MI, Borresen-Dale AL, Hainaut P, Olivier M. TP53 mutations in human cancers: functional selection and impact on cancer prognosis and outcomes. *Oncogene.* 2007;26(15):2157-2165.

124. Matsushima AY, Cesarman E, Chadburn A, Knowles DM. Post-thymic T cell lymphomas frequently overexpress p53 protein but infrequently exhibit p53 gene mutations. *Am J Pathol.* 1994;144(3):573-584.

125. Newton RH, Turka LA. Regulation of T cell homeostasis and responses by pten. *Front Immunol.* 2012;3:151.

126. Gerard B, Cave H, Guidal C, Dastugue N, Vilmer E, Grandchamp B. Delineation of a 6 cM commonly deleted region in childhood acute lymphoblastic leukemia on the 6q chromosomal arm. *Leukemia.* 1997;11(2):228-232.

127. Gaidano G, Hauptschein RS, Parsa NZ, et al. Deletions involving two distinct regions of 6q in B-cell non-Hodgkin lymphoma. *Blood.* 1992;80(7):1781-1787.

128. Cai Y, Crowther J, Pastor T, et al. Loss of Chromosome 8p Governs Tumor Progression and Drug Response by Altering Lipid Metabolism. *Cancer Cell.* 2016;29(5):751-766.

129. Tabares-Seisdedos R, Rubenstein JL. Chromosome 8p as a potential hub for developmental neuropsychiatric disorders: implications for schizophrenia, autism and cancer. *Mol Psychiatry.* 2009;14(6):563-589.

130. Tschaharganeh DF, Bosbach B, Lowe SW. Coordinated Tumor Suppression by Chromosome 8p. *Cancer Cell.* 2016;29(5):617-619.

131. Liu JC, Voisin V, Wang S, et al. Combined deletion of Pten and p53 in mammary epithelium accelerates triple-negative breast cancer with dependency on eEF2K. *EMBO Mol Med.* 2014;6(12):1542-1560.

132. Chow LM, Endersby R, Zhu X, et al. Cooperativity within and among Pten, p53, and Rb pathways induces high-grade astrocytoma in adult brain. *Cancer Cell.* 2011;19(3):305-316.

133. Ishii N, Maier D, Merlo A, et al. Frequent co-alterations of TP53, p16/CDKN2A, p14ARF, PTEN tumor suppressor genes in human glioma cell lines. *Brain Pathol.* 1999;9(3):469-479.

134. Pessoa IA, Amorim CK, Ferreira WAS, et al. Detection and Correlation of Single and Concomitant TP53, PTEN, and CDKN2A Alterations in Gliomas. *Int J Mol Sci.* 2019;20(11).

135. Hamid AA, Gray KP, Shaw G, et al. Compound Genomic Alterations of TP53, PTEN, and RB1 Tumor Suppressors in Localized and Metastatic Prostate Cancer. *Eur Urol.* 2019;76(1):89-97.

136. Aziz MH, Shen H, Maki CG. Acquisition of p53 mutations in response to the non-genotoxic p53 activator Nutlin-3. *Oncogene.* 2011;30(46):4678-4686.

137. Quelle DE, Zindy F, Ashmun RA, Sherr CJ. Alternative reading frames of the INK4a tumor suppressor gene encode two unrelated proteins capable of inducing cell cycle arrest. *Cell.* 1995;83(6):993-1000.

138. Saporita AJ, Maggi LB, Jr., Apicelli AJ, Weber JD. Therapeutic targets in the ARF tumor suppressor pathway. *Curr Med Chem.* 2007;14(17):1815-1827.

139. Greenblatt MS, Bennett WP, Hollstein M, Harris CC. Mutations in the p53 tumor suppressor gene: clues to cancer etiology and molecular pathogenesis. *Cancer Res.* 1994;54(18):4855-4878.

140. Halldorsdottir AM, Lundin A, Murray F, et al. Impact of TP53 mutation and 17p deletion in mantle cell lymphoma. *Leukemia.* 2011;25(12):1904-1908.

141. Malcikova J, Smardova J, Rocnova L, et al. Monoallelic and biallelic inactivation of TP53 gene in chronic lymphocytic leukemia: selection, impact on survival, and response to DNA damage. *Blood.* 2009;114(26):5307-5314.

142. Lang GA, Iwakuma T, Suh YA, et al. Gain of function of a p53 hot spot mutation in a mouse model of Li-Fraumeni syndrome. *Cell.* 2004;119(6):861-872.

143. Oren M, Rotter V. Mutant p53 gain-of-function in cancer. *Cold Spring Harb Perspect Biol.* 2010;2(2):a001107.

144. Srividya MR, Thota B, Shailaja BC, et al. Homozygous 10q23/PTEN deletion and its impact on

outcome in glioblastoma: a prospective translational study on a uniformly treated cohort of adult patients. *Neuropathology.* 2011;31(4):376-383.

145. Chen Z, Trotman LC, Shaffer D, et al. Crucial role of p53-dependent cellular senescence in suppression of Pten-deficient tumorigenesis. *Nature.* 2005;436(7051):725-730.

146. de Leval L, Gaulard P. Pathology and biology of peripheral T-cell lymphomas. *Histopathology.* 2011;58(1):49-68.

147. Heavican TB, Bouska A, Yu J, et al. Genetic drivers of oncogenic pathways in molecular subgroups of peripheral T-cell lymphoma. *Blood.* 2019;133(15):1664-1676.

148. Donehower LA, Harvey M, Vogel H, et al. Effects of genetic background on tumorigenesis in p53-deficient mice. *Mol Carcinog.* 1995;14(1):16-22.

149. Dudgeon C, Chan C, Kang W, et al. The evolution of thymic lymphomas in p53 knockout mice. *Genes Dev.* 2014;28(23):2613-2620.

150. Iacopetta B. TP53 mutation in colorectal cancer. *Hum Mutat.* 2003;21(3):271-276.

151. Lai SL, Perng RP, Hwang J. p53 gene status modulates the chemosensitivity of non-small cell lung cancer cells. *J Biomed Sci.* 2000;7(1):64-70.

152. Lin H, Bondy ML, Langford LA, et al. Allelic deletion analyses of MMAC/PTEN and DMBT1 loci in gliomas: relationship to prognostic significance. *Clin Cancer Res.* 1998;4(10):2447-2454.

153. Wang SI, Puc J, Li J, et al. Somatic mutations of PTEN in glioblastoma multiforme. *Cancer Res.* 1997;57(19):4183-4186.

154. Furnari FB, Fenton T, Bachoo RM, et al. Malignant astrocytic glioma: genetics, biology, and paths to treatment. *Genes Dev.* 2007;21(21):2683-2710.

155. Li YL, Tian Z, Wu DY, Fu BY, Xin Y. Loss of heterozygosity on 10q23.3 and mutation of tumor suppressor gene PTEN in gastric cancer and precancerous lesions. *World J Gastroenterol.* 2005;11(2):285-288.

156. Whang YE, Wu X, Suzuki H, et al. Inactivation of the tumor suppressor PTEN/MMAC1 in advanced human prostate cancer through loss of expression. *Proc Natl Acad Sci U S A.* 1998;95(9):5246-5250.

157. Sato N, Tsunoda H, Nishida M, et al. Loss of heterozygosity on 10q23.3 and mutation of the tumor suppressor gene PTEN in benign endometrial cyst of the ovary: possible sequence progression from benign endometrial cyst to endometrioid carcinoma and clear cell carcinoma of the ovary. *Cancer Res.* 2000;60(24):7052-7056.

158. Kurose K, Zhou XP, Araki T, Cannistra SA, Maher ER, Eng C. Frequent loss of PTEN expression is linked to elevated phosphorylated Akt levels, but not associated with p27 and cyclin D1

expression, in primary epithelial ovarian carcinomas. *Am J Pathol.* 2001;158(6):2097-2106.

159. Di Cristofano A, Pandolfi PP. The multiple roles of PTEN in tumor suppression. *Cell.* 2000;100(4):387-390.

160. Suzuki A, Yamaguchi MT, Ohteki T, et al. T cell-specific loss of Pten leads to defects in central and peripheral tolerance. *Immunity.* 2001;14(5):523-534.

161. Liu X, Karnell JL, Yin B, et al. Distinct roles for PTEN in prevention of T cell lymphoma and autoimmunity in mice. *J Clin Invest.* 2010;120(7):2497-2507.

162. Hagenbeek TJ, Spits H. T-cell lymphomas in T-cell-specific Pten-deficient mice originate in the thymus. *Leukemia.* 2008;22(3):608-619.

163. Newton RH, Lu Y, Papa A, et al. Suppression of T-cell lymphomagenesis in mice requires PTEN phosphatase activity. *Blood.* 2015;125(5):852-855.

164. Soond DR, Garcon F, Patton DT, et al. Pten loss in CD4 T cells enhances their helper function but does not lead to autoimmunity or lymphoma. *J Immunol.* 2012;188(12):5935-5943.

165. Wang S, Liu JC, Kim D, Datti A, Zacksenhaus E. Targeted Pten deletion plus p53-R270H mutation in mouse mammary epithelium induces aggressive claudin-low and basal-like breast cancer. *Breast Cancer Res.* 2016;18(1):9.

166. Trotman LC, Niki M, Dotan ZA, et al. Pten dose dictates cancer progression in the prostate. *PLoS Biol.* 2003;1(3):E59.

167. Akashi K, Richie LI, Miyamoto T, Carr WH, Weissman IL. B lymphopoiesis in the thymus. *J Immunol.* 2000;164(10):5221-5226.

168. Anderson G, Jenkinson EJ. Lymphostromal interactions in thymic development and function. *Nat Rev Immunol.* 2001;1(1):31-40.

169. Inaba K, Hosono M, Inaba M. Thymic dendritic cells and B cells: isolation and function. *Int Rev Immunol.* 1990;6(2-3):117-126.

170. Tokoro Y, Sugawara T, Yaginuma H, et al. A mouse carrying genetic defect in the choice between T and B lymphocytes. *J Immunol.* 1998;161(9):4591-4598.

171. Radtke F, Wilson A, Stark G, et al. Deficient T cell fate specification in mice with an induced inactivation of Notch1. *Immunity.* 1999;10(5):547-558.

172. Kawashima H, Takatori H, Suzuki K, et al. Tumor suppressor p53 inhibits systemic autoimmune diseases by inducing regulatory T cells. *J Immunol.* 2013;191(7):3614-3623.

173. Park JS, Lim MA, Cho ML, et al. p53 controls autoimmune arthritis via STAT-mediated regulation of the Th17 cell/Treg cell balance in mice. *Arthritis Rheum.* 2013;65(4):949-959.

174. Fray MA, Bunnell SC. p53 keeps bystanders at the gates. *Immunity.* 2014;40(5):633-635.

175. Whiteside SK, Snook JP, Williams MA, Weis JJ. Bystander T Cells: A Balancing Act of Friends and Foes. *Trends Immunol.* 2018;39(12):1021-1035.

176. Watanabe M, Moon KD, Vacchio MS, Hathcock KS, Hodes RJ. Downmodulation of tumor suppressor p53 by T cell receptor signaling is critical for antigen-specific CD4(+) T cell responses. *Immunity.* 2014;40(5):681-691.

177. el-Deiry WS, Tokino T, Velculescu VE, et al. WAF1, a potential mediator of p53 tumor suppression. *Cell.* 1993;75(4):817-825.

178. Harper JW, Adami GR, Wei N, Keyomarsi K, Elledge SJ. The p21 Cdk-interacting protein Cip1 is a potent inhibitor of G1 cyclin-dependent kinases. *Cell.* 1993;75(4):805-816.

179. Chen J. The Cell-Cycle Arrest and Apoptotic Functions of p53 in Tumor Initiation and Progression. *Cold Spring Harb Perspect Med.* 2016;6(3):a026104.

180. Serrano M, Hannon GJ, Beach D. A new regulatory motif in cell-cycle control causing specific inhibition of cyclin D/CDK4. *Nature.* 1993;366(6456):704-707.

181. Kastenhuber ER, Lowe SW. Putting p53 in Context. *Cell.* 2017;170(6):1062-1078.

182. Perri F, Pisconti S, Della Vittoria Scarpati G. P53 mutations and cancer: a tight linkage. *Ann Transl Med.* 2016;4(24):522.

183. Shay JW, Pereira-Smith OM, Wright WE. A role for both RB and p53 in the regulation of human cellular senescence. *Exp Cell Res.* 1991;196(1):33-39.

184. Campisi J. Senescent cells, tumor suppression, and organismal aging: good citizens, bad neighbors. *Cell.* 2005;120(4):513-522.

185. Radu A, Neubauer V, Akagi T, Hanafusa H, Georgescu MM. PTEN induces cell cycle arrest by decreasing the level and nuclear localization of cyclin D1. *Mol Cell Biol.* 2003;23(17):6139-6149.

186. Aubrey BJ, Kelly GL, Janic A, Herold MJ, Strasser A. How does p53 induce apoptosis and how does this relate to p53-mediated tumour suppression? *Cell Death Differ.* 2018;25(1):104-113.

187. Lotem J, Sachs L. A mutant p53 antagonizes the deregulated c-myc-mediated enhancement of apoptosis and decrease in leukemogenicity. *Proc Natl Acad Sci U S A.* 1995;92(21):9672-9676.

188. Singh N, Huang L, Qin H. Defective T-cell receptor-induced apoptosis of T cells and rejection of transplanted immunogenic tumors in p53(-/-) mice. *Eur J Immunol.* 2010;40(2):559-568.

189. Weng L, Brown J, Eng C. PTEN induces apoptosis and cell cycle arrest through phosphoinositol-3-kinase/Akt-dependent and -independent pathways. *Hum Mol Genet.* 2001;10(3):237-242.

190. Stambolic V, MacPherson D, Sas D, et al. Regulation of PTEN transcription by p53. *Mol Cell.*

2001;8(2):317-325.

191. Mayo LD, Donner DB. A phosphatidylinositol 3-kinase/Akt pathway promotes translocation of Mdm2 from the cytoplasm to the nucleus. *Proc Natl Acad Sci U S A.* 2001;98(20):11598-11603.

192. Kurose K, Gilley K, Matsumoto S, Watson PH, Zhou XP, Eng C. Frequent somatic mutations in PTEN and TP53 are mutually exclusive in the stroma of breast carcinomas. *Nat Genet.* 2002;32(3):355-357.

193. Kato H, Kato S, Kumabe T, et al. Functional evaluation of p53 and PTEN gene mutations in gliomas. *Clin Cancer Res.* 2000;6(10):3937-3943.

194. Freeman DJ, Li AG, Wei G, et al. PTEN tumor suppressor regulates p53 protein levels and activity through phosphatase-dependent and -independent mechanisms. *Cancer Cell.* 2003;3(2):117-130.

195. Hirahara K, Poholek A, Vahedi G, et al. Mechanisms underlying helper T-cell plasticity: implications for immune-mediated disease. *J Allergy Clin Immunol.* 2013;131(5):1276-1287.

196. Zhou L, Chong MM, Littman DR. Plasticity of CD4+ T cell lineage differentiation. *Immunity.* 2009;30(5):646-655.

197. Banerjee A, Thyagarajan K, Chatterjee S, et al. Lack of p53 Augments Antitumor Functions in Cytolytic T Cells. *Cancer Res.* 2016;76(18):5229-5240.

198. Fox JG, Sheppard BJ, Dangler CA, Whary MT, Ihrig M, Wang TC. Germ-line p53-targeted disruption inhibits helicobacter-induced premalignant lesions and invasive gastric carcinoma through down-regulation of Th1 proinflammatory responses. *Cancer Res.* 2002;62(3):696-702.

199. Ohkusu-Tsukada K, Tsukada T, Isobe K. Accelerated development and aging of the immune system in p53-deficient mice. *J Immunol.* 1999;163(4):1966-1972.

200. Lin JX, Leonard WJ. The role of Stat5a and Stat5b in signaling by IL-2 family cytokines. *Oncogene.* 2000;19(21):2566-2576.

201. Fung MM, Rohwer F, McGuire KL. IL-2 activation of a PI3K-dependent STAT3 serine phosphorylation pathway in primary human T cells. *Cell Signal.* 2003;15(6):625-636.

202. Chen M, Pratt CP, Zeeman ME, et al. Identification of PHLPP1 as a tumor suppressor reveals the role of feedback activation in PTEN-mutant prostate cancer progression. *Cancer Cell.* 2011;20(2):173-186.

203. Singh N, Yamamoto M, Takami M, et al. CD4(+)CD25(+) regulatory T cells resist a novel form of CD28- and Fas-dependent p53-induced T cell apoptosis. *J Immunol.* 2010;184(1):94-104.

204. Chen L, Flies DB. Molecular mechanisms of T cell co-stimulation and co-inhibition. *Nat Rev Immunol.* 2013;13(4):227-242.

205. Nogai A, Siffrin V, Bonhagen K, et al. Lipopolysaccharide injection induces relapses of experimental autoimmune encephalomyelitis in nontransgenic mice via bystander activation of autoreactive CD4+ cells. *J Immunol.* 2005;175(2):959-966.

206. Mills CD, Kincaid K, Alt JM, Heilman MJ, Hill AM. M-1/M-2 macrophages and the Th1/Th2 paradigm. *J Immunol.* 2000;164(12):6166-6173.

207. Shojaee S, Chan LN, Buchner M, et al. PTEN opposes negative selection and enables oncogenic transformation of pre-B cells. *Nat Med.* 2016;22(4):379-387.

208. Carracedo A, Alimonti A, Pandolfi PP. PTEN level in tumor suppression: how much is too little? *Cancer Res.* 2011;71(3):629-633.

209. Liu Y, Chen C, Xu Z, et al. Deletions linked to TP53 loss drive cancer through p53-independent mechanisms. *Nature.* 2016;531(7595):471-475.

210. Markert EK, Mizuno H, Vazquez A, Levine AJ. Molecular classification of prostate cancer using curated expression signatures. *Proc Natl Acad Sci U S A.* 2011;108(52):21276-21281.

211. Wang L, Xiong H, Wu F, et al. Hexokinase 2-mediated Warburg effect is required for PTEN- and p53-deficiency-driven prostate cancer growth. *Cell Rep.* 2014;8(5):1461-1474.

212. Li Y, Guessous F, Kwon S, et al. PTEN has tumor-promoting properties in the setting of gain-of-function p53 mutations. *Cancer Res.* 2008;68(6):1723-1731.

213. Scian MJ, Stagliano KE, Ellis MA, et al. Modulation of gene expression by tumor-derived p53 mutants. *Cancer Res.* 2004;64(20):7447-7454.

214. Haupt S, di Agostino S, Mizrahi I, et al. Promyelocytic leukemia protein is required for gain of function by mutant p53. *Cancer Res.* 2009;69(11):4818-4826.

215. Buckler JL, Walsh PT, Porrett PM, Choi Y, Turka LA. Cutting edge: T cell requirement for CD28 costimulation is due to negative regulation of TCR signals by PTEN. *J Immunol.* 2006;177(7):4262-4266.

216. Foulds KE, Zenewicz LA, Shedlock DJ, Jiang J, Troy AE, Shen H. Cutting edge: CD4 and CD8 T cells are intrinsically different in their proliferative responses. *J Immunol.* 2002;168(4):1528-1532.

217. Wilcox RA. A three-signal model of T-cell lymphoma pathogenesis. *Am J Hematol.* 2016;91(1):113-122.

218. Strano S, Fontemaggi G, Costanzo A, et al. Physical interaction with human tumor-derived p53 mutants inhibits p63 activities. *J Biol Chem.* 2002;277(21):18817-18826.

219. Di Como CJ, Gaiddon C, Prives C. p73 function is inhibited by tumor-derived p53 mutants in mammalian cells. *Mol Cell Biol.* 1999;19(2):1438-1449.

220. Alexandrova EM, Yallowitz AR, Li D, et al. Improving survival by exploiting tumour dependence on stabilized mutant p53 for treatment. *Nature.* 2015;523(7560):352-356.

221. Hiraki M, Hwang SY, Cao S, et al. Small-Molecule Reactivation of Mutant p53 to Wild-Type-like p53 through the p53-Hsp40 Regulatory Axis. *Chem Biol.* 2015;22(9):1206-1216.

222. Horwitz SM, Koch R, Porcu P, et al. Activity of the PI3K-delta,gamma inhibitor duvelisib in a phase 1 trial and preclinical models of T-cell lymphoma. *Blood.* 2018;131(8):888-898.

223. Okkenhaug K, Vanhaesebroeck B. PI3K in lymphocyte development, differentiation and activation. *Nat Rev Immunol.* 2003;3(4):317-330.

224. Trotman LC, Pandolfi PP. PTEN and p53: who will get the upper hand? *Cancer Cell.* 2003;3(2):97-99.